SURFACTANT MICELLES: SOLUBILIZATION AND RELATED PHENOMENA

by

MICHAEL JON GUMKOWSKI

A thesis submitted in partial fulfillment of the
requirements for the degree of
Doctor of Philosophy
(Pharmacy)

at the

UNIVERSITY OF WISCONSIN - MADISON

1986

For Francine
and
my parents,
with love and appreciation.

ACKNOWLEDGEMENTS

I wish to express my sincere appreciation to:

Professor P. Mukerjee for his concern for my training as a research scientist and for his physical insight without which this work would have been impossible;

The American Foundation for Pharmaceutical Education and the CIBA-GEIGY Corp for three years of financial support associated with the 1980-82 CIBA-GEIGY Pharmaceutics Scholarship;

The University of Wisconsin-Madison Graduate School, the National Science Foundation, and Abbott Laboratories for financial support;

The pharmaceutics faculty for their varied avuncular contributions to my training;

Dr. Ravi Sharma and Mr. Chun Chan for out collaboration on the work discussed in Chapter Eight of this thesis, for many helpful discussions, and for our lasting comradship;

Mr. Paul Bummer, a fellow graduate student and excellent friend, who always extended his assistance and support;

Prof. Edward M. Arnett for his patient understanding while the writing of this work was in progress;

My parents, Walter and Jean, whose teaching, example, sacrifice, and unconditional love will always be responsible for whatever good work I may accomplish;

And, Francine, my loving wife, for typing and organizing the compilation of this thesis and for the past and future which we shall share for our lifetimes.

TABLE of CONTENTS

	PAGE
TITLE PAGE	i
Dedication	ii
Acknowledgements	iii
Table of Contents	v
List of Tables	xi
List of Figures	xvii
I. INTRODUCTION	
A. General Background and Review of Previous Work	1
B. Scope and Aim	16
II. EXPERIMENTAL	
A. Materials	21
B. Apparatus	25
1. Drop Volume Apparatus	25
2. Dialysis	25
a. solids	25
b. liquids	26
3. Vapor Transfer	26
4. Spectrophotometers	27
C. Methods	28

1. Surface and Interfacial Tension Measurements 28
2. Solubility Determinations 30
a. solids 30
b. liquids by dialysis 30
c. vapor transfer 32
d. analysis 33
3. Partition Coefficient Determinations 34
4. Measurement of Microenvironmental Polarity by Absorption Spectra 35
5. Cmc Determinations of Perfluorocarbons by UV Spectroscopy 36
6. Determination of the Dissociation Constant of Perfluorocarboxylic Acids 36

III. PARTITIONING OF AROMATIC COMPOUNDS BETWEEN ORGANIC LIQUIDS AND WATER
A. Introduction 37
B. Results 39
C. Discussion 47

IV. SURFACE PROPERTIES OF BINARY MIXTURES OF BENZENE AND SOME ALKYLBENZENES AND POLYCYCLIC AROMATICS WITH DECANE AT THE AIR-LIQUID AND WATER LIQUID INTERFACES
A. Introduction 54
B. Scope and Aim 58
C. Results 61

D. Discussion 88

1. Surface and Interfacial Tension of Binary Mixtures of Liquids 88

a. background 88

b. surface tension results 92

c. interfacial tension studies 97

2. Interfacial Adsorption From Dilute Solution 103

3. Surface Activity Coefficients in Dilute Solution 110

4. Work of Adhesion 119

V. SOLUBILIZING POWER OF MICELLES: RELATION TO MICELLAR LAPLACE PRESSURES AND INTERFACIAL ACTIVITIES OF SOLUBILIZATES

A. Micellar Laplace Pressures and Relation to Gas Solubilities in Micelles 129

1. Background 129

2. Scope and Aim 135

3. Estimates of Laplace Pressure From Gas Solubility Data 136

4. Estimates of Laplace Pressure From Micelle Models 143

B. Solubilization of Interfacially Active Species and the Application of the Two-State Model

1. Background 160

2. Scope and Aim 162
3. The Two-State Model 164
4. Data Analysis on the Basis of the Two-State Model 174
C. Assessment of Head Group Effects: Comparison of Solubilization by SDS and CTAB Micelles 189

VI. SOLUBILIZATION CAPACITY OF MICELLES AND A NEW METHOD FOR ITS DETERMINATION
A. Background 201
B. Scope and Aim 208
C. Results 208
1. Methods Testing and Validation 208
a. liquids 208
b. solids 214
2. Solubilization Capacity Measurements 216
D. Discussion 219
1. General Considerations 219
2. Aromatic Liquids at Saturation in SDS 223
3. Solubility of Solids in Micelles of SDS 230
4. Effect of Added Electrolyte on the Solubilization Capacity of Micelles 235
5. Solubilization of Benzene and Toluene in Sodium Perfluorooctanoate Micelles 239

VII. MICROENVIRONMENTAL POLARITY STUDIES IN SDS AND SPFO MICELLES

A. Review of Previous Work 246

B. Scope and Aim 251

C. Results and Discussion 252

1. Microenvironmental Polarity of Toluene in SDS and the Relationship of Microenvironmental Polarities of Aromatics to Interfacial Adsorptivity at the Micelle-Water Interface 252

2. Microenvironmental Polarity of Benzene in SPFO Micelles 265

3. Effects of Additives on the Microenvironmental Polarity of p-Xylene and Benzene in SDS Micelles 274

VIII. DETERMINATION OF ACID DISSOCIATION CONSTANTS OF PERFLUOROCARBOXYLIC ACIDS AND CRITICAL MICELLE CONCENTRATIONS OF THEIR SALTS BY UV SPECTROSCOPY

A. Background 283

B. Scope and Aim 289

C. Results and Discussion 290

1. Chain Length Dependance 290

2. Approach Toward Determination of Dissociation Constants for Perfluorocarbons 295

3. Determination of the Cmc of Salts of Perfluorocarboxylic Acids by UV Spectroscopy 307

IX. REFERENCES 319

LIST OF TABLES

		PAGE
TABLE 3.1	Distribution Coefficients for Benzene Between n-Decane and Benzene Binary Mixtures and Water at 25°C	40
TABLE 3.2	Distribution Coefficients for Toluene Between n-Decane and Toluene Binary Mixtures and Water at 25°C	42
TABLE 3.3	Distribution Constants for Ethylbenzene Between n-Decane and Ethylbenzene Binary Mixtures and Water at 25°C	44
TABLE 4.1	Surface Tensions of n-Butylbenzene + n-Decane Mixtures Against Air at 25°C	62
TABLE 4.2	Surface Tensions of Naphthalene + n-Decane Mixtures Against Air at 25°C	64
TABLE 4.3	Surface Tensions of Phenanthrene + n-Decane Mixtures Against Air at 25°C	66
Table 4.4	Surface Tensions of p-di-tert-Butylbenzene + n-Decane Mixtures Aganist Air at 25°C	68
TABLE 4.5	Surface Tensions of 1-Dodecene to n-Decane Mixtures Against Air at 25°C	70
TABLE 4.6	Interfacial Tensions of n-Butylbenzene + n-Decane Mixtures Against Water at 25°C	72

TABLE 4.7 Interfacial Tensions of Naphthalene + n-Decane Mixtures Against Water at 25°C 74

TABLE 4.8 Interfacial Tensions of Phenanthrene + n-Decane Mixtures Against Water at 25°C 76

TABLE 4.9 Interfacial Tensions of Pyrene + n-Decane Mixtures Against Water at 25°C 78

TABLE 4.10 Interfacial Tensions of p-di-tert-Butylbenzene + n-Decane Mixtures Against Water at 25°C 80

TABLE 4.11 Interfacial Tensions of 1-Dodecene + n-Decane Mixtures Against Water at 25°C 82

TABLE 4.12 Interfacial Tensions of Benzene + Perfluoro-n-hexane Mixtures Against Water at 25°C 84

TABLE 4.13 Interfacial Tensions of Orange OT + n-Decane Mixtures Aganist Water at 25°C 86

TABLE 4.14 Comparison of the Interaction Parameters χ and $\ln f/(1-\Phi_1)^2$ Calculated From Experimental Values of the Activity Coefficient, V_1A_{12}/RT, Calculated From Regular Solution Theory and β/kT From Air-Liquid Surface Tension Data 93

TABLE 4.15 Comparison of the Interaction Parameter, χ, Calculated From Experimental Values of the Activity Coefficient, V_1A_{12}/RT Calculated From Regular Solution Theory, and β/kT From Air-Liquid and Water-Liquid Interfacial Tension Data

99

TABLE 4.16 Initial Slopes of Interfacial Tension Against Water vs Mole Fraction of Some Aromatics in Binary Mixtures With Decane 106

TABLE 4.17 Surface Activity Coefficients, f^m, of Aromatics at Infinite Dilution in Binary Mixtures With Decane at 25°C 114

TABLE 4.18 Surface Activity Coefficients, f^m, of Decane at Infinite Dilution in Binary Mixtures With Aromatics at 25°C 115

TABLE 4.19 Activity Coefficient, f^m, of Aromatics at Infinite Dilution in Binary Mixtures With Decane From Interfacial Tension Data at 25°C 116

TABLE 4.20 Relationship Between Work of Adhesion, the Dispersion Component of the Work of Adhesion, and the Initial Slope 126

TABLE 5.1 Free Energies of Transfer From Gas at One Atmosphere to Micelle at 25°C Kcal mol^{-1} 138

TABLE 5.2 Free Energies of Transfer of Gases at One Atmosphere toSolution at 298 K 139

TABLE 5.3 Partial Molar Volumes of Gases in Liquid Hydrocarbons at 25°C 140

TABLE 5.4 Micellar Laplace Pressures (atm.) Calculated from Gas Solubilities in Aqueous Surfactant Solutions 141

TABLE 5.5	Interfacial Tensions of Alkane/SDS Aqueous Solutions at 69.1 A^2/ SDS Monomer at 25°C	151
TABLE 5.6	Comparison of Experimental and Calculated Laplace Pressures, ΔP (atm)	155
TABLE 5.7	Effect of Sodium Dodecyl Sulfonate on the Adsorption of Dimethyl Ether at the Heptane-Water Interface (Data of Jho and King, 1981)	172
TABLE 5.8	Comparison of SDS Micelle/Water Partition Coefficients, Km/w, From Experimental Measurements and From the Two-State Model For Several Compounds of Varying Interfacial Activity	175
TABLE 5.9	Comparison of Micelle/Water Partition Coefficients For n-Amides and n-Alkanols From Experimental Measurements and From the Two-State Model	179
TABLE 5.10	Solubilization of Benzene	183
TABLE 5.11	Mole Fraction Solubility of Benzene, Naphthalene, Anthracene, Biphenyl, and Pyrene in SDS and CTAB Micelles	193
TABLE 6.1	Reported Values of Benzene Solubility in Aqueous SDS solutions at 25°C	202
TABLE 6.2	Benzene Solubility in Water and in 5mM SDS at 25°C by Dialysis and Vapor Transfer Methods	212

TABLE 6.3	Benzene Solubility in SDS Solution in Concurrent Experiments Performed By Dialysis and Vapor Transfer at 25°C	213
TABLE 6.4	Solubilization Values for Benzene, Toluene, Ethylbenzene, Naphthalene and Orange OT in Aqueous Solutions of SDS and SPFO and in Aqueous Sodium Chloride Solution of SDS at 25°C in Terms of the Mole Fraction of Solubilizate in the Micelle	217
TABLE 6.5	Comparison of Micelle/Water Partition Coefficients for Benzene, Toluene, Ethylbenzene and Butylbenzene from Experimental Measurements at Saturation and from the Two-State Model at Infinite Dilution.	225
TABLE 6.6	Comparison of Micellar Solubility for Naphthalene, Pyrene and Orange OT from Experimental Measurements at Saturation and from The Two-State Model at Infinite Dilution	231
TABLE 6.7	Comparison of Micelle/Water Partition Coefficients for Benzene in SPFO, SDS and SOS From Experimental Measurements and From the Two-State Model at Infinite Dilution	241
TABLE 7.1	Comparison of the H Parameter and the Fraction of Solubilizate at the Micelle-Water Interface From the Two-State Model For Benzene and Four Alkylbenzenes in SDS Micelles	260

TABLE 7.2	ϵ_s/ϵ_p Ratios For Benzene	272
TABLE 7.3	Microenvironmental Polarity of Benzene and p-Xylene Aqueous Solutions of SDS and SDS + Additive	278
TABLE 8.1	Chain Length Effect on the Absorptivity of Aqueous Solutions of Perfluorocarboxylic Acids and Their Salts at 205nm.	291

LIST OF FIGURE LEGENDS

		PAGE
Figure 3.1	Partition Coefficients, $x_{organic\ phase}/x_{aqueous\ phase}$, for benzene in binary mixture with decane plotted as a function of the mole fraction of benzene in the organic liquid.	41
Figure 3.2	Partition Coefficients, $x_{organic\ phase}/x_{aqueous\ phase}$, for toluene in binary mixture with decane plotted as a function of the mole fraction of toluene in the organic liquid.	43
Figure 3.3	Partition Coefficients, $x_{organic\ phase}/x_{aqueous\ phase}$, for ethylbenzene in binary mixture with decane plotted as a function of the mole fraction of ethylbenzene in the organic liquid.	45
Figure 3.4	Activity Coefficients, f_o, of Benzene, Toluene and Ethylbenzene in binary mixtures with decane plotted as function of the mole fraction of aromatic compound in the organic mixture, x_o.	50
Figure 4.1	Structures of Compounds Studied.	55
Figure 4.2	Surface tensions of n-butylbenzene + n-decane mixtures at 25°C plotted as a function of the mole fraction of n-butylbenzene.	63

Figure 4.3 Surface tensions of naphthalene + n-decane mixtures at 25°Cplotted as a function of the mole fraction of naphthalene. 65

Figure 4.4 Surface tensions of phenanthrene + n-decane mixtures at 25°Cplotted as a function of the mole fraction of phenanthrene. 67

Figure 4.5 Surface tensions of p-di-tert-butylbenzene + n-decane mixtures at 25°C plotted as a function of the mole fraction of p-di-tert-butylbenzene. 69

Figure 4.6 Surface tensions of 1-docecene + n-decane mixtures at 25°Cplotted as a function of the mole fraction of 1-dodecene. 71

Figure 4.7 Interfacial tensions of n-butylbenzene + n-decane mixtures against water at 25°C plotted as a function of the mole fraction of benzene in the organic phase. 73

Figure 4.8 Interfacial tensions of naphthalene + n-decane mixtures against water at 25°C plotted as a function of the mole fraction of naphthalene in the organic phase. 75

Figure 4.9 Interfacial tensions of phenanthrene + n-decane mixtures against water at 25°C plotted as a function of the mole fraction of phenanthrene in the organic phase. 77

Figure 4.10 Interfacial tensions of pyrene + n-decane mixtures against water at 25°C plotted as a function of the mole fraction of pyrene in the organic phase. 79

Figure 4.11 Interfacial tensions of p-di-tert-butylbenzene + n-decane mixtures against water at 25°C plotted as a function of the mole fraction of p-di-tert-butylbenzene in the organic phase. 81

Figure 4.12 Interfacial tensions of 1-dodecene + n-decane mixtures against water at 25°C plotted as a function of the mole fraction of 1-dodecene in the organic phase. 83

Figure 4.13 Interfacial tensions of benzene + perfluoro-n-hexane mixtures against water at 25°C plotted as a function of the mole fraction of benzene in the organic phase. 85

Figure 4.14 Interfacial tensions of Orange OT + n-decane mixtures against water at 25°C plotted as a function of the mole fraction of Orange OT in the organic phase. 87

Figure 4.15 Number of double bonds, n, in compounds listed below plotted as a function of the initial slope, $\delta\gamma/\delta x$, of the interfacial tension vs mole fraction curve. 108

Figure 4.16 Work of adhesion of benzene, n-butylbenzene and 1-dodecene in binary mixtures with decane plotted as a function of the mole fraction of the unsaturated compound in the organic liquid. 121

Figure 4.17 Work of adhesion of phenanthrene, naphthalene, and p-di-tert- butylbenzene in binary mixtures with decane plotted as a function of the mole fraction of the unsaturated compound in the organic liquid. 122

Figure 4.18 Initial slope, $\delta\gamma/\delta x$, of the interfacial tension vs mole fraction curve plotted as a function of the difference between experimental work of adhesion, W_A(expt.), for the pure compounds and that calculated, W_A(calc.), as $2(20.63\gamma)^{1/2}$ where γ is the surface tension of the pure liquid. 127

Figure 5.1 Hydrocarbon/aqueous surfactant solution interfacial tension at 20°C plotted as a function of area per surfactant molecule from data of Haydon and Taylor. 146

Figure 5.2 log $K_{m/w}$ plotted as a function of log $K_{\text{hydrocarbon alkane/water}}$ 187

Figure 5.3 Natural logarithm of the ratio of the mole fraction of listed compounds in CTAB micelles to that in SDS micelles plotted as a function of the molar volume of the solubilizate. 194

Figure 6.1 Ln micelle-water partition coefficient at saturation, $K_{m/w}^{(sat)}$, plotted as a function of the ln $K_{m/w}^{\infty}$ calculated at infinite dilution on the basis of the two-state model for micellar solubilization for benzene, toluene, ethylbenzene,and butylbenzene in SDS and potassium laurate. 226

Figure 7.1 R_C values for toluene ($a_{264.8}/a_{263.8}$), lower curve, and ethylbenzene , ($a_{264.4}/a_{263.3}$), plotted as a function of the H-parameter of the solvent. 254

Figure 7.2 R_c of toluene in aqueous solutions of SDS plotted as a function of $(R_c - R_{c,a})\ \Phi a/\Phi m$. 258

Figure 7.3 Difference spectrum of benzene in SPFO micelles. 269

Figure 7.4 UV spectra of benzene in perfluorohexane, and in water. 270

Figure 8.1 UV absorbance of SPFO at 205 nm plotted as a function of the molar concentration of SPFO in water. 293

Figure 8.2	UV absorbance of HPFO at 205 nm plotted as a function of the molar concentration of HPFO in water.	294
Figure 8.3	Linear plotting form for determination of K_a of trifluoroacetic acid at 25°C.	303
Figure 8.4	Linear plotting form for determination of K_a of perfluorobutyric acid at 25°C.	304
Figure 8.5	Difference plot for determination of cmc of SPFO in water at 25°C.	311
Figure 8.6	Difference plot for determination of cmc of tetraethyl ammonium perfluorooctanoate in water at 25°C.	313

INTRODUCTION

A. General Background and Review of Previous Work

The hydrophobic interaction is responsible for the self-association of molecules in aqueous solution. (1,2) If a molecule contains moieties which interact favorably with water as well as hydrophobic regions, it is called amphipathic (3). Molecules which possess a flexible hydrophobic chain with a polar group at one end are examples of amphipaths. These may be ionic, such as sodium dodecyl sulfate,(SDS), or hexadecyltrimethyl ammonium bromide,(CTAB), nonionic, such as octyl glucoside or polyoxyethylene lauryl ether, or zwitterionic, such as dodecyl N-betaine.

In low concentrations such molecules exist as monomers and reduce the surface tension of aqueous solutions. They adsorb to an air-water or hydrocarbon-water interface in large numbers.(4) They orient in such a manner that their hydrophobic portions escape the aqueous environment. Any molecule which has a strong tendency to adsorb to a surface from aqueous solution is called a surfactant.

The aggregation of flexible chain surfactants can be detected by the abrupt change in the concentration dependence of a number of physical

properties of solution.(5,6) Such properties will be dependent upon the concentration of monomers, aggregates, or an unequally weighted combination of the two. (7) If a large aggregate is formed consisting of more than about twenty monomers, the change in the solution property will occur over a narrow range of concentrations.(6) Such aggregates are called micelles.

Operationally, the intercept of the two linear portions of the solution property plot is referred to as the critical micellization concentration, abbreviated cmc. (6) Above the cmc the solution activity of monomers increases only slightly with large increases in total surfactant concentration. (1,8) Therefore, the surface tension decreases much less rapidly above the cmc; this makes surface tension a useful method of cmc detection. (5) Other methods used include light scattering, conductance, equivalent conductivity, colligative properties, and the change in the absorbance spectrum of the surfactant or an indicator molecule upon micellization. For most surfactants, the cmcs determined by different methods agree within a few percent. (1,5)

Micelles have found use in research and industry. (9). Of particular interest to the biophysical sciences, micelles are thermodynamically

stable and reproducible representatives of other assemblies of lipid molecules such as bilayers, membranes and vesicles.(10) Micelles can be used as model systems in fundamental studies to investigate the nature of hydrophobic forces and interactions of molecules with hydrophobically associated systems.(1) Complex biological enzymes and membranes can be simulated in a simple way by micelles. The micelle can provide an environment for some reactions leading to a catalytic change in reaction rate.(11)

The structure of the micelle has been extensively studied. (12,13, 14,15) At concentrations near the cmc, most micelles of flexible chain surfactants are roughly spherical (13,14). Compressibility and fluidity measurements indicate that the aggregated hydrophobic chains are in an environment similar to the liquid from which they were derived.(1,16) Some evidence for restrictions of their motion has been noted, however. (17,18) The polar or ionic headgroups remain in contact with water as well as, perhaps, the first one or two carbon atoms (19), making the surface of the micelle rough. The repulsive interactions between the headgroups, especially the ionic ones, contribute positively to the free energy of micelle formation. (20) The micelle which forms at the

cmc is nearly monodisperse since it best satisfies the competing effects of hydrophobic aggregation, head group repulsion and head group interaction with the hydrophobic core. (20) The association equilibria for successsive monomer addition to the aggregate are cooperative up to a small optimal region after which they become rapidly anti-cooperative. (20) Addition of salt can reduce the headgroup repulsion of ionic surfactants allowing larger, more polydisperse, rod-shaped micelles to form.(20) The monomers are in dynamic equilibrium with the micelle. The average lifetime of a micelle is on the order of 10^{-2} sec. (21) The rate constant for dissociation of monomers is about 10^{7} sec^{-1} for SDS micelles. (22) Association is nearly diffusion controlled. (22)

At concentrations above the cmc, aqueous solutions of surfactants can dissolve most organic compounds to a greater extent than can pure water.(23,24) McBain called this effect solubilization(23). If the amount solubilized is small enough that micellar properties are not greatly altered, the equilibrium solublility of a compound can be used to detect the cmc. Dyes such as Orange OT and dimethylaminoazobenzene (DMAB) have been used extensively for this purpose. (25,26,27) For most compounds no solubilization takes place below the cmc.

As seen with micellization, solubilization is a dynamic process as solubilizates are not rigidly fixed at a particular location. (28) Solubilized compounds have been shown to leave the micelle more than 50,000 times per second, their mean lifetime being on the order of 1-100 microseconds. (29) The reentry is close to diffusion controlled.(29) The solubilizate then has enough time to diffuse to, and to sample, different environments in the micelle. The amount of time a solubilizate can spend in favorable locations as opposed to unfavorable locations will be reflected in its equilibrium uptake into a micelle. Any preferential location of a solubilizate in a micelle will depend upon its molecular structure and that of the solubilizing surfactant. (28)

Solubilization is important to technological and research interests. For example, an understanding of the preferable locations of solubilized molecules within micelles provides better insight into micellar catalysis. The partitioning of drugs and toxicants into micelles serves as a model for their interactions with biological membranes or liposomes. In addition, micellar solutions are widely employed as vehicles for drugs.(32) A knowledge of the transition from micellar solubilization to microemulsions is also of interest in oil recovery.(34) Solubilization has

thus been studied extensively. A review was written as early as 35 years ago (30) and several others have followed. (24,31,23,33)

The ability of the micelle itself to solubilize molecules is referred to as the solubilization capacity of the micelle. A measure of the solubilization capacity is the ratio of the number of moles of a solubilizate associated with a micelle (total concentration of solubilizate - aqueous solubility) to the number of moles of aggregated surfactant in solution (total concentration of surfactant - cmc). This ratio is usually constant above the cmc but has been shown to increase at higher surfactant concentrations in some systems. (23,24).

Major trends in the factors influencing solubilization in ionic micelles have been examined. Increase in chain length of the surfactant has been shown to enhance solubilization. Klevens (30) found a general increase in the solubilization of ethylbenzene as the chain length of potassium carboxylates was increased from eight to sixteen. Kolthoff and Stricks (25) studied the solubilization of water in the insoluble dye dimethylaminoazobenzene in a series of potassium carboxylates of chain length 12 to 18 and found a similar increase in uptake of dye with chain length. In general the cationic surfactants have been found to have a

greater solubilization capacity for hydrocarbons than anionics of equal chain length. (30,35) For example, the mole ratio of micellized benzene to micellized surfactant is 0.95 for SDS and 1.60 in dodecylpyridinium chloride. (35) The solubilization capacity of quaternary ammonium surfactants for Orange OT has been shown to increase as the size of the alkyl chain attached to the nitrogen increases. (36)

The properties of the solubilizate which have been most closely studied are the molar volume and polarity. Within a homologous series of solubilizates of similar chemical composition, compounds of larger molecular weight are solubilized to a lesser extent. (30,37,38) For example, Stearns and coworkers (37) studied the solubilization of n-alkanes, benzene, and n-alkylbenzenes. They found that the volumes of these compounds solubilized by potassium laurate micelles was inversely proportional to the molar volume of the solubilizate. For molecules of similar molar volumes, the aromatics were found to be more soluble than the alkanes. Klevens (38) found a decrease in the solubilization of polycyclic aromatics as their molar volume was increased. Increased polarity of the solubilizate has been shown to enhance its solubility in micelles. (30,39) Thus ethers, ketones, esters, and slightly polar aromatic

hydrocarbons as well as molecules which are themselves amphipathic, such as heptanol, are solubilized to a greater extent than non-polar hydrocarbons.(23) For example heptanol is more than twice as soluble as heptane in potassium laurate.(39) A similar difference in solubilization of octane and octanol in cetyl pyridinium chloride (CPC) has been seen.(23,24) Methyl isobutyl ketone is more than twice as soluble in CPC and more than four times as soluble in dodecyl ammonium chloride than is ethylbenzene, although both of these solubilizates have the same molar volume. (24) As noted above, aromatic compounds have been found to be solubilized to a greater extent than hydrocarbons of similar size. (24,37)

Additives can also influence the solubilization of other molecules. Electrolytes can change the size, shape and cmc of micelles. (15,27,40,41) The effects of electrolytes on the solubilization capacity of ionic micelles is not well defined since it is dependent upon these complex structural changes.(26,33) In some cases electrolytes have no effect while in other cases an increase in solubilization capacity is seen.(23,23)

Cosolubilization of nonelectrolytes has also been examined.(30,42,43) Medium and long chain alkanols have been the most widely examined. They have been found to increase the micellar solubility of hydrocarbons.

Koltoff and Graydon (43) studied the effects of amyl alcohol and octyl alcohol on the solubilization of several water insoluble compounds in potassiumn laurate. In general the solubilization capacity increased as the concentration of alcohol in solution increased. Solubilization of n-heptane in potassium tetradecanoate micelles was found by Klevens (30) to increase with chain length of the alkanol from heptanol to dodecanol. Octyl mercaptan and octylamine were found to have a greater effect than octyl alcohol.(30) Hoskins and King have found that the solubility of ethane in sodium dodecyl sulfate (SDS) micelles was enhanced by the presence of pentanol.(42)

Certainly, the solubilization of highly water insoluble molecules, such as alkanes,(30,37), by micelles indicates that the associated hydrophobic chains are responsible for solubilization. However, the micelle acts as a solvent differently than the hydrocarbon chains from which it was derived. The partition coefficient of solubilizate between the micelle and water at low solubilizate concentrations gives an indication of these differences. At low concentrations the micelle structure is not perturbed by the presence of solubilizate. An aliphatic hydrocarbon such as decane has a micelle/water partition coefficient in SDS of about one tenth

the value of its hydrocarbon/water partition coefficient.(44) As will be shown later, butanol, a polar molecule, has a micelle/water partition coefficient in SDS about 200 times its hydrocarbon/water partition coefficient.(45) Some major anomalies of the solubilization process are revealed by this example. The micelle favors the more polar species by a factor of l000 unlike the expected behavior of a hydrocarbon. Also, the solubilizing power of the micelle is greater than hydrocarbon in one case and less than hydrocarbon in the other. Any solubilization theory would need to explain both types of behavior.

The location of the solubilizate in the micelle is of fundamental interest. It determines the amount of contact the solubilizate has with the aqueous phase and with compounds, such as ions, located only in the aqueous phase. Many investigators have attempted to define the location of molecules solubilized by micelles. A number of techniques have been employed including UV spectroscopy (46-52), NMR (53,54), ultrasonic spectroscopy (55), and fluorescence (56). In an attempt to quantitatively describe the environment of solubilized molecules, Cardinal and Mukerjee (49) identified some UV spectral parameters sensitive to solvent polarity. The polarity was measured by the dielectric constant. A parameter,H, was

defined as the volume concentration of -OH dipoles in a solvent relative to that in water (55.4 mol/l). It was found to be related to the dielectric constant and could also provide a solvent polarity parameter (57). Micellar solutions of benzene, n-alkylbenzenes and naphthalene were studied. The effective dielectric constant of benzene in SDS and CTAB micelles was found to be similar to a fifty percent ethanol/water mixture (H = 0.65).

In the case of the alkylbenzenes the estimated average polarity of the microenvironments decreased in a gradual manner with increasing alkyl substitutions. This was inconsistent with a single homogenous environment for solubilizates be it polar or non-polar. The solubilizate molecules were thus shown to be sampling more than one environment in the micelle. This led Mukerjee and Cardinal (50) to suggest a two-state model for micellar solubilization. Solubilizate molecules were considered to be distributed between the hydrophobic core, a "dissolved state", and the micelle/water interface, an "adsorbed" state. The amount adsorbed to the micelle/water interface was related to the tendency of a molecule to decrease the interfacial tension between the micelle and water. Since the "adsorbed" and "dissolved" states are in equilibrium, the amount at the interface was controlled by the amount in the hydrophobic core. Since the

micelle has such a large surface area relative to its volume, the total amount of solubilizate adsorbed could be extensive even for slightly interfacially active molecules.

These workers also presented an analysis of previous work of Rehfeld (58) on the interfacial tensions of aliphatic hydrocarbons and benzene against aqueous solutions of SDS. The interfacial tension for benzene paralleled in a rough manner that of the alkane systems as the SDS concentration was increased. The difference in interfacial tension was found to be nearly constant over the region 88.8-66.4 $Å^2$ per adsorbed SDS molecule. In the micelle the surface area of adsorbed SDS molecule is about 69 $Å^2$ per molecule. This behavior suggested that the presence of SDS would not abolish the interfacial activity of benzene dissolved in hydrocarbons against an aqueous solution. Therefore, the interfacial activities of benzene and other solubilizates have been estimated from interfacial tension measurements on systems without surfactants. (50,59)

The two-state model suggests that alkylbenzenes are adsorbed at the micellar interface to a lesser degree. Increasing the size of the alkyl substituent decreases the interfacial tension against water, and decreases its interfacial activity. Alkylbenzenes would thus be expected to

experience a more hydrophobic average environment and this was seen experimentally. (50) The model is also consistent with some experimental observations which suggest that as concentration of solubilizate in the micelle increases the fraction of solubilizate in the core of the micelle relative to that at the surface would increase. (23,53,60,61)

Mukerjee introduced the concept of micellar Laplace pressure in a discussion of odd-even chain length effects on micellization.(18) This pressure arises from the curved interface of the micelle. Laplace presure opposes the entry of molecules into the micelle. As a pV work term in the chemical potential of the solubilizate, this effect increases with the molar volume of the solubilizate. Mukerjee has addressed the role of micellar Laplace pressure on solubilization in reviews of the subject. (23,62) He analyzed the data of Nakagawa and Tori (63) on the solubilization of n-octane, n-decane and n-dodecane in decyl polyoxyetheylene decyl ether micelles. (23) A Laplace pressure of about 299 atm. was consistent with an interfacial tension for the micelle of reasonable order of magnitude. Also, the available data of Wishnia (64) on the solubility of four hydrocarbon gases at one atm. pressure in SDS micelles in 0.I NaCl were analyzed by Mukerjee. The free energies of

transfer of these gases from liquid hydrocarbons to SDS micelles agreed with values calculated on the basis of a Laplace pressure of 296 atm.

More recently, Pyter, Ramachandran and Mukerjee (52) have extended the two-state model to the nitroxides 2,2,6,6,- tetramethyl piperidinyl-l-oxy (TEMPO) and 4-oxo-2,2,6,6,- tetramethylpiperidinyl-l-oxy (OTEMPO). They determined the micelle-water partition coefficients in several surfactant systems. The partition coefficients between dodecane and water and interfacial activities at the dodecane-water interface were also measured. These workers took account of the Laplace pressure effect on the partitioning of these solubilizates into micelles. They estimated the value of the Laplace pressure using interfacial tensions of SDS at alkane/water interfaces and the micellar radius. The dodecane-water partition coefficients corrected for the Laplace pressure effect gave an estimate of the partitioning into the micellar core from water. The experimental micelle-water partition coefficients were found to be 71 times higher for TEMPO and l600 times higher for OTEMPO. On the basis of the two-state model, these values are the ratio of nitroxide adsorbed at the micelle-water interface to that in the core. From the interfacial adsorptions to the dodecane-water interface this ratio was

estimated to be about 400 for TEMPO and 5300 for OTEMPO. These large adsorbed/dissolved ratios from both methods indicated the dominant role of the micelle - water interface for these molecules. For the highly polar nitroxide groups specific head group effects may be influential in their surface activities. From the results cited above for two methods of estimating the adsorbed/dissolved ratio, the adsorption to a dodecane-water interface gave values 5.6 times higher in the case of TEMPO and 33 times higher for OTEMPO than the comparison of partitioning between the micelle and water and hydrocarbon and water. An understanding of the reason for these differences is one of the major objectives of this research.

Recently, Blatt, Sawyer and Ghiggino (65) found evidence for the existence of two states for solubilized methyl-9-anthroate. The fluorescence decay patterns of this compound in SDS micelles could not be adequately described by a single exponential decay function. A double exponential decay was needed. The longer lifetime was associated with the non-polar, hydrocarbon environment. The shorter lifetime gave evidence of a polar environment similar to methanol. Quenching experiments also suggested the occupation of two states by this

solubilizate in SDS. In CTAB micelles similar experiments could be interpreted with only one state, the surface region of the micelle. Differences between quaternary ammonium cationic micelles and anionic micelles with respect to the fraction of solubilization in the surface state will be addressed in this work.

B. Scope and Aim

The ultimate goal behind this work was the understanding of the nature of the interaction of nonelectrolytes with surfactant micelles and other lipid assemblies in aqueous solution. This involves the solubilizate location in the micelle, distribution between the micelle and water, uptake into the micelle, and orientation at the micelle-water interface, when located in that region. Two concepts pertinent to micellar solubilization have recently been introduced in the literature.The presence of a high Laplace pressure in the micelle was examined.(18,52) Laplace pressure values for several surfactants determined from literature data on gas solubilities in micelles have been compared with calculations based upon a fluid model of the micelle. (18,23) The two-state distribution of solubilizate between the hydrophobic core and the micelle/water interface for interfacially active compounds was investigated.(50,52) The present

work was an investigation of the usefulness of these concepts as a framework for a general theory of solubilization. Through the analysis of several systems another important feature has been illuminated. The solubilizate must compete for the micelle/water interface with the polar groups of the aggregated surfactant monomers. A new thermodynamic approach has been developed which provides a suitable correction of hydrocarbon/water interfacial activity data to account for the presence of the polar groups. The two-state model has been tested, with encouraging results, against recent literature data of micelle/water partition coefficients, including some systems where 99.9% of the molecules are at the interface.

Solubilization studies performed in this work have centered on the aromatic compounds benzene, n-alkyl benzenes and polycyclic aromatics. These compounds are simple molecules facilitating data interpretation in terms of theory. Also they are of biological importance as potential carcinogens.(66) Interactions between micelles and these solubilizates provides an indication of the nature of their interaction with all lipid assemblies including physiological membranes. In this work solubilization in both hydrocarbon and perfluorocarbon surfactant micelles has been

studied to test the qualitative conclusions of the solubilization model in two different types of surfactant micelles.

We have successfully investigated and validated a new method for the determination of the solubilization capacity of micelles. Through the use of porous membranes, the liquid or solid pure solubilizate phase was kept separate from the sampled solution while equilibration took place in dialysis cells. The microenvironmental polarity of solubilized aromatics in trace concentrations has been studied by UV spectroscopy.(49,50) Such studies in perfluorocarbon surfactants required a new method of data analysis. The effects of additives, which themselves interact with the micelle, on the microenvironmental polarity of solubilized benzene and p-xylene has also been examined.

Results of solubilization capacity studies and microenvironmental polarity studies are analyzed in terms of the solubilization model under investigation. Effects of micellar Laplace pressures and interfacial tension as well as the interfacial activity, the hydrocarbon/water partitioning, and the molar volume of the solubilizate are examined. Consistency between the thermodynamic model and spectroscopic findings lends strong support to the present analysis.

Phenomena related to solubilization have also been studied and analyzed to reveal significant findings. The most fundamental interaction involved in solubilization is the interaction between the hydrophobic chains of the micelle and the solubilizate. Partitioning studies of aromatics between hydrocarbon or perfluorocarbon organic phases and water were performed. Comparison of activity coefficients determined from liquid/liquid partitioning and from literature data on vapor pressure studies in the absence of water indicated the insignificant role of water on the activity of benzene in decane.

Interfacial activities of solubilizates determine their ability to adsorb to the micelle-water interface. The hydrocarbon or perfluorocarbon - water interfaces have been used as a model for the micelle-water interface. Interfacial activity was measured by the change in interfacial tension upon addition of solubilizate. Therefore, interfacial tensions of aromatic + alkane mixtures have been measured. Further understanding of the interactions occurring across interfaces has been gained by analysis of these data on the basis of thermodynamic theories of interfaces. Measurements of surface tensions of these mixtures against air have been used along with thermodynamic models to investigate the perturbing

effects of water on the interactions occurring at an interface. The relation of interfacial activity to the extent of aromaticity has also been examined. Activity coefficients at the air-liquid and water-liquid interfaces have been estimated on the basis of experiment and theory. The work of adhesion was also determined for these mixtures and analyzed in terms of interactions occurring across interfaces.

The UV spectrum of perfluorocarboxylic acids and their salts has been examined and exploited to provide information on two interesting and important physical properties of these types of molecules. The acid dissociation constants of the moderately strong acids perfluoroacetic acid and perfluorobutyric acid have been determined from UV spectral changes occurring upon increasing acid concentration. The critical micelle concentrations of perfluorooctanote salts have been evaluated from changes in their UV spectrum upon micellization.

EXPERIMENTAL

A. MATERIALS

Benzene, toluene, and n-decane (Aldrich, 99+% Gold Label) were passed through Florisil™ (activated Magnesium Silicate, J.T. Baker) to adsorb contaminants prior to use in experiments.(67)

Ethylbenzene (Aldrich 99%) was distilled and then passed through Florisil™ when used for partition studies. Ethylbenzene (Aldrich 99%) was distilled for solubilization studies.

n-Butyl benzene was obtained from Aldrich (99%) and passed through a Florisil™ column prior to use.

Naphthalene (Aldrich, Scintillation Grade, 99+%, Gold Label) was dissolved in n-decane (Aldrich, 99%, Gold Label) and passed through Florisil™ twice. No significant change in interfacial tension was noted between the first and second treatments, and the the mole fraction of naphthalene in the final Florisil ™ treated solution was shown to be within 2% of the original by spectroscopic determinations. This solution was diluted by weight. For solubilization experiments the above material was used as received.

p-Di-tert-Butylbenzene (Aldrich, 98%) was recrystallized from methanol (68) and then dissolved in n-decane (Aldrich, (98+%) and passed through Florisil™ before use. The final concentration of p-di-tert butylbenzene was within 2% of the starting concentration.

Phenanthrene (Aldrich, 98+%) was purified by dilution in decane and passaged through Florisil™ twice before use for interfacial tension experiments. The final concentration was within 5% of the original by spectroscopic determination.

Pyrene (Aldrich, 99+%) was dissolved in n-decane and passed through Florisil™ twice before use. The UV spectrum was indistinguishable from that of a sample which had been recrystallized twice from ethanol with addition of decolorizing charcoal. The final concentration was within 1% of the starting concentration.

1-Dodecene (Aldrich, 95%) was vacuum distilled (b.p. 93.5°C) and then passed through Florisil™ before use for interfacial tension or surface tension measurements.

Orange OT (l-o-tolylazo-2-naphthol) was synthesized by R. Cataldi of this laboratory. It had been recrystallized once from an acetone/water mixture and three times from ethanol (M. Murata, l977). Some of this

material was also recrystallized from ethanol by this worker. The two recrystallized batches gave interfacial tensions in agreement.

Perfluorohexane (PCR) was passed through Florisil™ prior to use.

Sodium dodecyl sulfate (BDH) was recrystallized twice from an ethanol-water (1:1) mixture and from water. Following one extraction from ethyl ether, the surface tension of this material showed no minimum with concentration. Also the BDH product (99.25% C_{12} sulfate) was used as received except for drying over calcium sulfate. It gave a minimum in surface tension of 1 dyne/cm and was used for some solubilization studies. It gave solubilization capacity values equal to the pure compound within experimental error. This product was extracted with ethyl ether six times and recrystallized from water five times. This material was also used for solubilization studies once it was found to be equivalent to the pure compound with respect to solubilization of benzene.

Perfluorooctanic acid (PCR,Inc.) was used as received, after drying under vacuum. Sodium perfluorooctanoic acid was recrystallized from a basic (pH 11.7) aqueous solution of perfluorooctanic acid and sodium hydroxide. Previous data from this laboratory have shown that this product does not exhibit a minimum in surface tension with respect to composition.(68)

Sodium hydroxide was taken from a saturated solution.

HCl used was electronic grade (Hi-pure chem). For HCl concentrations less than 6M, the HCl was distilled from an azeotropic mixture with water.

Trifluoroacetic acid and heptafluorobutyric acid were distilled before use. Due to the hygroscopicity of these compounds, aqueous stock solutions prepared after distillation were titrated against standard sodium hydroxide.

NaCl (MCB) was precipitated from water by introduction of acetone or methanol. After filtration and partial drying, it was dried completely by roasting.

Tetraethylammonium hydroxide 20% solution (Aldrich) was used as received.

Distilled deionized water was again distilled from alkaline potassium permanganate prior to use.

n-Heptane (Akdrich Gold Label, 99+%, Spectrophotometric Grade) was used as received.

Ethanol (Midwest Solvent Company of Illinois) was used as received.

Methanol (Fisher, ACS or Mallinckrodt, absolute acetone free) was used as received.

95% ethanol (Hydrite Chemical Co.) was used as received.

p-xylene (Aldrich Chemical Co.) was redistilled prior to use.

1-Hexanol (Aldrich, Gold Label 99+%) was used as received.

Tetrabutylammonium bromide (Aldrich 99%) was used as received.

Zwittergent™ 3-12 (N-dodecyl-N, N-dimethyl-3-ammonio-1-propane sulfonate) (Calbiochem, 99%) was dried prior to use.

B. APPARATUS

1. Drop Volume Apparatus

Surface and interfacial tension measurements were performed using a drop volume apparatus which had been designed in this laboratory (70). An Alga™ syringe with a tip ground so as to produce a flat unbeveled surface was connected to a micrometer and fitted to a thermostatted container. This apparatus allowed for measurement of interfacial tensions by the falling drop or rising drop methods.

2. Dialysis

a. Solids: A spectrum equilibrium dialysis unit was used for the determination of the solubilities of solids. This unit consisted of five Teflon™ dialysis cells, each with a total half cell volume of 1.36 ml and a

membrane surface area of 4.5 cm^2 . The cells were mounted onto a holder and connected to a motor which provided continuous rotation of the unit. Polycarbonate membranes (Nucleopore™) with a 500Å pore size were used in these studies.

b. Liquids: Stainless steel dialysis cells were constructed after it was realized that the aromatic liquids studied here were sorbed to the Teflon™ of the above apparatus.(70,72) The stainless steel cells also had a total half cell volume of 1.36 ml and a membrane surface area of 4.5 cm^2. Regenerated cellulose membranes (Spectrum™ #2), precut in the form of discs, and with a molecular weight cut off of 12000-14000, were employed.

3. Vapor Transfer

Two devices were constructed for the measurement of solubility by transfer through the vapor phase. The first was a 50ml ground glass stoppered Erylenmeyer flask to which a side arm was added for introducing and sampling by syringe. A tight fitting Teflon™ stopper was fashioned to close the side arm. The volatile liquid was placed in a small test tube which fit within the flask. The aqueous solution was placed on the bottom of the flask. The flask was placed in a temperature-controlled water bath

covered by a cork which allowed the air above the water to attain the same temperature as the bath. The whole system was placed on a magnetic stir plate so that the aqueous solution could be agitated. The flask method was shown to be useful in studies against the dialysis method.

Some design improvements were implemented to remove the need for a moveable test tube, the need for grease on the stopper, and to allow for the sampling of more than one solution. An all glass (Pyrex) six-port dialysis vapor transfer apparatus was constructed. Six test tubes were connected via a common manifold above them. On the top side of the manifold, above each tube, were glass capillaries through which samples were delivered and removed via syringe. Capped Teflon™ sleeves were constructed to fit tightly over the capillaries for stoppering. No weight loss was detected 48 hours after 9.1 grams of water and benzene were introduced to the apparatus. For solubility studies the cell was placed in a water bath and shaken horizontally on a moveable platform.

4. Spectrophotometers

The Varian 2200 UV-Vis spectrophotometer was used for all studies unless otherwise indicated. The Perkin Elmer 559 was used for some readings in solubilization capacity experiments. The Cary 14 recording

spectrophotometer and Cary 16 fixed wavelength spectrophotometer were used for partitioning studies of aromatics between decane and water. All spectrophotometers were equipped with units to regulate the cell compartment temperature to within ± 0.1°C. Capped cells were used for all studies.

C. METHODS:

I. Surface and Interfacial Tension Measurements

Surface tension and interfacial tension measurements were performed using the drop volume technique. An Agla ™ syringe with a tip ground so as to produce a flat unbevelled surface was connected to a micrometer and fitted to a thermostatted container. This apparatus (70) allowed for the measurement of interfacial tensions by the falling drop or rising drop methods. The surface or interfacial tension, γ, is related to the drop volume,V, by equation (2.1)

$$\gamma = \frac{V(\Delta\rho)gf}{r} \qquad (2.1)$$

where $\Delta\rho$ is the difference between the densities of the two phases

studied,

g is the acceleration due to gravity,

r is the radius of the syringe tip, and,

f is a function of r and $V^{1/3}$ and corrects for the deviation from sphericity of the drop formed on the syringe tip.

The function f was interpolated from the tables of Lando and Oakley, (73). The radius of the syringe tip was determined using literature values for the surface tensions of water and decane in equation (2.1). Each value of surface tension reported is a mean of ten drops. Each value of interfacial tension reported is a mean of at least two drops. Phases were preequilibrated for at least one day prior to reading the interfacial tensions.

Based on repeat measurements taken during the same experiment and in different experiments, the surface and interfacial tensions were found to be generally reproducible to within ± 0.1 dyne/cm.

Density was measured using one ml or two ml capillary pycnometers. The method described by Bauer and Levin (74) was employed. The pycnometers were filled at room temperature, covered, and allowed to equilibrate in a 25°C water bath. After about 15 minutes in the bath, they

were removed and the capillaries inserted. They were returned to the bath for a few more minutes and then dried and weighed. The pycnometers were calibrated with double-distilled water.

2. Solubility Determinations

a. Solids: The solid was placed on one side of a 500Å diameter pore size polycarbonate membrane in a Teflon™ dialysis cell. Using a syringe the surfactant solution was placed on each side of the membrane. The cells were placed in a holder and connected to a motor which provided constant rotation. The cells were placed in a thermostatted waterbath and sampled from the bath.

b. Liquids by dialysis Stainless steel dialysis cells were constructed for measurement of the solubilization of the liquid aromatics in aqueous surfactant solutions. Cellulose membranes with a molecular weight cut off of I2000-14000 were employed. The membranes were treated to remove sulfur and heavy metals and allowed to soak overnight prior to use. The organic liquid, previously saturated with water, was placed on one side of the membrane and an aqueous surfactant solution placed on the other side. The cells were filled so that no part of the membrane could dry out. The cells were placed in a water bath until the time of sampling.

In order to estimate the amount of time necessary to achieve saturation, the rate of transfer was determined by measuring the amount of solubilization in the aqueous phase as a function of time. Fick's law for the transport through water-filled porous membranes in which no micelles are present and into a micellar solution gives:

$$\frac{dC_T}{d_t} = \frac{DA}{Vl} (C_{sf} - C_f) \qquad (2.2)$$

where C_T is the total concentration of solubilizate in solution at time t,

C_f is the free (non-micellized) solubilizate in solution at time t,

C_{sf} is the solubility of the solubilizate in water, (the continuous phase),

D is the diffusion coefficient of the solubilizate in water,

A is the area available for transport,

V is the volume of aqueous solution, and

l is the thickness of the membrane.

Assuming that the ratio of solubilizate in the micelle to that in free solution is constant up to saturation, integration yields

$$\frac{DA}{Vl} = \frac{(l + k)\ \ln(1/1-x)}{t} \qquad (2.3)$$

where, $K = \frac{\text{moles of micellized solute /l solution}}{\text{moles of free solute/l solution}}$

and x is the degree of under saturation, $(C_s-C)/C_s$.

For any given solubilizate and membrane,m, the value on the right hand side of equation (2.3) is a constant. Its value can be determined from evaluation of the time to achieve a certain degree of saturation. It cannot be predicted since diffusivities through porous membranes and effective A and l parameters are not known precisely. The value of DA/Vl for benzene was $1.4h^{-1}$. The value of K was estimated from saturation studies by this or other methods. Using this constant, the time required to reach an appropriate degree of saturation was estimated. The kinetics indicated that one day was required to achieeve 99.9% saturation for benzene in 0.1M SDS solutions. Therefore, these samples were allowed to equilibrate for at least 48 hours. The time of equilibration for other liquids was determined by their K values.

c. Vapor transfer methods have been completely described by way of the description of the devices in the apparatus section.

d. Analysis: The samples were analyzed by removal of a portion of the aqueous solution with a syringe. This portion was placed into a mixture of water and 95% ethanol (1:4) containing an additional amount of 95% ethanol equal to four times the volume of the aqueous sample. In this way, the final solution was a 1:4 vol:vol mixture of water and 95% ethanol. A 1:4 mixture of water and 95% ethanol was used as a reference.

For the volatile compounds studied in this work such as benzene, toluene, and naphthalene special care was necessary to avoid loss due to evaporation from saturated aqueous solution. For example, at 20°C benzene has an Ostwald adsorption coefficient of 5.1 between saturated aqueous solution and vapor.(90) This means that at equilibrium about 20% of the benzene in the aqueous phase will escape into an equal volume of air. Contact with air was minimized through the use of syringes. The use of this alcohol/water mixture reduced the vapor pressure of these compounds in solution. Even in this mixture, transfer to the spectrophotometric cell by means of a 10ml gas-tight syringe improved precision considerably.

Sodium dodecyl sulfate and NaCl did not absorb in the UV or visible regions of interest. Sodium perfluorooctanote did absorb in the UV and a correction of approximately 2% was taken for its influence. All dilutions

were made by weight. Since the final dilution was a dilute solution of surfactant and solubilizate in the 1:4 water:95% ethanol mixture, the density of the pure mixture was used to convert weight to volume needed for use in Beer's Law calibration. For SDS the error of using the pure solution density was 0.2%, an order of magnitude lower than the overall error. For SPFO the apparent molar volume of the surfactant in the ethanol: water mixture was used to calculate the final volume.

3. Partition Coefficient Determinations

The partition coefficients of benzene, toluene and ethylbenzene between decane and water across the entire composition range were determined. Water, decane, and the aromatic compound were weighed into the spectrophometric cell and the cell was capped tightly with a Teflon™ stopper. Typically, the cell was then inverted 100 times and placed into a themostatted bath so that only the stopper was exposed. After about four hours the cell was again inverted 100 times. Twenty-four hours after the start of the experiment the aqueous phase of the sample was read in the Cary Model 14 or Cary Model 16 spectrophotometer against a water blank. In this way the sample was not exposed to air so that no loss of volatile aromatics occurred. The interface between organic and aqueous phases was

kept well above the light path of the spectrophotometer. Dilutions for Beer's Law calibrations were made by addition of the aromatic compound to a known large volume of water (250-500ml) via a calibrated syringe. The solutions were removed via syringe and placed into a spectrophotometric cell which was rapidly stoppered.

Since perfluorohexane is more dense than water, the partitioning of benzene between these liquids could not be measured by the above method. The liquids were weighed into capped culture tubes and shaken or vortexed. They were then allowed to separate in a water bath. The aqueous phase was sampled by syringe and placed into a 1/4 v/v 95% ethanol/water mixture and measured on the Varian 2200 spectrophotometer as described in the preceding section.

4. Measurement of Microenvironmental Polarity by Absorption Spectra

To surfactant solution or solvent in a spectrophotometric cell was introduced a μl quantity of test solubilizate. The absorbance in the region of interest was between 0.4 and 1.2. The cells were placed in the thermostatted cell compartments of the Varian 2200. The surfactant solution was used as the blank. A spectral band width of 0.2 nm was used in all cases except in SPFO where 0.1 nm was employed.

5. Cmc Determinations of Perfluorocarbons by UV Spectroscopy

Experiments performed in collaboration with Dr. R. Sharma and Mr. C. Chan.

A stock solution of the perfluorooctanoate salt of interest was diluted by weight with water. The samples were read in the Varian 2200 containing a thermostatted cell compartment. The absorbance of the perfluorinated salt was read at 205 nm.

6. Determination of the Dissociation Constant of Perfluprocarboxylic Acids

Experiments performed in collaboration with Dr. R. Sharma and Mr. C. Chan.

Solutions of perfluorocarboxylic acids in various concentrations of HCl were prepared by dilution of stock solutions. Samples were read on the Varian 2200 at 25°C. An HCl solution of the same concentration was used as the reference.

PARTITIONING OF AROMATIC COMPOUNDS BETWEEN ORGANIC LIQUIDS AND WATER

A. Introduction:

A complete understanding of the solubilization process at a fundamental level requires a knowledge of the interactions between the solubilizate and the hydrophobic chains of the micelle. A thermodynamic measure of this interaction is the activity coefficient. Mixtures of solubilizates with n-alkanes provide a good model for determining the interactions between the solubilizate and the hydrophobic chain of the micelle. Activity coefficients over the entire composition range are required, since the interactions between the solubilizate and the chains are a function of the solubilizate composition in the micelle.

Experimental determination of activity coefficients is required, since no predictive theory exists for the aromatic + alkane mixtures of interest here. (76) Vapor pressure measurements of such mixtures have been used by other workers to determine activity coefficients over the entire range of compositions (76-80). In the method used by these workers the total vapor pressure of the aromatic + alkane mixture was measured. The results are fitted to a polynomial to extract activity coefficients.(81) These results

may not be trustworthy for dilute solutions since polynomial fits are known to produce serious errors in extrapolation.

In the present study activity coefficients were determined from measurements of partition coefficients betwen alkane + aromatic mixtures and water. Unlike the total vapor pressure method, this procedure provides a direct measurement of the amount of aromatic in each phase of the system. Moreover, the presence of the aqueous phase in the partitioning method provides a closer model to the micellar system. Since micelles exist in an aqueous medium, solubilizates dissolved in micelles are in distribution equilibrium with the aqueous phase. Interactions of water with the solubilizate may influence its interactions with and partitioning into the organic or micellar phase. In the case of aromatics such effects may result in the formation of self-associated dimers (82) or hydrated forms arising from hydrogen bond interactions between aromatics and water.(83-86) Comparison of activity coefficients from partitioning data with those from liquid-vapor data can indicate any significant effects of water. The partition values are themselves useful numbers. They provide a basis of interaction between solubilizate, alkyl chain, and water upon which a model for micellar solubilization will be built.

The present study is an investigation of the partition coefficients between water and the organic phase for the mixtures decane + benzene, + toluene, + ethylbenzene, and perfluorohexane + benzene . The decane-water partition coefficients were measured across the entire composition range. The perfluorohexane-water partition coefficient for benzene was measured at one concentration.

A new method which prevented evaporation loss of the aromatics was used for the decane-water measurements. This was discussed in detail in the experimental section. Briefly, the organic liquids and water were weighed into a spectrophotometric cell. The two-phase system was shaken and allowed to separate. The cell was then transferred to the spectrophotometer for measurement of the aqueous phase concentration.

B. Results:

The distribution coefficients for the aromatic component of the binary mixtures of decane + benzene, + toluene, and + ethyl benzene are listed in Tables 3.1-3.3, and plotted against the mole fraction of aromatic in the organic phase in Figures 3.1-3.3. The values for the mole fraction of aromatic in each phase are given as well as the distribution coefficient

TABLE 3.1

Distribution Coefficients for Benzene Between n-Decane and Benzene Binary Mixtures and Water at 25°C

$X_{organic\ phase}$	$10^4\ X_{aqueous\ phase}$	$10^{-3}\ X_o/X_a$
0.1478	0.859	1.72
0.2482	1.39	1.79
0.5156	2.67	1.93
0.7025	3.32	2.12
1.00	4.32 (4.12 ref. 87,88) (4.21 ref. 90) (4.14 ref.89)	2.31

x = mole fraction benzene

Figure 3.1 Partition Coefficients, $x_{organic\ phase}/x_{aqueous\ phase}$, for benzene in binary mixture with decane plotted as a function of the mole fraction of benzene in the organic liquid.

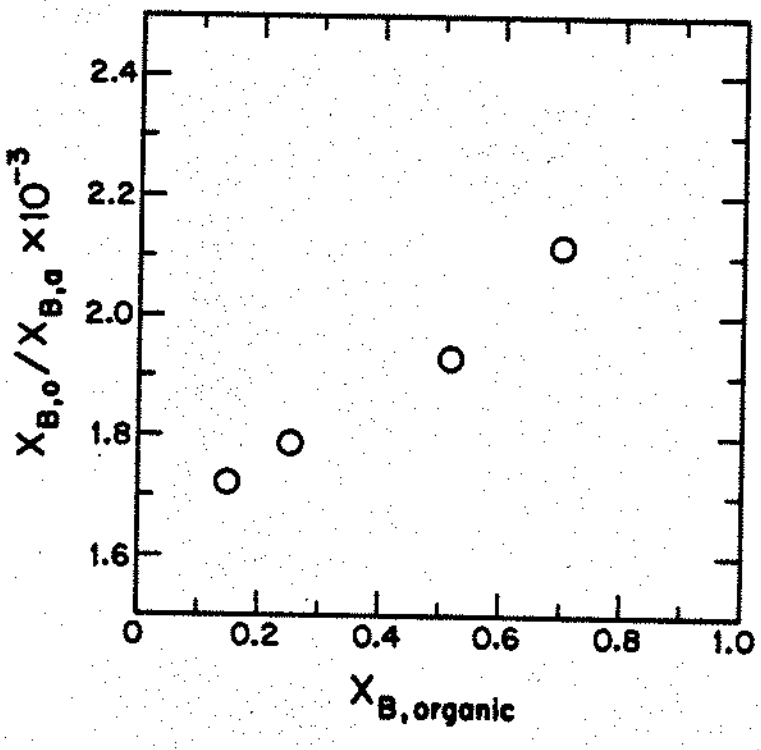

TABLE 3.2

Distribution Coefficients for Toluene Between n-Decane and Toluene Binary Mixtures and Water at 25°C

$X_{organic\ phase}$	$10^5\ X_{aqueous\ phase}$	$10^{-3}X_o/X_a$
0.1530	2.37	6.45
0.2739	4.07	6.77
0.4788	6.59	7.25
1.0000	12.29 (10.49 ref.87,88) (12.10 ref. 90) (12.28 ref.89)	8.13

x = mole fraction toluene

Figure 3.2 Partition Coefficients, $x_{organic\ phase}/x_{aqueous\ phase}$, for toluene in binary mixture with decane plotted as a function of the mole fraction of toluene in the organic liquid.

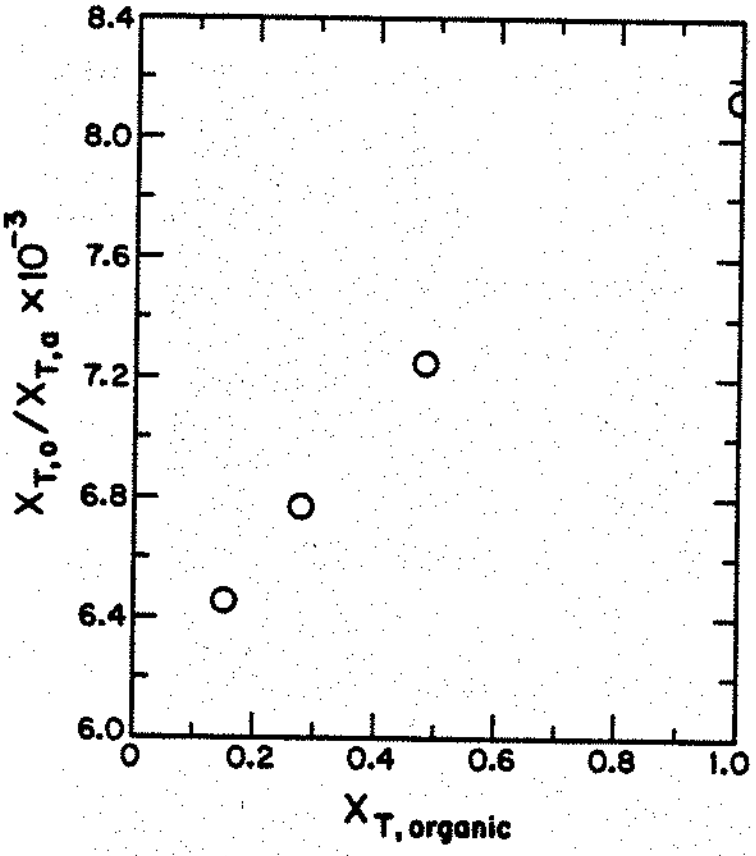

TABLE 3.3

Distribution Coefficients for Ethylbenzene Between n-Decane and Ethylbenzene Binary Mixtures and Water at 25°C

$X_{organic\ phase}$	$10^5 X_{aqueous\ phase}$	$10^{-4} X_o/X_a$
0.2524	1.12	2.26
0.4444	1.81	2.45
0.5933	2.34	2.53
0.7990	2.96	2.70

x = mole fraction ethylbenzene

Figure 3.3 Partition Coefficients, $x_{organic\ phase}/x_{aqueous\ phase}$, for ethylbenzene in binary mixture with decane plotted as a function of the mole fraction of ethylbenzene in the organic liquid.

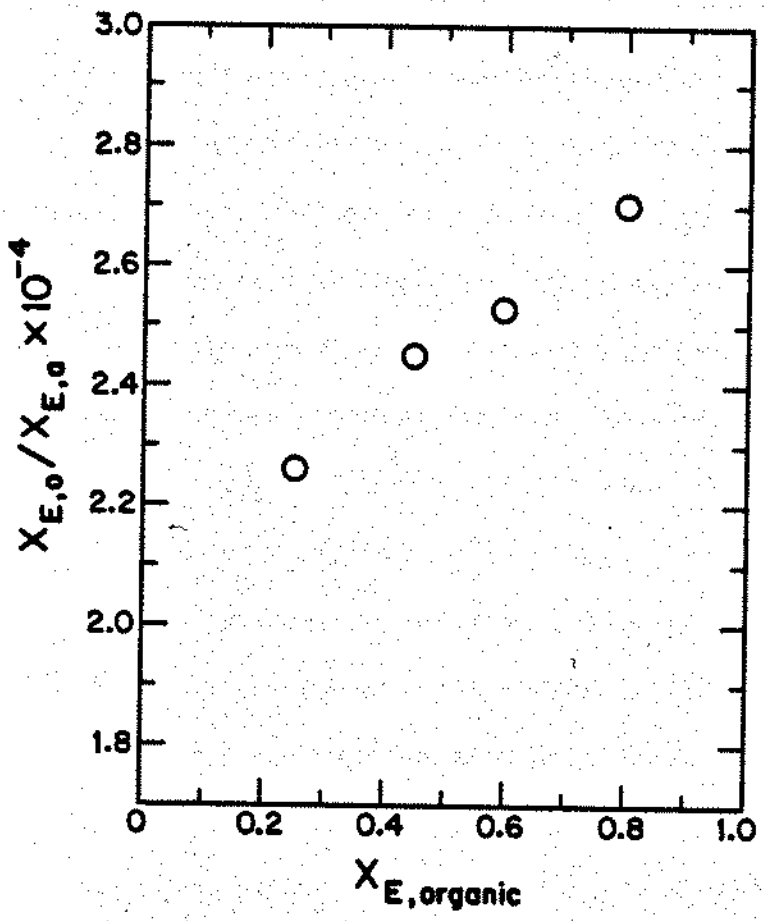

$x_{organic\ phase}/x_{aqueous\ phase}$. As expected the distribution coefficient increases as the amount of aromatic in the organic phase increases. Based upon deviations from smooth curves, the distribution coefficients are reliable to ± 2%.

The values for the aromatic in the aqueous phase at saturation are compared with literature values. For benzene the present value, 4.32×10^{-4} mole fraction, is 5% higher than an average from a compilation of literature values used by Abraham (87) and Mackay and Shiu.(88) The value is also 6% higher than that which was obtained by the dialysis and vapor transfer measurements to be described in Chapter 6. The deviation is likely due to the high absorbance value, 2.6, for this sample. Moreover, the instrument had not been calibrated in this region. Due to the uncertainty of this value, the average literature value 4.12×10^{-4} was used in calculation of the activity coefficient.

In the case of toluene, a mole fraction value, 12.29×10^{-4}, which is 9% higher than the literature average, was determined. This value is in good agreement, however, with the data of Bohon and Clausson,(89) and Ben-Naim. (90) The latter worker confirmed his value by two methods. Since there was no reason to doubt the experimental value found in the present work, it will be employed in further calculations.

For ethylbenzene a literature value was needed since the solubility of ethylbenzene in water had not been determined in this study. The value chosen was 3.60×10^{-5} mole fraction, which was also obtained by Ben-Naim (90) and Bohon and Claussen (89) and confirmed by two methods of Ben-Naim.(90) This value is higher than the literature average by about 25%. However, any lower value for ethylbenzene solubility would have given activity coefficients of ethylbenzene in decane which were significantly higher than in toluene.

The partitioning of benzene between perfluorohexane and water was also determined at between 0.05 and 0.06 mole fraction benzene in perfluoro- hexane. The value of 205 ± 20 was obtained for the ratio $X_{B,organic}/ X_{B,aqueous}$. This suggests an activity coefficient of about 11.4. Regular solution theory (91) predicts that the activity coefficient at infinite dilution is 5.2. The differences of these values indicate the extent of the deviation from regular solution behavior and the significant non-idealities of this system.

C. Discussion:

Determination of the activity coefficient from partitioning data

provides a measure of the nonidealities of interaction of the aromatics and alkanes. It also allows for comparison with theory and with results from vapor-liquid methods. Equation 3.1 introduces activity coefficients into the expression for the partition coefficient, K.

$$K = \frac{x_o f_o}{x_a f_a} = \frac{1}{x_{a,sat} f_{a,sat}} \qquad (3.1)$$

where, x is the mole fraction,

f is the activity coefficient,

subscripts o and a stand for organic and aqueous phase respectively, and subscript sat stands for saturation conditions.

Rearranging equation 3.1 gives equation 3.2.

$$f_o = \frac{x_a f_a}{x_o x_{a,sat} f_{a,sat}} \qquad (3.2)$$

If the activity coefficient in water is constant at all concentrations, then

$$f_a/f_{a,sat} = 1 \text{ and } f_o = \frac{x_a}{x_o x_{a,sat}} \qquad (3.3)$$

In this way the activity coefficient, f_o, can be determined from partition experiments.

Figure 3.4 is a plot of the activity coefficients of the benzene, toluene, and, ethylbenzene binary mixtures with decane as a function of the mole fraction of the aromatic component. Along with the values determined in this study, values calculated from regular solution theory using solubility parameters are shown for each of these systems. In addition the activity coefficients of benzene from the vapor-liquid experiments of Rubio, Renuncio, and Diaz Peña (79) for benzene + decane mixtures are presented. Since these workers fitted their data to empirical equations, a smooth curve results. Their actual experimental data ranged between 0.1 and 0.75 mole fraction of benzene in decane. Based upon uncertainties stated for the partition coefficients, the experimental activity coefficient values are reliable to ± 0.025.

The activity coefficients of toluene and ethylbenzene overlap within error as expected from the regular solution prediction. The values are slightly higher than regular solution calculations (91) but follow the regular solution trend, with slope tending toward zero at high aromatic composition. The nonideality of interaction between benzene and decane is

Figure 3.4 Activity Coefficients, f_o, of Benzene, Toluene and Ethylbenzene in binary mixtures with decane plotted as function of the mole fraction of aromatic compound in the organic mixture, x_o.

X Benzene, from Partitioning Data
O Toluene, from Partitioning Data
Δ Ethylbenzene, from Partitioning Data

Curve A Benzene from Vapor Pressure Data. Ref. 79
Curve B Benzene Solubility Parameter Theory
Curve C Toluene Solubility Parameter Theory
Curve D Ethylbenzene Solubility Parameter Theory

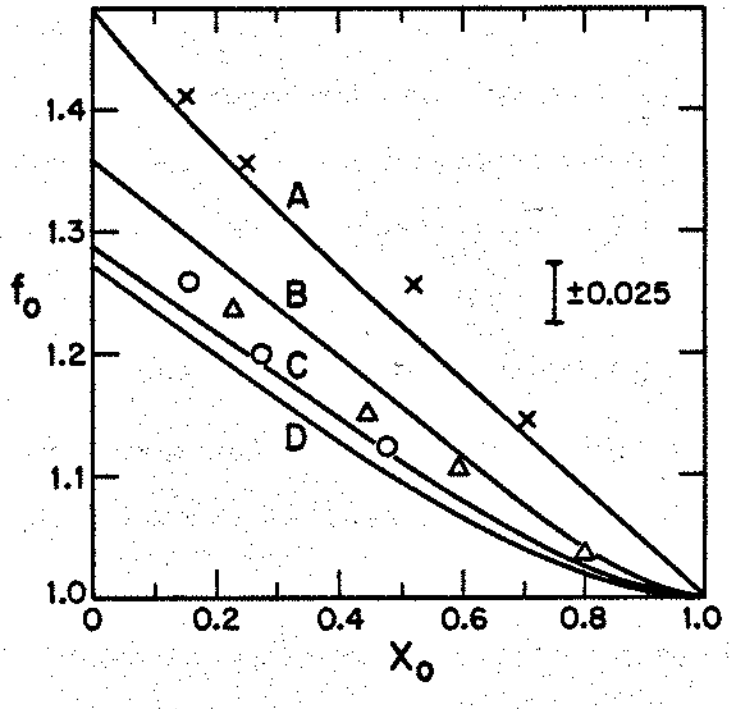
1.4
1.3
1.2
1.1
1.0
f_o
0
0.2
0.4
0.6
0.8
1.0
X_o
A
B
C
D
±0.025

much more pronounced. The activity coefficients are significantly higher than regular solution prediction, and do not follow the regular solution trend at high benzene mole fraction. The region over which benzene obeys Raoult's Law is much smaller than can be detected by these data. The region where toluene and ethylbenzene obey Raoult's Law may extend to 0.95 mole fraction as suggested by regular solution theory.

One further question regarding the calculation of the activity coefficient from these data is in regard to the constancy of f_a with concentration. Green and Frank (92) found no difference in the activity coefficient of benzene in water between that at 10% of saturation and saturation. Tucker and Christian,(82) however, noted a linear decrease in activity coefficient of about 3.9% at 35°C between infinite dilution and saturation. They attributed this to self-association of benzene in water. This effect increases the value of the calculated activity coefficient. The ΔH of the dimerization process has been stated by these workers to be relatively large and positive. Therefore, this effect will cause dimerization to occur to a lesser degree at 25°C than at 35°C. Taking these effects into consideration the calculated activity coefficients for benzene in decane may be somewhat higher than those displayed in Figure 3.1. They

are expected, however, to be within the ± 0.025 range of the value calculated from partitioning data.

Activity coefficients determined from partitioning data and from vapor pressure measurements (79) are seen to agree. This indicates that water does not significantly influence the interactions between benzene and decane. Partitioning of aromatics between alkanes and water can, therefore, be calculated from vapor-liquid data. This permits use of available vapor-liquid data in the micelle solubilization models to be discussed.

In summary, this work confirms the vapor pressure data on benzene + decane mixtures. This mixture is significantly more non-ideal than regular solution predictions. Toluene or ethylbenzene in mixtures with decane behave much more like regular solutions. The presence of the aqueous phase does not have a significant influence on the nonidealities of aromatics + hydrocarbon alkane mixtures.

SURFACE PROPERTIES OF BINARY MIXTURES OF BENZENE AND SOME ALKYLBENZENES AND POLYCYCLIC AROMATICS WITH DECANE AT THE AIR-LIQUID AND WATER-LIQUID INTERFACES

A. Introduction

Aside from its intrinsic interest, a knowledge of the adsorption of molecules to a hydrocarbon-water interface is required in terms of the micellar solubilization model described in the introduction.(50,52) The two-state model is based upon the adsorption of molecules to the micelle-water interface. An initial assessment of the magnitude of that adsorption is obtained from evaluation of adsorption to the hydrocarbon-water interface. In order for meaningful conclusions to be drawn from tests of models of molecular interactions, such as solubilization, the molecules employed in such tests must have the simpliest possible molecular structure. A series of molecules which varies in a continuous manner with respect to a certain feature of molecular structure, such as the chain length of an alkyl group, allows for relative comparisons and facilitates interpolation and extrapolation of effects. Furthermore, as micellar solubilization has implications for the interactions of molecules with biological membranes, the study of a

simple molecular series which is at the same time of biological importance would certainly be of interest to several fields of research.

The compounds benzene, toluene, ethylbenzene, butylbenzene, p-di-tert-butylbenzene, naphthalene, phenanthrene, pyrene, and 1-dodecene were chosen for the study of interfacial tensions in binary mixtures with decane against water. From these data adsorption of these compounds to the decane-water interface was determined. These compounds provide a series of simple molecules which also hold biological interest. The location, distribution, and orientation of these molecules in biological membranes may be related to their known or postulated carcinogenic potential.(66) This series also provides a basis for extension of insights gained here to other more complex molecules, such as drugs containing aromatic moieties, and more potent carcinogens, such as benzpyrene.(66)

Evaluation of the adsorption of a molecule to a hydrocarbon-water interface requires the determination of the derivative of the interfacial tension with respect to the thermodynamic activity of that molecule in solution.(4,93) Assessment of the surface excess, Γ, by this method may not be feasible in many cases. Therefore, the usefulness of existing

mixture theories for predicting Γ should also be examined.(94,100) Since such theories are based upon the mixing of two components, results from the surface tensions against air of binary mixtures provides a test of these theories. The surface tensions of the binary mixtures listed above were also measured. The perturbing effects of water on the interfacial properties of binary mixtures can be analyzed by comparison with surface tension results. Mixture theories will be discussed further in the discussion section at the points where they are employed.

The effect of water on the interactions at the interface is expected to be significant in the systems studied, since aromatic compounds are known to be hydrogen bond acceptors. (83-86) The hydrogen bonding of phenol to hexamethylbenzene was found to have a $\Delta G = 0.03$ kcal mol^{-1}, $\Delta H = -1.7 \pm 0.5$ kcal mol^{-1}, and $\Delta S = -5.5 \pm 1.7$ e.u. at 25°C in carbon tetrachloride.(86) Monte Carlo simulations and calculation of quantum mechanical potentials suggest that the energy minimum of the interaction of a water molecule with a benzene molecule is obtained when water is tilted slightly away from the symmetry axis of benzene with the hydrogens of water pointing toward the benzene molecule.(85) The most favorable orientation is that of water hydrogen bonding with the π system

of benzene. This specific interaction between the aromatic ring and water can be expected to influence the forces acting across the interface. Surface tension data provide a comparative system where these specific effects are absent. An important question raised in this work is the degree to which additional aromatic groups influence this specific interaction with water.

In any analysis of surface effects it must be understood that surface thermodynamic properties arise from the asymmetric forces upon molecules at the surface, as opposed to the bulk. While a molecule in the bulk has other molecules surrounding it in all directions, those at the surface are influenced by significantly fewer neighboring molecules. (4, 99,101) Therefore, all properties, such as the activity coefficient, which are dependent upon intermolecular interactions (91) are expected to be different at the surface than in the bulk. In the case of the activity coefficient, which will be treated in detail in this chapter, the lower number of interactions at the surface is expected to reduce its value. Indeed models for the surface often consider it as ideal.(97,100,102,103) At a liquid-liquid interface the molecules are similarly influenced by an asymmetric distribution of forces, although they are surrounded by other

molecules.(4,101,104,105) The forces acting across the interface, that is, between molecules of the different phases, distinguishes the liquid-liquid interface from the vapor-liquid surface. In the discussion to follow, the interface will be considered as a monolayer of the organic mixture in question against water. The influence of water on the interactions occurring in the organic monolayer will be examined.

B. Scope and Aim

This chapter reports the results of surface tension measurements against air, and interfacial tension measurements against water, of binary mixtures of decane plus one of several aromatic compounds or an olefin. The compounds chosen for study are pictured in Figure 4.1. The hydrocarbon compounds were chosen for their simplicity of molecular character and their biological importance as outined in the introduction to this chapter. They include the series benzene, toluene, ethylbenzene, and butylbenzene through which the effects of increasing alkyl chain length and molecular asymmetry have been investigated. The data on the first three compounds of this series has been reported in the master's thesis prepared by this investigator.(59) Further analysis of the surface and interfacial tension results for these compounds is presented here. P-di-tert-butylbenzene

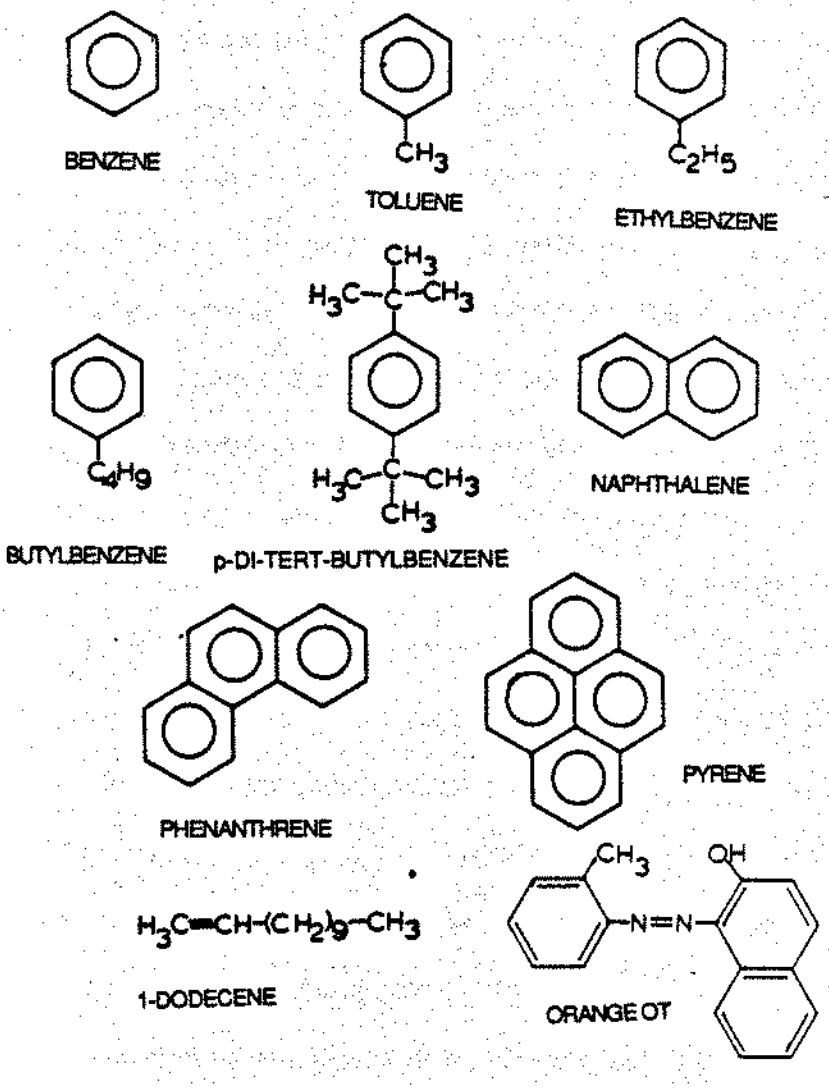

Figure 4.1 Structures of compounds studied

contains two bulky t-butyl groups, and in contrast to the series above this molecule is symmetrical with respect to the positioning of alkyl groups on the ring. The molecules benzene, naphthalene, phenanthrene, and pyrene provide a series of planar molecules with an increasing number of double bonds in the form of aromatic rings. The degree to which hydrogen bonding of aromatics with water across interfaces is influenced by the extent of aromaticity is examined by this series. 1- Dodecene was studied to investigate the effect of a single double bond on a long chain hydrophobic molecule.

It is the aim of this chapter to present and analyze the results of surface and interfacial tension measurements in an attempt to provide greater insight into the nature of the interactions occurring at and across interfaces. Theories of surface tension of mixtures are employed to test their usefulness in describing these systems. Deviations from theory and parameters derived from theory are analyzed in terms of the information they can provide about the interface. A new method for determining the activity coefficients of molecules at the surface based on a monolayer theory is described. The work of adhesion was also determined for these

mixtures and analyzed with respect to theories of interaction across interfaces.

C. Results

The surface and interfacial tension results for n-butylbenzene, p-di-tert-butylbenzene, naphthalene, phenanthrene, pyrene, and 1-dodecene are displayed in Tables 4.1-4.1l and Figures 4.2-4.12. Based upon replicate measurements taken during the same experiment and in different experiments, the surface and interfacial tensions were found to be generally reproducible to within ± 0.1 dyne cm^{-1}. Deviations around a smooth curve were usually within this range.

For use in modelling micellar solubilization, the interfacial tensions of two other binary systems against water were also measured. Table 4.12 and Figure 4.13 report the interfacial tensions of binary mixtures of benzene + perfluorohexane against water. The initial slope of 107 dynes cm^{-1} compared to 33 dynes cm^{-1} for the benzene + n-decane system reflects the nonidealities of mixing of benzene and the perfluoroalkane, as also noted from partitioning work reported in the preceding chapter. Table 4.13 and Figure 4.14 report the interfacial tensions of Orange OT (also pictured in Figure 4.1) in decane against water. The initial slope of 2150

TABLE 4.1

Surface Tensions of n-Butylbenzene + n-Decane Mixtures Against Air at 25°C

Mole Fraction n-Butylbenzene	Surface Tension/dynes cm^{-1}
0.00	23.37 (23.38, ref. 110)
0.0105	23.42
0.0255	23.54
0.0505	23.54
0.0755	23.61
0.150	23.73
0.227	23.99
0.400	24.72
0.599	25.96
0.800	27.20
1.0	28.58 (28.72 ref.(110))

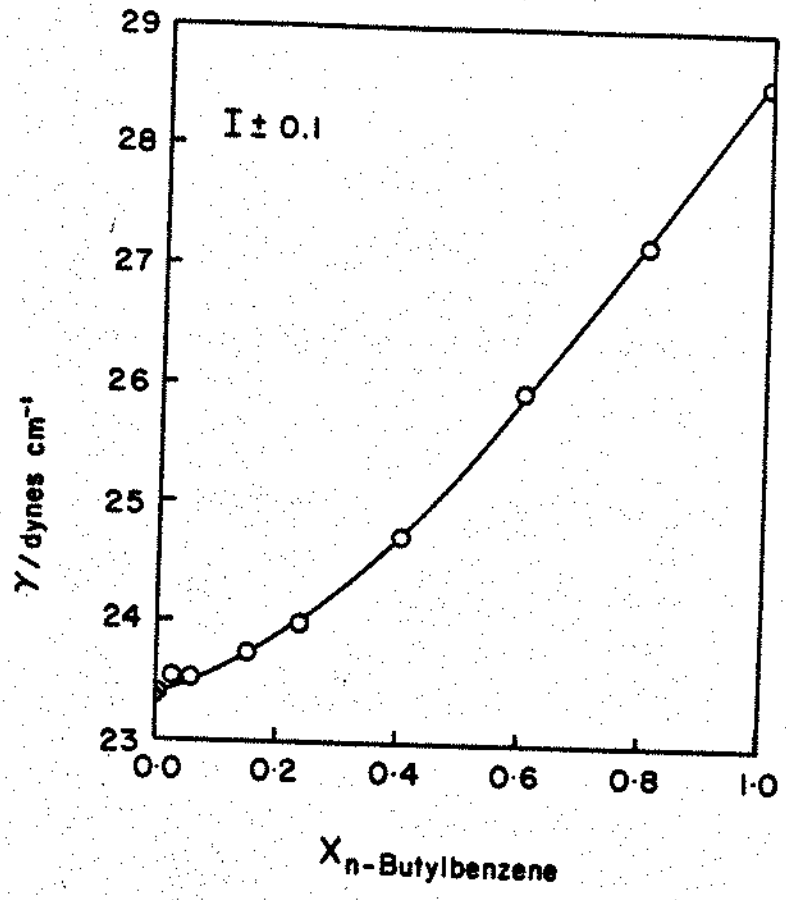

Figure 4.2. Surface tensions of n-butylbenzene + n-decane mixtures at 25°C plotted as a function of the mole fraction of n-butylbenzene.

TABLE 4.2

Surface Tensions of Naphthalene + n-Decane Mixtures Against Air at 25°C

Mole Fraction Naphthalene	Surface Tension/dynes cm^{-1}
0.00	23.38
0.0387	23.52
0.763	23.75
0.121	24.06
0.154	24.24

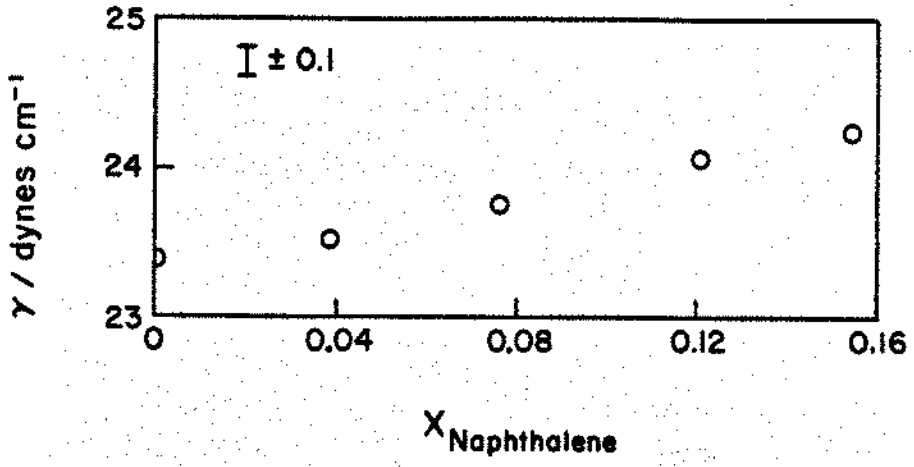

Figure 4.3 Surface tensions of naphthalene + n-decane mixtures at 25°C plotted as a function of the mole fraction of naphthalene.

TABLE 4.3

Surface Tensions of Phenanthrene + n-Decane Mixtures Against Air at 25°C

Mole Fraction Phenanthrene	Surface Tension/dynes cm^{-1}
0.00	23.37
0.0203	23.69
0.310	23.74
0.0505	23.85

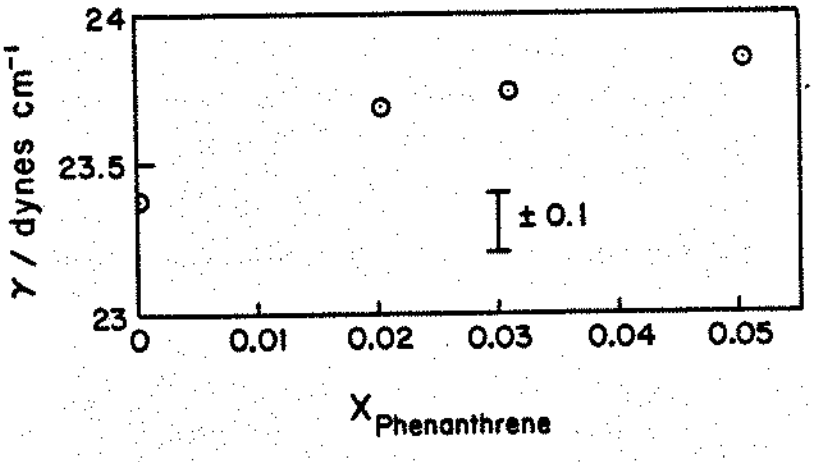

Figure 4.4 Surface tensions of phenanthrene + n-decane mixtures at 25°C plotted as a function of the mole fraction of phenanthrene.

Table 4.4

Surface Tensions of p-di-tert-Butylbenzene + n-Decane Mixtures Aganist Air at 25°C

Mole Fraction p-di-tert-Butylbenzene	Surface Tension/dynes cm^{-1}
0.00	23.38
0.0388	23.52
0.0685	23.58
0.0988	23.72
0.149	23.86

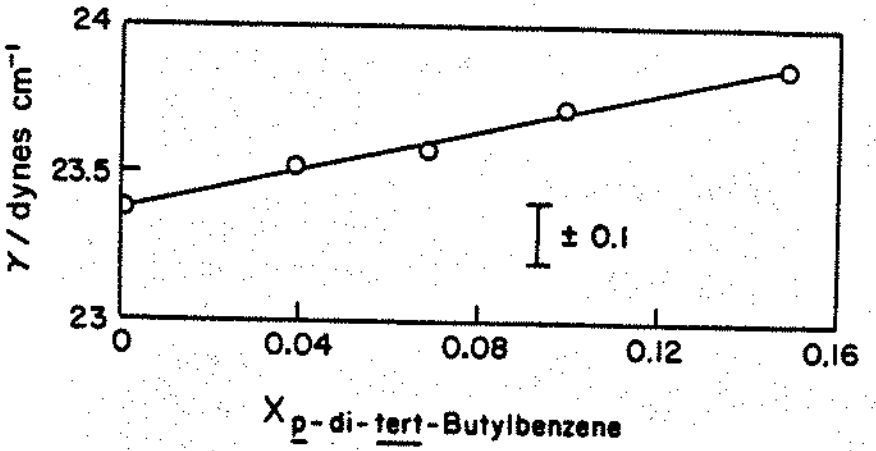

Figure 4.5 Surface tensions of p-di-tert-butylbenzene + n-decane mixtures at 25°C plotted as a function of the mole fraction of p-di-tert-butylbenzene.

TABLE 4.5

Surface Tensions of 1-Dodecene to n-Decane Mixtures Against Air at 25°C

Mole Fraction 1-Dodecene	Surface Tension/dynes cm^{-1}
0.00	23.37
0.190	23.76
0.396	24.10
0.594	24.47
0.796	24.89
1.00	25.25 (25.15 ref. (110))

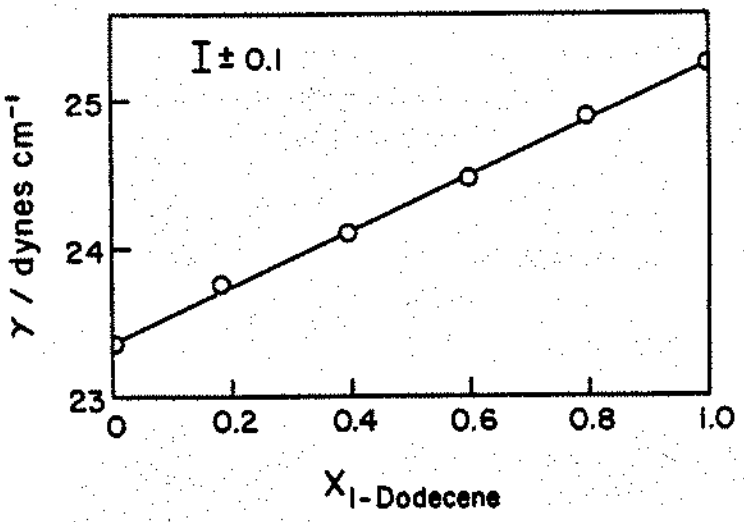

Figure 4.6 Surface tensions of 1-docecene + n-decane mixtures at 25°C plotted as a function of the mole fraction of 1-dodecene.

TABLE 4.6

Interfacial Tensions of n-Butylbenzene + n-Decane Mixtures Against Water at 25°C

Mole Fraction n-Butylbenzene	Interfacial Tension/dynes cm^{-1}
0.00	51.60 (51.7, ref.(58))
0.0105	51.26 (50.8, ref.(114))
0.0255	51.17
0.0505	50.64
0.0755	50.27
0.101	49.50
0.150	48.76
0.227	47.59
0.400	45.60
0.599	43.58
0.800	41.96
1.00	40.25 (39.6, ref (113))

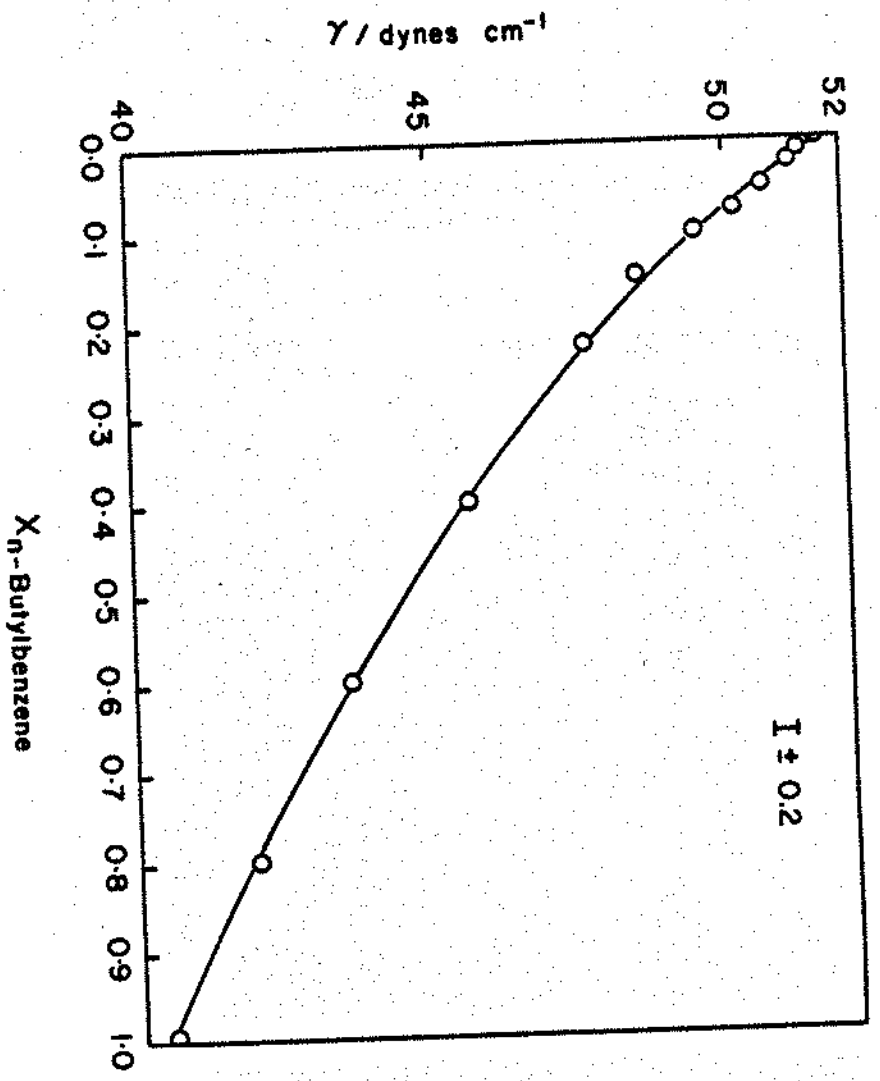

Figure 4.7 Interfacial tensions of n-butylbenzene + n-decane mixtures against water at 25°C plotted as a function of the mole fraction of benzene in the organic phase.

TABLE 4.7

Interfacial Tensions of Naphthalene + n-Decane Mixtures Against Water at 25°C

Mole Fraction Naphthalene	Interfacial Tension /dynes cm^{-1}
0.00	51.60
0.0155	50.95
0.0387	49.90
0.0763	48.80
0.121	47.28
0.154	46.34

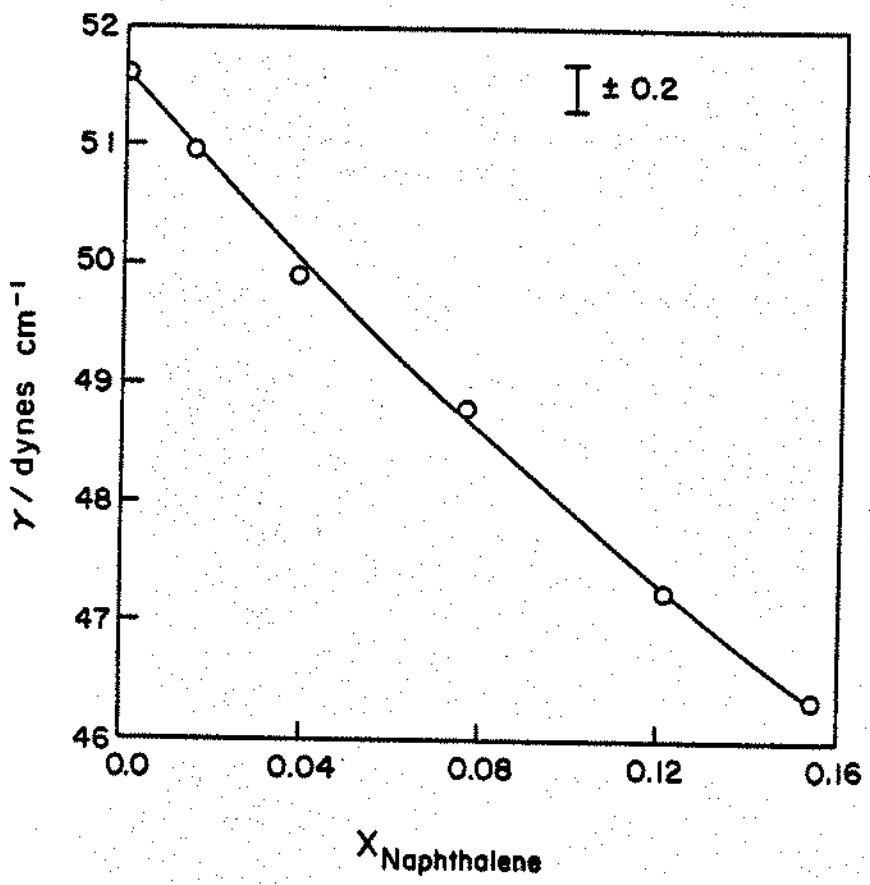

Figure 4.8 Interfacial tensions of naphthalene + n-decane mixtures against water at 25°C plotted as a function of the mole fraction of naphthalene in the organic phase.

TABLE 4.8

Interfacial Tensions of Phenanthrene + n-Decane Mixtures Against Water at 25°C

Mole Fraction Phenanthrene	Interfacial Tension /dynes cm^{-1}
0.00	51.60
0.0203	50.32
0.0310	49.83
0.0505	48.82

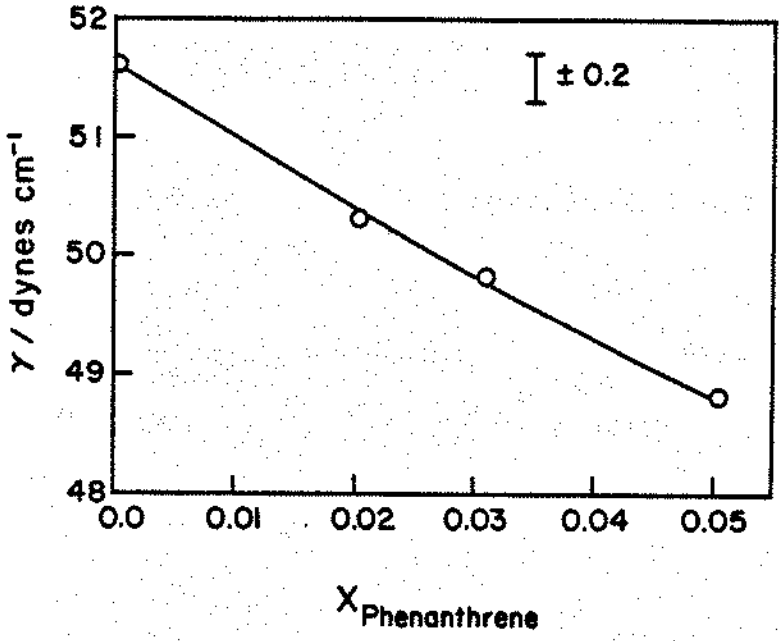

Figure 4.9 Interfacial tensions of phenanthrene + n-decane mixtures against water at 25°C plotted as a function of the mole fraction of phenanthrene in the organic phase.

TABLE 4.9

Interfacial Tensions of Pyrene + n-Decane Mixtures Against Water at 25°C

Mole Fraction Pyrene	Interfacial Tension /dynes cm^{-1}
0.00	51.60
0.0051	51.29
0.0102	50.86
0.0153	50.51

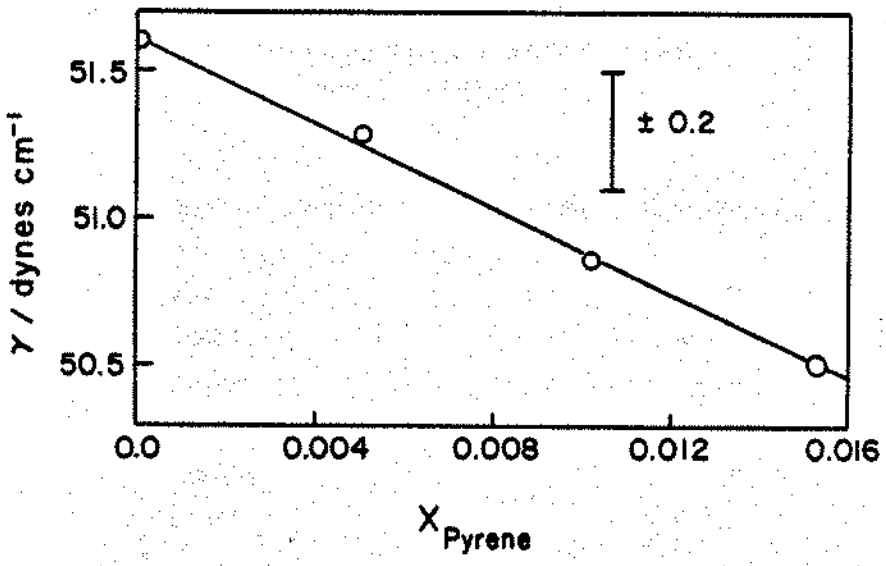

Figure 4.10 Interfacial tensions of pyrene + n-decane mixtures against water at 25°C plotted as a function of the mole fraction of pyrene in the organic phase.

TABLE 4.10

Interfacial Tensions of p-di-tert-Butylbenzene + n-Decane Mixtures Against Water at 25°C

Mole Fraction p-di-tert-Butylbenzene	Interfacial Tension /dynes cm^{-1}
0.00	51.60
0.00970	51.46
0.0383	50.56
0.0671	50.03
0.0970	49.38
0.149	48.40

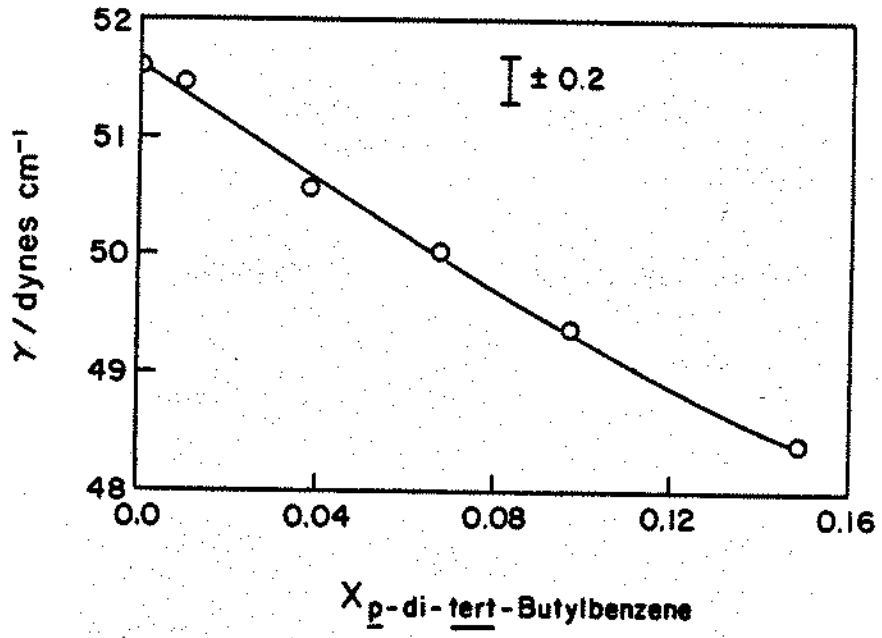

Figure 4.11 Interfacial tensions of p-di-tert-butylbenzene + n-decane mixtures against water at 25°C plotted as a function of the mole fraction of p-di-tert-butylbenzene in the organic phase.

TABLE 4.11

Interfacial Tensions of 1-Dodecene + n-Decane Mixtures
Against Water at 25°C

Mole Fraction 1-Dodecene	Interfacial Tension /dynes cm^{-1}
0.00	51.60
0.0165	51.46
0.0429	51.31
0.100	51.15
0.190	50.66
0.396	49.92
0.594	49.34
0.796	48.92
1.00	48.47

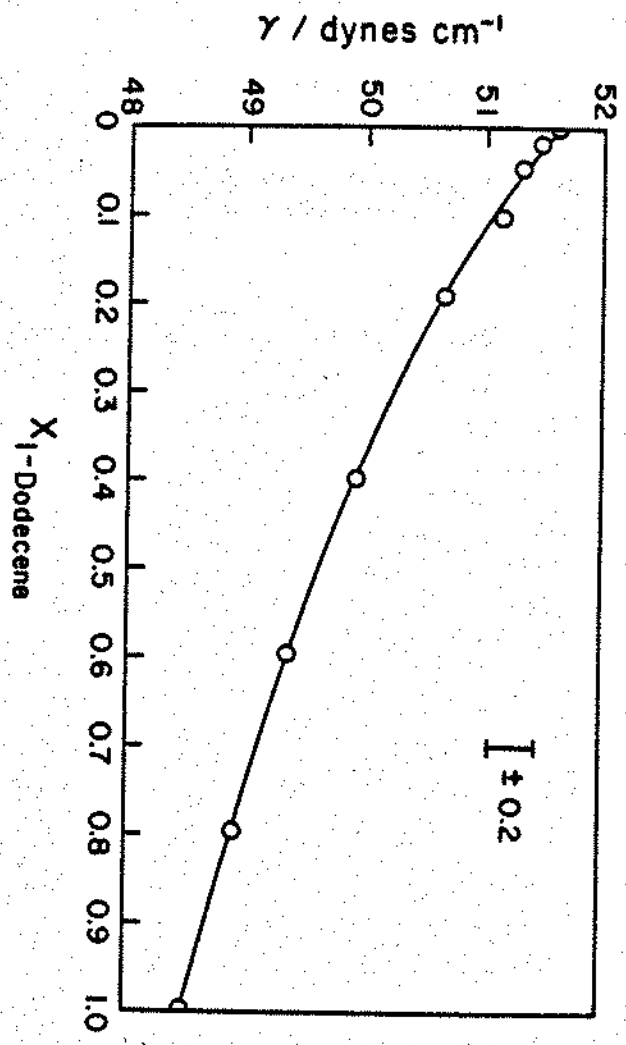

Figure 4.12 Interfacial tensions of 1-dodecene + n-decane mixtures against water at 25°C plotted as a function of the mole fraction of 1-dodecene in the organic phase.

TABLE 4.12

Interfacial Tensions of Benzene + Perfluoro-n-hexane Mixtures Against Water at 25°C

Mole Fraction Benzene	Interfacial Tension /dynes cm^{-1}
0.00	57.35 (56.45, ref (100))
0.00646	56.68
0.0180	55.36
0.0241	54.90
0.0774	48.72

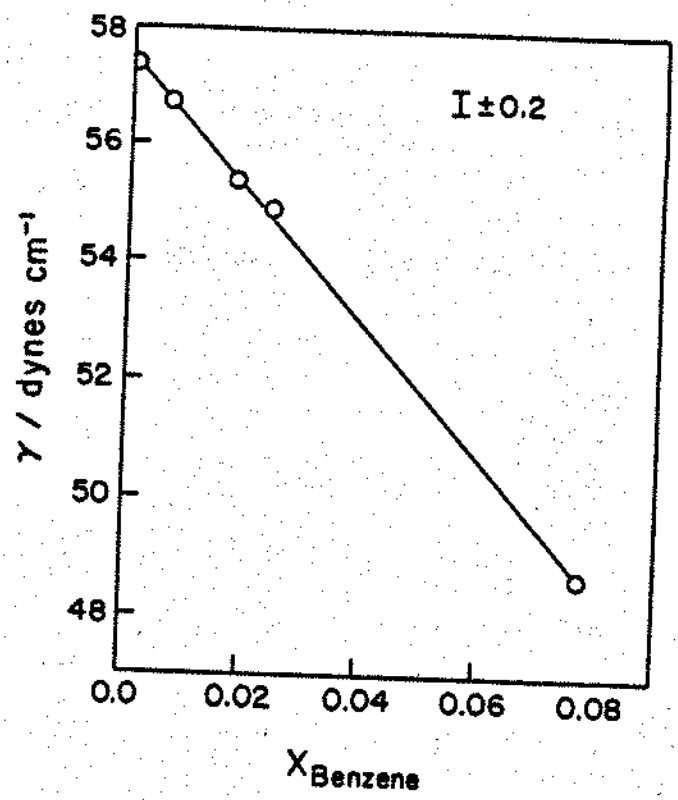

Figure 4.13 Interfacial tensions of benzene + perfluoro-n-hexane mixtures against water at 25°C plotted as a function of the mole fraction of benzene in the organic phase.

TABLE 4.13

Interfacial Tensions of Orange OT + n-Decane Mixtures
Aganist Water at 25°C

Mole Fraction Orange OT(10^4)	Interfacial Tension /dynes cm^{-1}
0.00	51.70
1.45	51.37
4.30	50.76
8.01	49.94
8.79	49.82
11.60	48.87
15.2	48.09
20.0	47.04
24.0	44.37

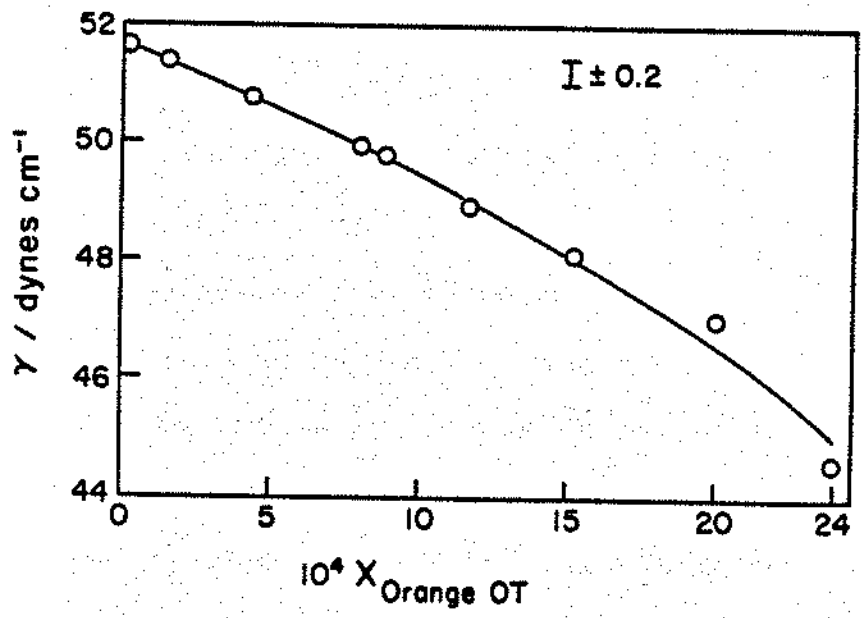

Figure 4.14 Interfacial tensions of Orange OT + n-decane mixtures against water at 25°C plotted as a function of the mole fraction of Orange OT in the organic phase.

dynes cm^{-1} reflects the effect of an -OH group on a molecule containing three aromatic rings and an azo group.

D. Discussion

1. Surface and Interfacial Tension of Binary Mixtures of Liquids

a. Background

In this section the results of surface and interfacial tension measurements of binary mixtures of the liquids benzene, toluene, ethylbenzene, butylbenzene, and 1-dodecene with decane are analyzed. Past work on the analysis of binary mixtures of liquids has largely centered on the development of descriptive models and equations. Liquids lend themselves to such analysis since the tensions of mixtures can be described as some empirically (106) or theoretically (94-100) derived average of the experimentally determinable pure liquid tensions. Through the use of an existing model (98,99), which will be shown to describe air-liquid surface tensions data for mixtures well,(59) the alteration in the surface brought about by the presence of water is evaluated.

As described in the introduction to this chapter, the molecules at the surface have fewer nearest neighbors with which to interact.(99,101)

They are therefore expected to behave in a more nearly ideal manner. The extent to which this effect is reflected by theory underscores the reasonableness of the theory's predictions.

The theory which will be employed here was developed by Prigogine and Marechal (98,99) on the basis of Flory-Huggins mixing of molecules of unequal size. According to the theory the surface is a monolayer of molecules on a lattice. The smaller of the two molecules occupies one site on the lattice. The larger molecule occupies r sites, where r is a ratio of the sizes of the molecules and is usually taken as the ratio of molar volumes. Those molecules which occupy more than one site on the lattice are assumed to lie parallel to the surface. For this reason the model is often referred to as the parallel layer model. For non-athermal solutions the resulting equations require estimates of lattice coordination numbers. Gaines (102,103,107) simplified the model by assuming the surface to behave ideally. The resulting expression for the surface tension, σ, for a binary mixture is given by equations 4.1a and 4.1b.

$$\sigma = \sigma_2 \underset{ar}{kT} [\ln (\Phi_2^s/\Phi_2^b) + (r-1)(\Phi_2^s - \Phi_2^b)] - \beta(\Phi_1)^2 \qquad (4.1a)$$

$$\sigma = \sigma_1 + \frac{kT}{a}\left[\ln\left(\Phi_1^{s}/\Phi_1^{b}\right) + \frac{(r-1)}{r}\left(\Phi_1^{b} - \Phi_1^{s}\right)\right] - \beta(\Phi_2)^2/a \qquad (4.1b)$$

where σ_1 is the surface tension of pure component 1,

σ_2 is the surface tension of pure component 2,

a is the area of the molecule of smaller size, component one,

r is the ratio of the molar volume of components one and two, V_2/V_1,

Φ_1 is the volume fraction of component I,

β is the interaction parameter,

and superscripts s and b stand for surface and bulk respectivly.

These equations can be solved numerically for Φ_1^{s} at any given value of β. The value of β which is consistent with a known value of σ can also be determined. The value of a is not known. It is usually ascribed on the basis of some convention. A typical convention is the use of $V^{2/3} N^{1/3}$, where V is the molar volume of component one, and N is Avogadro's number.

Gaines has commented that, since surface properties reflect

differences between the surface and bulk, β may be related to a differential or excess interaction energy between the surface and bulk.(102,103) He also suggested that β absorbs deviations due to effects not included in lattice theories, such as volume changes on mixing. On this basis, if surface interactions matched bulk interactions, β would be zero. The expected result is a value of β somewhat smaller than that of an interaction parameter derived on the basis of bulk interactions. Such a result would reflect the incomplete cancellation of bulk interactions by the more nearly ideal surface. Gaines found that equation 4.1 could describe the surface tension of mixtures of polydimethylsiloxanes and toluene or tetrachloroethylene (102) over the entire composition range using β as an adjustable parameter. He also applied equation 4.1 to the data of Schmidt, Randall, and Clever (108) on the surface tensions of benzene + hexane and benzene + dodecane binary mixtures. (103) In these systems a single β value in equation 4.1 described the data to within 0.2 dynes cm^{-1}. Edmonds and McLure also employed equation 4.1 to describe the surface tensions of n-alkane - dimethyl siloxane mixtures. (109) They found that their data could be fitted using one value for β.

b. Surface Tension Results.

In the master's thesis prepared by this investigator (59), surface tensions against air and interfacial tensions against water for binary mixtures of benzene, toluene, and ethylbenzene with decane across the entire composition range were reported. It was found that the surface tensions could be described by a single value of β. The present work extends these considerations to butylbenzene and 1-dodecene. It also investigates an interaction parameter, χ, which is based upon Flory-Huggins mixing as a suitable bulk parameter for comparison with β/kT.

Table 4.14 lists the values of β (in units of kT) found in the master's study along with the values for n-butylbenzene + decane and 1-dodecane + decane mixtures determined recently. Also tabulated are the values of β/kT determined by Gaines (103) from the data of Schmidt et al (108) on benzene + hexane and benzene + dodecane mixtures. The benzene + decane value lies between the benzene + hexane and benzene + dodecane values as expected.

In order to evaluate the reasonableness of these values of β/kT, the values of bulk interaction parameters for these systems are also

TABLE 4.14

Comparison of the Interaction Parameters χ and $Inf/(1-\Phi_1)^2$ Calculated From Experimental Values of the Activity Coefficient, V_1A_{12}/RT, Calculated From Regular Solution Theory, and β/kT From Air-Liquid Surface Tension Data

System	β/kT	χ	$Inf/(1-\Phi_1)^2$	V_1A_{12}/RT
Benzene + Decane	0.21	0.61-0.76[a]	0.39-0.59[a]	0.30
		0.63-0.76[b]	0.40-0.59[b]	
Toluene + Decane	0.14	0.42-0.38[b]	0.28-0.26[b]	0.25
Ethylbenzene + Decane	0.13	0.38-0.48[b]	0.30-0.41[b]	0.24
Butylbenzene+ Decane	0.06			0.18
1-Dodecene + Decane	0.002			0.01[c]
Benzene + Hexane	0.12[d]	0.58[e]	0.52[e]	0.55
		0.59-0.52[f]	0.47-0.53[f]	
Benzene + Dodecane	0.28[d]	0.6-0.78[g]	0.3-0.56[g]	0.28

a. calculated from data in ref. 79.
b. calculated from partitioning data presented in Chapter 3.
c. maximum probable value based on a difference of solubility paramenters of 0.10.
d. reference (103).
e. reference (77).

presented in Table 4.14. The χ value is the interaction parameter for Flory-Huggins mixing.(111) It has been evaluated from experimentally determined values of the activity coefficient, f_1, for these systems, according to equation 4.2.(112)

$$\chi = \frac{\ln f_1}{(1-\Phi_1)^2} + \frac{\ln (x_1/(1-\Phi_1))}{(1-\Phi_1)^2} + \frac{1}{(1-\Phi_1)} ((V_1/V_2) - 1) \qquad (4.2)$$

where Φ_1 is the volume fraction of component 1

X_1 is the mole fraction of component 1,

and V is the molar volume.

χ is a reasonable interaction parameter to compare with β /kT, since they both arise from Flory-Huggins mixing theory for which the entropy of mixing is based upon Flory-Huggins statistics.(111) If the entropy of mixing were ideal on the basis of mole fraction the last two terms in equation 4.2 would be zero. The value of the leading term of equation 4.2 is also tabulated in Table 4.14. This is the form of the relationship between the interaction parameter of regular solution theory and the activity coefficient. The values of χ and $\ln f/(1-\Phi_1)^2$ listed, represent the range of values calculated from available activity coefficient data. For the benzene

+ alkane systems, activity coefficients were available in the literature from vapor pressure studies.(77-80) For decane + aromatic systems the reported values are from the partitioning data presented in the preceding chapter. The value of χ differs significantly from that of $\ln f/(1-\Phi_1)^2$ as the size difference between the two components increases. This reflects the difference in the entropy of mixing terms.

The predicted value of the regular solution theory interaction parameter, V_1A_{12}/RT, where A_{12} is the square of the difference of the solubility parameters of the two components, is listed in the last column. (91) In the master's thesis of this investigator (59), this interaction parameter was compared with β/kT. It was concluded that the β/kT values were of reasonable magnitude, since they are generally lower than those predicted by the bulk parameter, reflecting the partial cancellation of bulk interactions by surface interactions. The benzene + dodecane system was anomalous by this comparison since the β/kT value equalled the V_1A_{12}/RT value. Moreover, the trend of increasing β/kT with increasing chain length of the alkane, in the benzene + alkane mixtures was reversed in the regular solution prediction. Comparison of the surface tension values for β/kT with χ, however, clears the anomaly of the benzene + dodecane system,

since χ (0.6-0.78) is significantly higher than β/kT (0.28). The χ values reflect the trend in β/kT with increasing chain length of alkane as particularly reflected in the difference in χ between the benzene + dodecane mixture (0.6 -0.78) and the benzene + hexane system (0.52 - 0.59).

The χ value is also much greater than the β/kT values for the decane + aromatic mixtures. This result confirms the expected partial cancellation of the bulk interaction by surface interactions. The surface interactions, which are expected to be close to ideal behavior, do not cancel the bulk interaction completely. Thus the surface interactions are of lesser magnitude than those in the bulk. The interaction parameter derived from surface tension data is reporting differences between the bulk and surface interactions. That the magnitude of these interactions are different between bulk and surface is reflected in the non-zero value of β/k.

The values of χ and β/kT both decrease with increasing chain length of the alkyl substituent on the alkylbenzene. The more favorable interactions between decane and alkylaromatics of longer chain length is reflected in these interaction parameters. The new data on butylbenzene and 1-dodecene extend these trends. Since activity coefficients for these

systems were not available and χ could not be calculated, the regular solution parameter is provided in Table 4.14 as an indicator of bulk interactions. Since butylbenzene and 1-dodecene are more similar to decane in molecular size and the interactions are closer to ideality than the other molecules tested, the difference between χ and V_1A_{12}/RT is expected to be smaller.

From analysis of the surface tension values, it is concluded that the surface is partially cancelling the bulk interaction, reflecting the more nearly ideal behavior of the surface. Also the χ parameter is a more suitable parameter for comparison with β than the regular solution prediction.

c. Interfacial Tension Studies

In this section the interfacial tension data for the binary mixtures of benzene, toluene, ethylbenzene, butylbenzene and 1-dodecene with decane against water are analyzed on the basis of the Prigogine-Marechal parallel layer model for binary mixtures.(98,99) The interaction parameter β derived from application of the model to the data is compared with bulk interaction parameters and with the same parameter, β, derived from

surface tension measurements against air for the same binary mixtures. This work extends the work presented in the masters thesis on the interfacial tension of the first three mixtures listed in the above series. (59) Butylbenzene extends the alkyl chain series. 1-Dodecene describes the influence of one double bond in an alkyl chain, as opposed to the three double bonds of the aromatics on interactions at the interface. The χ value as a more appropriate comparative interaction parameter is also considered.

Table 4.15 lists the values of the β/kT parameter, determined from equation 4.1, for the surface tensions and interfacial tensions of the binary mixtures of benzene, toluene, ethylbenzene, butylbenzene, and 1-dodecene with decane. The χ value, calculated on the basis of equation 4.2, and the value V_1A_{12}/RT, which is the regular two-component solution interaction parameter, are also included. The interfacial tension data for the aromatic + decane mixture against water could not be described by a single interaction parameter across the entire composition range. The values listed are those β/kT values calculated from the interfacial tension values at mole fractions 0.1, 0.4 and 0.7 of aromatic in the mixture.

TABLE 4.15

Comparison of the Interaction Parameter, χ, Calculated From Experimental Values of the Activity Coefficient, V_1A_{12}/RT, Calculated From Regular Solution Theory, and β/kT From Air-Liquid and Water-Liquid Interfacial Tension Data[a]

System	(β/kT) S.T.	(β/kT) I.T. 0.1	0.4	0.7	χ	V_1A_{12}/RT
Benzene + Decane	0.21	0.51	0.36	0.28	0.61-0.76 0.63-0.76	0.30
Toluene + Decane	0.14	0.38	0.28	0.23	0.42-0.38	0.25
Ethylbenzene + Decane	0.13	0.35	0.27	0.20	0.38-0.48	0.24
Butylbenzene + Decane	0.06	0.22	0.14	0.08		0.18
1-Dodecene + Decane	0.002	0.1	0.1	0.1		0.01

a. χ and V_1A_{12}/RT values are from the sources listed in Table 4.14.

In order to analyze these values of β, the meaning of β in the ternary system of an aromatic + alkane mixture against water must be considered. The β value arises from a monolayer surface model of a mixture of two components.(99) At the organic liquid-water interface the monolayer under consideration is that of the organic components alone. The same model that was used for surface tension of two component mixtures is extended to interfaces here. Aveyard (116) also used this approach to describe the interfacial tension of alkane mixtures against water. Water is treated as a perturbant to the interactions of the organic molecules at the interface. It was shown in the last chapter that for the benzene + decane system the presence of water does not significantly affect the activity coefficient, which is a measure of interactions in the bulk. The solubility of water in the alkyl-substituted systems studied is likely to be even lower, since water solubility in alkanes is known to be lower than in benzene.(117,118) It is therefore expected to have an even smaller influence on bulk interactions.

With surface tensions of these mixtures, a partial cancellation of bulk interactions, χ, by surface interactions was seen and is described in the preceding section. The β values derived from interfacial tension data

($\beta_{I.T.}$) are also somewhat smaller than the χ values but they are significantly larger than the β values derived from surface tension ($\beta_{S.T.}$). The cancellation of bulk interactions by interfacial interactions is less than the cancellation of bulk interaction by surface interactions. This would suggest that the organic-water interface is even more ideal than the organic-air interface. What is actually reflected here is the specific interaction of hydrogen bonding of the aromatic component with water, which is absent at the air-organic liquid surface.(83,86) The higher value of β in the system which includes water indicates that the interfacial tension of the mixtures is lower than would have been predicted on the basis of the non-specific dispersive interaction reported by the $\beta_{S.T.}$. The aromatics adsorb to the water-liquid surface thereby lowering interfacial tension to a greater extent than would have been expected from interpretation of air-liquid surface tension β values.

As seen with the surface tension results, the χ value is shown by these data to be a more suitable comparison for β/kT, than the regular solution parameter V_1A_{12}/RT, which is lower than $\beta_{I.T.}$ The χ value is higher than the $\beta_{I.T.}$ values as expected from cancellations of bulk properties by

surface interaction.

The β values decrease with increasing chain length of the alkyl substituent as is reflected in χ, V_1A_{12}/RT, and $\beta_{S.T.}$. This reflects the more favorable interactions with decane as alkyl chain length is increased. The new data on the butyl-benzene + decane and 1-dodecane system are consistent with this trend.

The $\beta_{I.T.}$ values are also seen in Table 4.15 to decrease with increasing aromatic composition of the mixture. The hydrogen bonding, which accounts for the value of β, requires a planar orientation of the π system at the interface.(85) In dilute solutions of aromatics, this planar orientation is more likely to be attainable than at high concentrations, at which aromatic molecules are in close contact with each other. Therefore, to the extent that hydrogen bonding is responsible for adsorption of aromatics to the water/liquid interface, the tendency of aromatics to adsorb will be most fully expressed in dilute solution. The fitted β value is consequently higher in the dilute region. The 1-dodecene data do not show this trend. The values are low since the system is quite close to ideality and it is expected to be difficult to find any trend in the data. On the other hand the most efficient hydrogen bonding between the π system

of this 1-olefin and water at an interface is not likely to require an orientation which occupies an extensive amount of surface. The π system of 1-dodecene involves only one π bond as opposed to a ring system in the aromatic. Favorable orientations for hydrogen bonding of these molecules are likely to be attainable at any interfacial concentration of 1-dodecene.

In summary, the model employed provides an adjustable interaction parameter β through which interactions in different systems can be compared. The experimental χ parameter can be used as a suitable comparison for β, to indicate the extent to which surface effects are cancelling bulk effects. Specific interaction at the organic liquid - water interface are reflected in the differences in χ, $\beta_{S.T.}$, and $\beta_{I.T.}$ Values of β cannot presently be predicted, so that experimental determination of the composition dependence of interfacial tension is necessary for assessing values of the tensions of mixtures and adsorption.

2. Interfacial Adsorption From Dilute Solution.

A phenomenon that is of interest in any system possessing an interface is the adsorption of molecules to that interface. In the present study a measure of adsorption to an alkane/water interface is required for the modelling of micellar solubilization to be presented in the next chapter.

As pointed out in the last section, theories of mixtures are unable to predict the composition dependence of interfacial tension for the liquids studied, to which adsorption is related. Also for solids no theories are available to predict adsorption to liquid-liquid interfaces. Therefore, experimental determination is required.

The surface excess, Γ in moles area $^{-1}$, for adsorption of molecules from solution is given by

$$\Gamma_1 = \frac{-1}{RT} \frac{\delta \gamma}{\delta \ln a_1} \qquad (4.3)$$

where, γ is the interfacial tension,

a is the activity of the molecule in solution,

R is the gas constant,

T is the temperature,

and subscript 1 refers to component 1.

At infinite dilution equation 4.3 becomes

$$\frac{\Gamma_1}{x_1} = \frac{-1}{RT} \frac{\delta \gamma}{\delta x_1} \qquad (4.4)$$

where x_1 is the mole fraction of component 1 in solution. If a molecule adsorbs to the surface, $\delta\sigma/\delta x$ will be negative. The absolute value of $\delta\sigma/\delta x$ is therefore, a measure of the distribution of molecules between the surface and the bulk. Table 4.16 lists the absolute values of the initial slopes for benzene, toluene, ethylbenzene, n-butylbenzene, p-di-tert-butylbenzene, naphthalene, phenanthrene, pyrene and 1-dodecene from mixtures with decane to the decane/water interface. These values are reliable to about ± 10% except for 1-dodecene, which carries a somewhat greater error of about 20% due to its smaller magnitude. The absolute values of the initial slopes in the range from six for 1-dodecene to 72 for pyrene indicates the magnitude of the interfacial activity of the compounds. A traditional surface active substance, butanol, has an initial slope of about -20000 at the dodecene/water interface (119). In the next chapter this mild interfacial activity of the aromatics will be shown to be magnified by the extensive interfacial area of surfactant micelles.

The general trend is toward a decrease of adsorptivity to the decane/water interface as the alkyl chain length of the n-alkyl benzenes increases. This reflects the more favorable interactions of these molecules with decane as chain length increases and the hydrophobic effect of the

TABLE 4.16

Initial Slopes of Interfacial Tension Against Water vs Mole Fraction of Some Aromatics in Binary Mixtures With Decane

	$\delta\sigma/\delta x$
Benzene	33
Toluene	30
Ethylbenzene	28
n-Butylbenzene	22
p-Di-tert-butylbenzene	27
Naphthalene	41
Phenanthrene	60
Pyrene	72
1-Dodecene	6

alkyl chain. The polycyclic aromatics show a trend of increasing adsorptivity as more rings are added. The activity coefficients for these compounds in decane are not available. Regular solution theory (91) predicts a small increase in the activity coefficient in decane as more rings are added. The addition of more rings also allows for more hydrogen bonding of these compounds with water.

The significant influence of the number of double bonds on adsorption is indicated by Figure 4.15. In this figure the absolute value of the initial slope is plotted against the number of double bonds in the molecule. Purely aliphatic compounds with no double bonds would have fallen near the origin on this graph. Indeed, Aveyard (116) found that the initial slopes of binary mixtures of aliphatic chains are less than the predictions from a linear dependence on mole fraction. The absolute value of the initial slope of a mixture of octane and hexadecane against water was found to be close to unity. The value of six for the absolute value of the initial slope of 1-dodecene indicates a significantly greater adsorptivity than expected for an alkane.

It is seen from Figure 4.15 that a roughly linear relationship exists between the number of double bonds and the adsorptivity. Since hydrogen

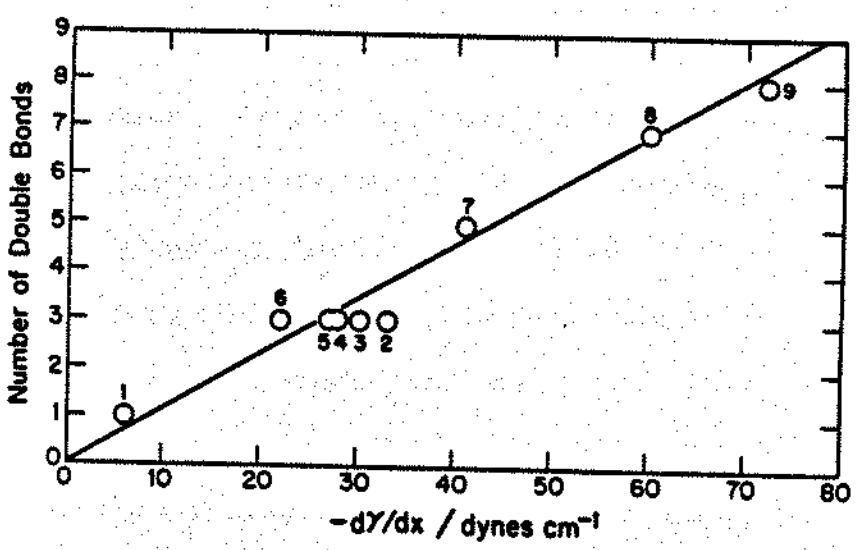

Figure 4.15 Number of double bonds, n, in compounds listed below plotted as a function of the initial slope, $\delta\gamma/\delta x$, of the interfacial tension vs mole fraction curve.

1. 1-dodecene
2. benzene
3. toluene
4. ethylbenzene
5. p-di-tert-butylbenzene
6. n-butylbenzene
7. naphthalene
8. phenanthrene
9. pyrene

bonding of these molecules with water occurs through the π bond system, the number of double bonds is likely to be a good indicator of the ability of these molecules to hydrogen bond. The proportionality between double bonds and adsorptivity to the decane-water interface indicates the additive character of hydrogen bonding at the interface.

The linearity of the relationship makes this a valuable correlation for interpolating and extrapolating adsorptivity estimates. Some large aromatic compounds are likely to be only slightly soluble in an organic medium making precise experimental determination of adsorptivity difficult.

The value of the initial slope of the p-di-tert-butylbenzene + decane mixture relative to the other alkyl benzenes may not be expected considering that it contains eight non-aromatic carbon atoms including six methyl groups. However, p-di-tert-butylbenzene is a symmetrical molecule. The orientation at the decane/water interface which would place a t-butyl group in the aqueous phase is overwhelmingly energetically unfavorable.(1,2) This compound must sit at the interface in a certain orientation, likely the most favorable one for H-bonding. The activity coefficient of this compound in decane is not known. Further study of

these possibilities should be considered.

3. Surface Activity Coefficients in Dilute Solution

The activity coefficient is a fundamentally important thermodynamic quantity for describing intermolecular interactions in any mixture. Activity coefficients at interfaces are not easily determined. They are usually assumed to be unity, that is ideal mixing at the interface. (97,103) In section A an effective interaction parameter, β, describing differences between surface and bulk was all that could be obtained from one theory. Even so its value provided insights into the nature of the interactions occurring at the interface. In view of the paucity of information on the magnitude of the surface activity coefficient and the value of such an estimate for understanding the surface state, any estimate of it is valuable.

A new approach toward estimation of the surface activity coefficient in dilute solution is outlined below. The method is based upon Butler's equation (94,99) which models the surface of a binary mixture as a monolayer of molecules. For a nonideal binary mixture

$$\sigma - \sigma_i = \frac{RT}{a_i} \ln \frac{x_i^m f_i^m}{x_i^l f_i^l} \qquad (4.5)$$

where σ is the surface tension

σ_i is the surface tension of pure component i

a_i is the partial molar area of component i

x_i is the mole fraction of component i

f_i is the activity coefficient of component i

and superscripts m and l refer to surface (monolayer) and bulk (liquid) respectively.

In the case of a dilute solution of component two, the mole fraction of component one in both the surface and the bulk approach unity and the activity coefficients of component one also approach unity. As $x_2 \rightarrow 0$,

$$\ln(x_1^m/x_1^l) = \ln[(1-x_2^m)/(1-x_2^l)] \approx x_2^l - x_2^m \qquad (4.6)$$

Substituting equation 4.6 into equation 4.5 gives,

$$\sigma_1 - \sigma \equiv \pi = \frac{RT}{a_1}(x_2^m - x_2^l) \qquad (4.7)$$

or

$$\pi / x_2^l = \frac{RT}{a_1}((x_2^m / x_2^l) - 1). \qquad (4.8)$$

In very dilute solution where $\delta\pi/\delta x_2^l$, the negative of the initial slope value, is independent of x_2^l, $\delta\pi/\delta x_2^l = \pi/x_2^l$. Therefore, the quantity x_2^m/ x_2^l can be estimated from equation 4.8, if the initial slope is known and the partial molar area of component one is estimated. Even for simple spherical molecules, such as argon, the partial molar area has not been determined.(99,120) In the present treatment the molar area, a, is estimated as $V^{2/3} N^{1/3}$, where V is the molar volume and N is Avogadro's number.(103) According to this approach molecules at the surface are in a square lattice arrangement with five nearest neighbors. This is likely to be an overestimate of the area of each molecule. Also $V^{2/3}$ treatment implies a random orientation at the interface which may not be the case. However, the molar volume of the molecules studied is known precisely and relative differences between molecules can be noted. Equation 4.5 can be rearranged to

$$\frac{x_2^m f_2^m}{x_2^l f_2^l} = \exp\left\{\frac{(\gamma_1-\gamma_2)a_2}{RT}\right\} \exp\left\{\frac{-\pi a_2}{RT}\right\} \qquad (4.9)$$

As π $(=\gamma_1 - \gamma)$ approaches zero at infinite dilution of component two

the second exponential on the right hand side of equation 4.9 goes to one. The activity coefficient of component two at the surface, f_2^m, can, therefore, be calculated from the x_2^m/x_2^l ratio obtained from equation 4.8 and the other quantities in equation 4.9 including f_2^l. Values of f_2^l of the aromatic compounds at infinite dilution in decane were estimated from the partitioning data presented in Chapter Three. They are likely to be reliable to within a few percent. The value for butylbenzene was calculated from regular solution theory. The f_2^l values for the aliphatic component in such binary mixtures at its infinite dilution can be estimated from the analysis of total vapor pressure data for benzene + heptane (77,78) and benzene + decane mixtures. (79) In the former case the estimated values from two sources differ by 25%. In the latter case a very large extrapolation is required. For these reasons, f_2^l for decane at infinite dilution has been calculated using the regular solution theory and solubility parameters.(91,115)

The surface and interfacial tension data of binary mixtures of the liquids benzene, toluene, ethylbenzene, and butylbenzene with decane have been analyzed to provide information on surface activity coefficients for these compounds. Tables 4.17 - 4.19 list the values of $\delta\pi/\delta x$ determined

TABLE 4.17

Surface Activity Coefficients, f^m, of Aromatics at Infinite Dilution in Binary Mixtures With Decane at 25°C

	$\delta\pi/\delta x$	x^m/x^l	f^l	f^m
Benzene	-0.96	0.89	1.48	1.19 ±0.05
Toluene	-1.10	0.87	1.32	1.07 ±0.05
Ethylbenzene	-1.85	0.78	1.32	1.11 ±0.05
Butylbenzene	-1.7	0.80	1.20	0.90 ±0.05

TABLE 4.18

Surface Activity Coefficients, f^m, of Decane at Infinite Dilution in Binary Mixtures With Aromatics at 25°C

	$\delta\pi/\delta x$	x^m/x^l	f^l	f^m
Benzene	34.4	3.34	2.06	1.09 ± 0.05
Toluene	18.4	2.41	1.58	1.10 ± 0.07
Ethylbenze	16.8	2.42	1.47	1.08 ± 0.07
Butylbenzene	8.5	1.84	1.25	1.24 ± 0.10

TABLE 4.19

Activity Coefficient, f^m, of Aromatics at Infinite Dilution in Binary Mixtures With Decane From Interfacial Tension Data at 25°C

	$\delta\pi/\delta x$	x^m/x^l	f^l	f^m
Benzene	33	4.8	1.48	1.00 ± 0.07
Toluene	30	4.5	1.32	1.00 ± 0.08
Ethylbenzene	28	4.3	1.32	1.02 ± 0.07
Butylbenzene	22	3.5	1.20	1.06 ± 0.09

from experiment, x_2^m/x_2^1 from equation 4.8, f^1, the infinite dilution activity coefficient, and f^m, values calculated from equation 4.9 using the other parameters listed in the tables and the surface or interfacial tensions of the pure components. Table 4.17 gives the appropriate values at infinite dilution of the aromatic compound in decane at the air-liquid surface. Table 4.18 gives the values at infinite dilution of decane in the aromatic component from air-liquid surface tension data. Table 4.19 lists the values at infinite dilution of the aromatic component in decane at the water/liquid interface. Error assessments of the low slopes from water/liquid interfacial tension data at infinite dilution of decane in the aromatics allow no conclusions to be drawn concerning activity coefficients at the interface. Therefore, these data are not tabulated or discussed further.

An examination of the tables indicates that the method is working reasonably well since the f^m values lie in the expected range, near unity. For all of the systems studied, it is seen from Tables 4.17-4.19 that the surface activity coefficient is lower than the bulk activity coefficient. This is consistent with the physical state at the surface, where molecules have fewer neighboring molecules with which to interact. For some

systems, such as decane in benzene, this difference is large the bulk activity coefficient being 2.06, whereas at the surface it is 1.09. Although these systems are not highly non-ideal, that is, the value of f^1 is not very large, the difference between f^1 and f^m is in most cases significant. For some systems closer to ideality in the bulk, such as butylbenzene + decane, the differences between surface and bulk are smaller. This is expected since the surface must approach the ideal limit. The closeness of most of these systems to ideality at the surface, $f^m = 1$, is supporting evidence for the usual assumption of ideality at the surface or interface.

There is some evidence in the case of benzene that at the interface against water this molecule has a lower activity coefficient than against air. For the other aromatics, results are equivocal since the values at air + water interface are the same within error. These results do not contradict that for benzene. The difference between the activity coefficient at the air/liquid surface and water/liquid interface for benzene is consistent with the findings for the interaction parameter β in section A. At the interface the hydrogen bonding interaction between benzene and water shows up as a high value of β due to a smaller interfacial activity coefficient and a correspondingly smaller cancellation of the bulk

parameter. It must also be noted that the f^m values are quite sensitive to the choice of the area parameters a_1 and a_2. For example a decrease of benzene area of 4.6Å², from 28.03 Å² to 23.4 Å², increases the air/liquid f^m from 1.19 to 1.26 and decreases the water/liquid f^m from 1.00 to 0.79.

In summary, relative comparison based upon a single convention for determining the area at the surface, $V^{2/3}$, yields the qualitative conclusions that f^m is lower than f^I and that f^m approaches unity.

4. Work of Adhesion

A complete description of the interfacial region requires an understanding of the intermolecular forces which act across the interface. At interfaces between condensed phases, such as the liquid-liquid interface, molecules at the surface are capable of interacting with molecules of the other phase. This interaction is absent at the liquid-vapor surface. A measure of the free energy per unit area of the interactions occurring across the interface is the work of adhesion, W_a,(4),

$$W_a = \gamma_1 + \gamma_2 - \gamma_{12} \qquad (4.10)$$

where γ_1 is the surface tension against vapor of pure component one

or phase one,

γ_2 is the surface tension against vapor of pure component two or phase two,

and γ_{12} is the interfacial tension between components or phases one and two.

Both surface tension and interfacial tension data on a number of systems including mixtures are available in this study. The work of adhesion was calculated as a function of composition of binary mixtures of aromatic compounds and decane over the whole composition range for four systems and over a limited range of concentration for three solid systems. Such data are not usually available in the literature. The calculated work of adhesion values for binary mixtures of benzene, butylbenzene, and 1-dodecene with decane across the entire composition range is shown in Figure 4.16. For toluene and ethylbenzene only the values at mole fraction of aromatic equal to unity are displayed, since the mixture values lie too close to benzene for clear resolution on the graph. The mixtures of phenanthrene, naphthalene, and p-di-tert-butylbenzene are shown in Figure 4.17.

The work of adhesion increases with increasing aromatic composition

Figure 4.16 Work of adhesion of benzene, n-butylbenzene and 1-dodecene in binary mixtures with decane plotted as a function of the mole fraction of the unsaturated compound in the organic liquid.

Curve A Benzene
Curve B n-Butylbenzene
Curve C 1-Dodecene
O Toluene
□ Ethylbenzene

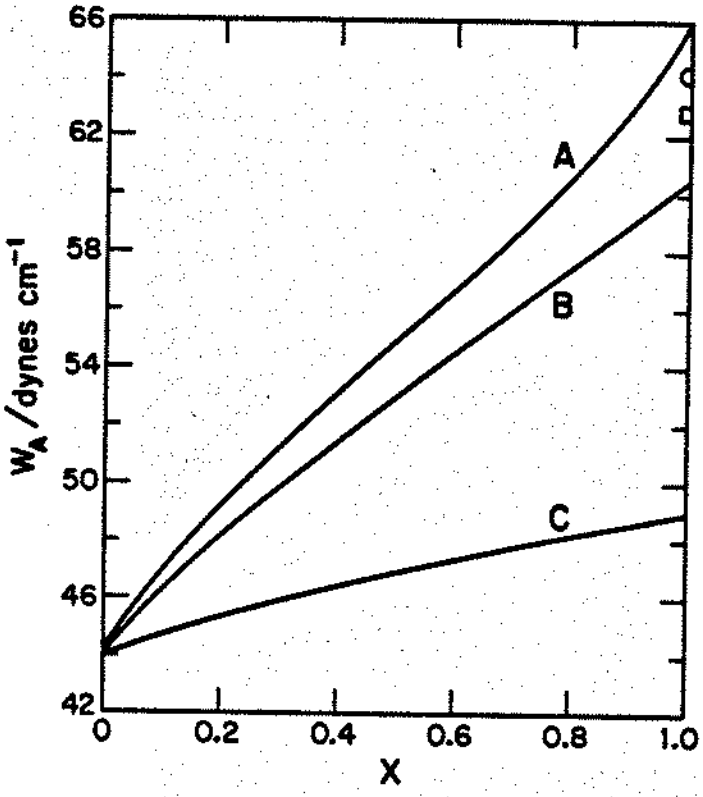

Figure 4.17 Work of adhesion of phenanthrene, naphthalene, and p-di-tert- butylbenzene in binary mixtures with decane plotted as a function of the mole fraction of the unsaturated compound in the organic liquid.

Curve A Phenanthrene
Curve B Naphthalene
Curve C p-di-tert-butylbenzene

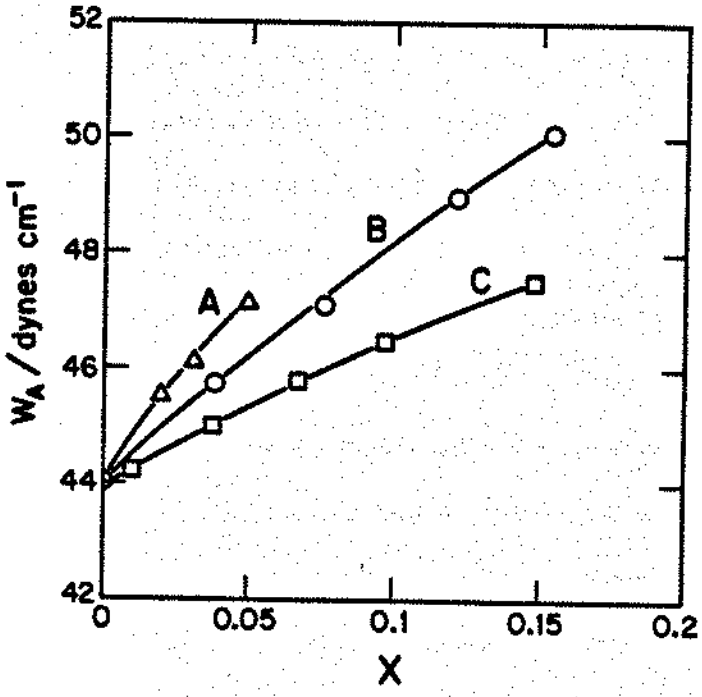

of the mixture. Therefore, greater interaction must be occurring across the organic-water interface as the composition of aromatic is increased. The rate of increase in W_a with aromatic mole fraction is greater for compounds with more double bonds. Thus, phenanthrene has a higher W_a than naphthalene at the same mole fraction. The proportionality between the number of double bonds and the interfacial activity has been demonstrated in Figure 4.15. The hydrogen bonding interactions across the interface show up in an increased adsorption from hydrocarbon and an increased work of adhesion as more double bonds are added.

As the alkyl chain is lengthened for the n-alkyl benzenes, the work of adhesion decreases as does the interfacial activity shown in Table 4.20. Indeed the rate of increase in work of adhesion parallels the interfacial activity demonstrated by the initial slopes of Table 4.15. The work of adhesion curve in Figure 4.16 is somewhat sigmoid for benzene, and monotonic for butylbenzene and 1-dodecene. However, the deviation from linearity is not greater than 1 dyne cm^{-1}. Therefore, if the pure liquid values are known, then either surface or interfacial tensions, known as a function of composition, can provide an estimate of the other.

The work of adhesion between water and alkanes has been described by an approximate theory as

$$W_a = 2 (\gamma_1^d \gamma_2)^{1/2} \qquad (4.11)$$

where γ_1^d is the dispersion component of the surface tension of water,

and γ_2 is the surface tension of alkanes, assumed to be entirely due to dispersion forces.

This theory is reasonably successful since dispersion forces are the only ones acting across the alkane-water interface.(105) For example, at 20°C a mean value of γ_1^d of 20.76 dynes cm^{-1} reproduces W_a data for nine alkanes from hexane to hexadecane within a mean error of 0.6 dynes cm^{-1}. A small trend in the data was considered to be significant by Fowkes.(105) He attempted to explain it in terms of anisotropy effects of dispersion forces.

For somewhat polar molecules, such as the aromatics studied here, both anisotropy of dispersion forces and additional polar interactions are expected.(4,101,105) In order to estimate these forces experimentally, the work of adhesion calculated from equation 4.11 has been compared with

the experimental W_a in Table 4.20. A γ_l^d value for water of 20.63 dynes cm^{-1}, obtained from the work of adhesion for decane, was used here. The experimental W_a values are much higher than the calculated W_a values, indicating that a significant polar component is present for W_a for such systems. The difference between W_a (experimental) and W_a (calculated) also listed in Table 4.20 can be used as a measure of the polar interactions at interfaces of the aromatic compounds.

Of considerable interest, the initial $-\delta\gamma/\delta x$ values for five systems, 1-dodecene, benzene and three alkyl derivatives of benzene in decane from interfacial tension studies against water are proportional to W_a(exp) - W_a(calc); this is shown in Figure 4.18. Thus the 50% reduction of $-\delta\gamma/\delta x$ for the aromatics studied here between benzene and butylbenzene, all of which contain the same number of double bonds, appears to be primarily due to variations in interfacial tensions of the benzene derivatives reflected in experimental W_a values. A correlation of this kind is likely to be useful for estimating $-\delta\gamma/\delta x$ values of other compounds from pure liquid interfacial tension data alone.

TABLE 4.20

Relationship Between Work of Adhesion, the Dispersion Component of the Work of Adhesion, and the Initial Slope of Interfacial Tension vs Mole Fraction Data

	W_a(exp)	W_a(calc)[a]	W_a(exp)-W_a(calc)	$\frac{-\delta\gamma/\delta x}{W_a(exp)-W_a(calc)}$	$-\frac{\delta\gamma}{\delta x}$
Benzene	65.98	48.33	17.65	1.87	33
Toluene	64.30	47.97	16.33	1.84	30
Ethylbenzene	62.99	48.42	14.57	1.92	28
Butylbenzene	60.43	48.56	11.87	1.85	22
1-Dodecene	48.97	45.65	3.27	1.83	6

a. $W_a(calc) = 2(20.63\gamma)^{1/2}$ where γ is the air-liquid surface tension of the unsaturated compound.

Figure 4.18 Initial slope, $\delta\gamma/\delta x$, of the interfacial tension vs mole fraction curve plotted as a function of the difference between experimental work of adhesion, W_A(expt.), for the pure compounds and that calculated, W_A(calc.), as $2(20.63\gamma)^{1/2}$ where γ is the surface tension of the pure liquid.

1. 1-Dodecene
2. n-Butylbenzene
3. Ethylbenzene
4. Toluene
5. Benzene

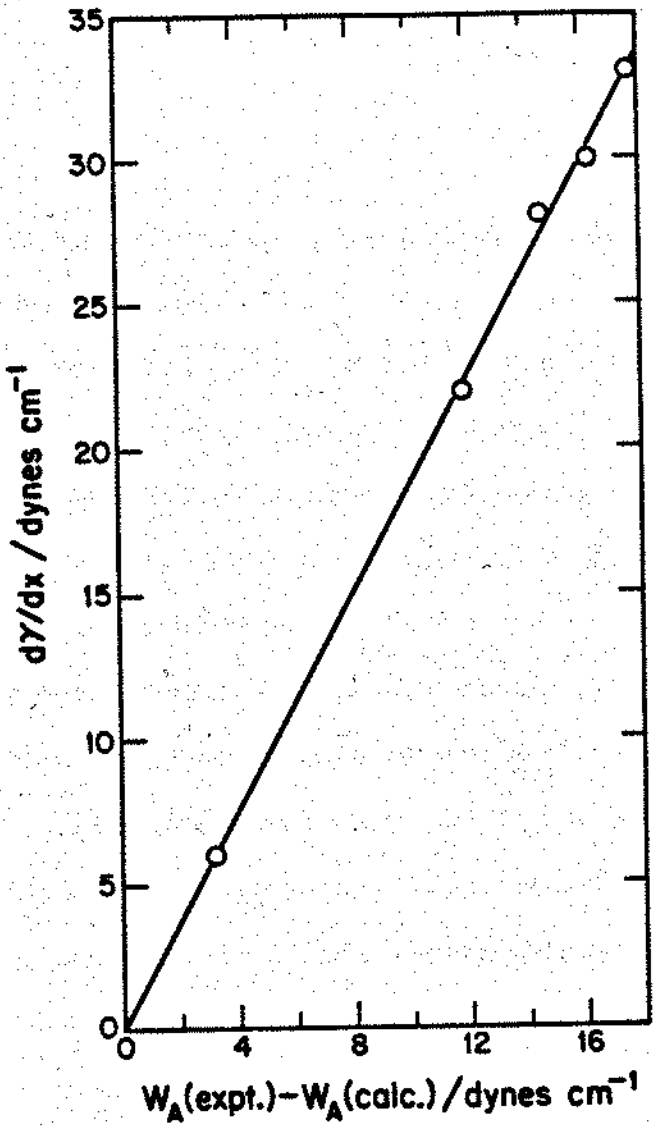
35
30
25
20
15
10
5
0
0
4
8
12
16
dγ/dx / dynes cm⁻¹
W_A(expt.)−W_A(calc.) / dynes cm⁻¹

SOLUBILIZING POWER OF MICELLES: RELATION TO MICELLAR LAPLACE PRESSURES AND INTERFACIAL ACTIVITIES OF SOLUBILIZATES

A. Micellar Laplace Pressures and Relation to Gas Solubilities in Micelles.

1.Background

The Laplace pressure of a micelle will influence the ability of the micelle to solubilize other molecules.(23,62,52) Considering the importance of solubilization in both its applications and as a model for hydrophobic association, any verified estimate of micellar Laplace pressure is a significant contribution.

The magnitude of the Laplace pressure in micelles is dependent upon the magnitude of the interfacial tension between the micelle and the aqueous medium and the curvature of the interface.(43,18) The micellar interfacial tension is a fundamental feature important for a complete understanding of micellar aggregation.(18,121-125) No experimental measure of micellar interfacial tension is available. A suitable model system is needed for estimation of this value. Experimental methods for the estimation of micellar Laplace pressure have been developed and employed, particularly

in the work of King and colleagues, through the measurement of gas solubilities in micelles.(42,126-130) The present work is an examination of the hydrocarbon/aqueous surfactant solution interface as a model for the micellar interface. Laplace pressure values from experiment are compared with those calculated from the model.

The concept of micellar Laplace pressure was first suggested by Mukerjee (18) in an examination of the evidence of some ordering effects within the micelle. Experimental evidence for micellar Laplace pressure is related to the effect of this pressure on the solubility of molecules within a micelle. Relative to a hydrophobic solvent of the same chemical composition as the hydrophobic tail of the micelle, the solubility of a molecule in a micelle is reduced due to Laplace pressure. The relation is

$$x_m/x_h = \exp(-\Delta P\bar{V}/RT) \qquad (5.1)$$

where x_m is the solubility in the micelle,

x_h is the solubility in the hydrophobic solvent,

ΔP is the Laplace pressure in the micelle, and

$\bar{V}$ is the partial molar volume of the solubilizate in the micelle.

An analogous treatment applies to the ratio of the micelle-water partition coefficient to the hydrocarbon-water partition coefficient. Similarly the difference in the free energy of transfer from gas to micelle and gas to hydrocarbon can also be employed as a measure of the Laplace pressure.

$$\Delta P = (\Delta G_{g \rightarrow micelle} - \Delta G_{g \rightarrow hydrocarbon})/\overline{V} \qquad (5.2)$$

The Laplace pressure effect is evident in the solubility of aliphatic hydrocarbons and hydrocarbon gases in hydrocarbon surfactant micelles. (23,126-130) As will be discussed in detail below, the mole fraction solubility of hydrocarbon gases in micelles at one atmosphere pressure is less than their solubilities in hydrocarbons. In a homologous series of solubilizates, micelles have been shown to solubilize smaller quantities of the larger molecules.(37,38) As seen from equation 5.1, a decrease of the micellar solubility of molecules with similar hydrocarbon solubility is expected as solubilizate molar volume increases. This effect also reflects the resistance of the micelle against the expansion required to solubilize larger molecules. An expansion of the micelle would increase its area of contact with water. The force acting against this expansion is the

interfacial tension.

A lower value of micellar solubility or micelle/water partitioning relative to a hydrocarbon is not detected for all molecules. As described in the introduction, if solubilized molecules are interfacially active in micelles, a significant portion of the uptake in micelles may be due to the "adsorbed state".(23,50) Experimental estimates of Laplace pressure effects require studies on systems where the interfacial activity is minimal. For this reason hydrocarbon gases or liquid hydrocarbons in hydrocarbon surfactant micelles are likely to be the best candidates for this analysis. Also, such gases at pressures near 1 atm. have low micellar solubilities (64,126-130) and therefore are not expected to alter micellar structure by their presence. On such systems a number of studies, primarily by King and coworkers, have recently become available.(64,126-130,131) However, interfacial activity may be important even for nonpolar gases in certain cases. Recent work has shown that in mixtures of fluorocarbons and hydrocarbons, each component is significantly interfacially active in dilute solution at the water-liquid interface.(100) Some evidence of the interfacial activity of carbon tetrafluoride in hydrocarbon micelles will be given later. In contrast, only very mild interfacial activities of mixtures of

aliphatic hydrocarbon-liquids at hydrocarbon liquid-water interfaces has been noted.(119) For a rough estimate of the uncertainty associated with the assumption that hydrocarbon gases in hydrocarbon micelles are not interfacially active the data of Aveyard and Haydon have been used.(132) These workers measured interfacial tension against water of a series of liquid alkanes. Extrapolation of their values to ethane gave a tension at the ethane /water interface of 47 dynes cm^{-1}. Using this value, the adsorption of ethane to a dodecane-water interface was estimated using equation 4.5. Using the procedure to be outlined later for highly interfacially active substances, the adsorption to a micelle-water interface was calculated. The results indicated that less than 3% of solubilized ethane was likely to be at the interface, thus providing support for the assumption of insignificant interfacial activity for the alkane gases in micelles.

The concept of micellar interfacial tension has been invoked in numerous theories and descriptions of micellar association. In a discussion of the effect of pressure within the micelle on its solvent action, Hartley (133) suggested a two dyne cm^{-1} interfacial tension. Mukerjee (18) pointed out that ordering of molecules within micelles was likely to be related to Laplace pressure. He suggested that the interfacial tension of a micelle

was roughly similar in magnitude to that of a hydrocarbon-water interface at which surfactant had adsorbed to a degree of coverage (area per molecule) equal to that found in micelles. Based upon the data of Kling and Lange,(134) Mukerjee(18) estimated a micellar interfacial tension of 20 dynes cm^{-1} . Later in the evaluation of the data of Wishnia on gas solubilities in micelles, Mukerjee (23) found that calculations based upon a mean Laplace pressure of 296 atm. reproduced the results within experimental error. Such a Laplace pressure was consistent with a micellar interfacial tension of 31.5 dynes/cm . He compared this with the 27.1 dynes/cm estimated from the work of Haydon and Taylor (135) at the petroleum ether/water interface containing SDS. Rusanov (121) made a theoretical estimate of the range of micellar interfacial tension to be between 3.6 and 24.4 dynes cm^{-1} for potassium octadecoanoate micelles at 25°C. Gunnarson, Jonsson and Wennerstrom (122) have used 18 dynes cm^{-1} for carboxylic soaps. Nagarajan and Ruckenstein (124) used the hydrocarbon/water interfacial tension around 50 dynes cm^{-1} to estimate the micellar interfacial tension. Isrealachvili, Mitchell and Ninham (123) viewed the tension as that exerted between each monomer and water. Therefore, they too employed a hydrocarbon /water tension near 50 dynes

cm^{-1} but then corrected it for the capacitance due to the ionized headgroups. Their final value was about 31 dynes cm^{-1} . Ericksson (125) has recently also used the sum of the hydrocarbon/water interfacial tension and an electrostatic contribution to the micelle/water interfacial tension to arrive at a micellar surface tension of about 34 dynes cm^{-1} . Theoretical estimates of the micellar surface tension are of course essential to the further understanding of the micelle. A model system which could provide experimental estimates is similarly valuable. Therefore, this study examines the use of the hydrocarbon/aqueous surfactant solution interface as such a model.

2. Scope and Aim

Two important and interrelated physical quantities associated with the structure of the micelle and its ability to solubilize molecules are the Laplace pressure and interfacial tension. In this section gas solubility measurements in micelles which are available in the literature are evaluated to determine the micellar Laplace pressure for several systems. Based upon a fluid model for the micelle (23), the hydrocarbon / aqueous surfactant solutions interfacial tension is used as a model for the micellar interfacial tension . Experimentally determined Laplace pressures and

those calculated from the model are compared. The results indicate that the hydrocarbon/aqueous surfactant solution provides a reasonable model for the micellar interface.

3. Estimates of Laplace Pressure From Gas Solubility Data.

In this section experimental estimates of Laplace pressure of several micellar systems are presented. The data were obtained from values available in the literature on solubilities of hydrocarbons in hydrocarbon micelles. King and coworkers (126-130) have measured the solubilities of methane, ethane, propane, and carbon tetrafluoride at one atmosphere pressure in several surfactants including sodium alkyl sulfates of carbon chain length eight (SOS), ten (SDeS), and twelve (SDS) and decyl (DeTAB) and cetyl trimethyl ammonium bromide (CTAB). Wishnia (64) had measured the solubilities of hydrocarbon gases in SDS solutions at 0.1M NaCl. Christian and coworkers (131) have measured the solubility of liquid cyclohexane in sodium octyl sulfate micelles. Free energies of transfer from gas to micelle estimated from these data are given in Table 5.1.

The free energies of transfer for specific gases from the gas phase to specific hydrocarbon liquids, needed for calculation of Laplace pressure by equation 5.2, are not available in all cases. A systematic survey of the

available data from the literature was performed.(136-139) These data are presented in Table 5.2. From the trends indicated by 18 experimental values for six compounds in four solvents, the required values for seven unavailable combinations were estimated.

Similarly the available data on the partial molar volumes of these gases in hydrocarbon from the studies by Handa, D'Arcy and Benson (140) are shown in Table 5.3 along with estimates in solvents they had not investigated. The value of the partial molar volume of butane given by these workers (140) is inconsistent with a constant increase per $-CH_2$ group. An examination of the difference between the molar volume of liquid hexane (144) and the partial molar volume of hexane in alkanes (141-143) provided a basis for estimating the partial molar volume of n-pentane and n-butane which were consistent with established trends.

Employing the data listed in Tables 5.1-5.3, Laplace pressures of micelles have been estimated and are given in Table 5.4. These values carry an overall error of about 10%. The results indicate that the micellar Laplace pressure can be as high as 600 atmospheres. Since data obtained on different gases for the same micellar system do not differ by much more than the experimental error of individual estimates, the pressures

TABLE 5.1

Free Energies of Transfer (Kcal mol^{-1}) From Gas at One Atmosphere to Micelle at 25°C

	SURFACTANT					
GAS	SOS	SDeS	SDS	SDS (0.1M NaCl)	DeTAB	CTAB
Methane			3.71[a]		3.78[b]	3.46[b]
Ethane	2.96[a]	2.76[a]	2.67[a]	2.60[c]	2.86[b]	2.47[b]
n-Propane	2.51[d]		2.02[d]	1.98[c]	2.29[b]	1.80[b]
n-Butane				1.29[c]		
n-Pentane				0.80[c]		
CF_4			4.50[b]		4.15[b]	4.64[b]
Cyclohexane	0.02[e]					

a. ref. 128
b. ref. 130
c. ref. 64
d. ref. 129
e. ref. 131

TABLE 5.2

Free Energies of Transfer (Kcal mol^{-1}) of Gases at One Atmosphere to Solution at 298 K

	SOLVENT			
GAS	Octane	Decane	Dodecane	Hexadecane
Methane		3.11[a,b]	3.09	3.05[a]
Ethane	2.008[b]	1.97[a,b]	1.98[c,d]	1.96[a]
n-Propane	1.22[b]	1.16[a,b]	1.156	1.19[a]
n-Butane	0.470[b]	0.424[a,b]	0.42	0.41[a]
n-Pentane		-0.25 [a,b]	-0.26	-0.28[a]
CF_4	3.69[c]	3.72[a]	3.76	3.84
Cyclohexane	-1.30[a]	-1.26		-1.36[a]

a. ref. 136
b. ref. 137
c. ref. 138
d. ref. 139

TABLE 5.3

Partial Molar Volumes (ml) of Gases in Liquid Hydrocarbons at 25°C and Infinite Dilution

SOLUTE	SOLVENT				
	Octane	Decane	Dodecane	Hexadecane	V°
Methane	53.8[a]	51.8[a]	51.2	50.0[a]	
Ethane	66.6[a]	65.0	64.5	63.5	
n-Propane	83.2[a]	82.2	81.6	80.6	
n-Butane	96.7[a]	99.7	99.4		101.0
	100.4				
n-Pentane	115.9	115.6	115.1		116.1[e]
n-Hexane	131.3[b]	130.9[b]	130.6[c]	129.7[d]	131.6[e]
CF_4	81.9[a]	79.9	79.3	78.1	
Cyclohexane	110.6[f]				108.7[e]
	109.9[g]				

a. ref. 140
b. ref. 141
c. ref. 142
d. ref. 143
e. ref. 144
f. ref. 145
g. ref. 146

TABLE 5.4

Micellar Laplace Pressures (atm.) Calculated from Gas Solubilities in Aqueous Surfactant Solutions

	LAPLACE PRESSURE, ΔP (atm.)					
GAS	SOS	SDeS	SDS	SDS (0.1M NaCl)	DeTAB	CTAB
CH_4			500		530	340
C_2H_6	590	510	440	400	590	330
C_3H_8	640		440	420	580	330
C_4H_{10}				360		
C_5H_{12}				380		
$c\text{-}C_6H_{12}$	500(satd.)					
CF_4(surface active)			340		420	220

calculated are verified to be intrinsic micellar properties. The data also indicate a systematic decrease in Laplace pressure with increasing chain length of the surfactant monomers. This is consistent with the expected relationship between micellar radius and Laplace pressure.

The effect of Laplace pressure of the magnitude reported here on the ability of the micelle to solubilize other molecules can be evaluated. A pressure of 400 atm., equivalent to about four times the hydrostatic pressure at the depth of the Mariana trench, decreases the solubility of a molecule with a molar volume of 100 ml at 25°C by a factor of five relative to that in the hydrocarbon . A molecule of twice that volume would have its solubility decreased by a factor of 26. For large molecules, therefore, the pressure effect can be very substantial.

The uniformly significantly lower Laplace pressure determined from the solubilization of carbon tetrafluoride indicates the interesting nature of the hydrocarbon - fluorocarbon interaction. As briefly discussed in the background of this section, in mixtures of fluorocarbon and hydrocarbon each component is significantly interfacially active in dilute solution at the water-liquid interface.(100) The lower Laplace pressure calculated for CF_4 as a solubilizate is a reflection of a higher x_m/x_h from equation 5.1 for

CF_4 than for the hydrocarbon gases. Carbon tetrafluoride is thus expected to be interfacially active in a hydrocarbon medium such as the micelles studied. A significant portion of this solubilizate is expected to be in an "adsorbed state". The micelle provides an extensive interfacial environment for the solubilization of this molecule which is not available in bulk solution. On the basis of these considerations, it is expected that CF_4 would have a higher x_m/x_h than the non-interfacially active hydrocarbon gases and, therefore, a lower Laplace pressure. The above Laplace pressure results indicate that approximately 30% of the CF_4 is at the surface of the micelle. The interfacial activity of nonpolar fluorocarbons in hydrocarbon micelles has ramifications for the interactions of fluorocarbon anesthetics and blood substitutes with physiological membranes. The location, distribution, accessibility and uptake of these important drugs will be affected by their interfacial activity in membranes.

4. Estimates of Laplace Pressure from Micelle Models.

Considering the effect such large micellar Laplace pressures, as shown in Table 5.4, have on micellar solubilization, it would be valuable to develop a means of estimating Laplace pressure of micelles without

experimental determination. Such a method first requires a model of the micelle. At low concentrations in water most micelles have been described as spheres.(3,12,20) The Laplace pressure of a sphere is related to its interfacial tension ,δ, and radius ,r, by equation 5.3. (4)

$$\Delta P = 2\delta/r \qquad (5.3)$$

Even if a spherical model is appropriate for a micelle , neither the interfacial tension for the micelle-water interface nor the radius at the true surface of tension of the micelle are experimentally available. A model of the micelle-water interface is, therefore, required. It is assumed that the hydrocarbon-water interface containing the same number of charged surfactant molecules per unit area as found at the micelle surface is similar to the micelle-water interface. Since micelle radii are as small as 10 Å, an initial consideration in the use of this model must be the effect of the curvature of the micelle on its interfacial tension. Existing theories (4,148), which would indicate major effects at high curvature, have been shown to be inadequate. Fisher and Israelachivili (149), for example, showed that even at a radius of 5 Å, the cyclohexane surface tension was not different from that measured at a planar interface. In these studies we have ignored the effect of curvature on interfacial tension .

Other factors which are likely to influence the magnitude of the micelle-water interfacial tension must be investigated. Toward this goal, Mukerjee has employed a model which has led to encouraging results. (18,23) The model is that of a fluid micelle with a polar coat.(150) It models the micelle's interior as a hydrocarbon fluid. Further, the model assumes that the interfacial tension is determined primarily by the nature of the headgroups and their surface charge density in the micelle. In order to test the extent to which this assumption holds at planar interfaces, literature data on interfacial tension of sodium alkyl sulfate systems have been compiled and compared.(134,135,151,58) These are the only systems for which a reasonable amount of data exists in the literature. Figure 5.1 shows a plot of the data of Haydon and Taylor (135,151) for the interfacial tension of aqueous solutions of SOS, SDeS, and SDS at various concentrations of NaCl. The SDS data (135) are against petroleum ether whereas the other systems are against decane.(151) The interfacial tensions are plotted against the area of interface available to each surfactant monomer, which was calculated by the authors from the derivative of the interfacial tension with respect to the log of the activity of the surfactant. The figure indicates that interfacial tension for these

Figure 5.1 Hydrocarbon/aqueous surfactant solution interfacial tension at 20°C plotted as a function of area per surfactant molecule from data of Haydon and Taylor (151,135).The curve drawn is according to equation 5.4.

Symbol	Surfactant	Hydrocarbon	NaCl conc.[M]
●	SOS	decane	0.05
▽	SOS	decane	0.1
o	SOS	decane	0.25
△	SDeS	decane	0.1
▲	SDeS	decane	0.25
□	SDS	petroleum ether	0.05
■	SDS	petroleum ether	0.1
◇	SDS	petroleum ether	0.25

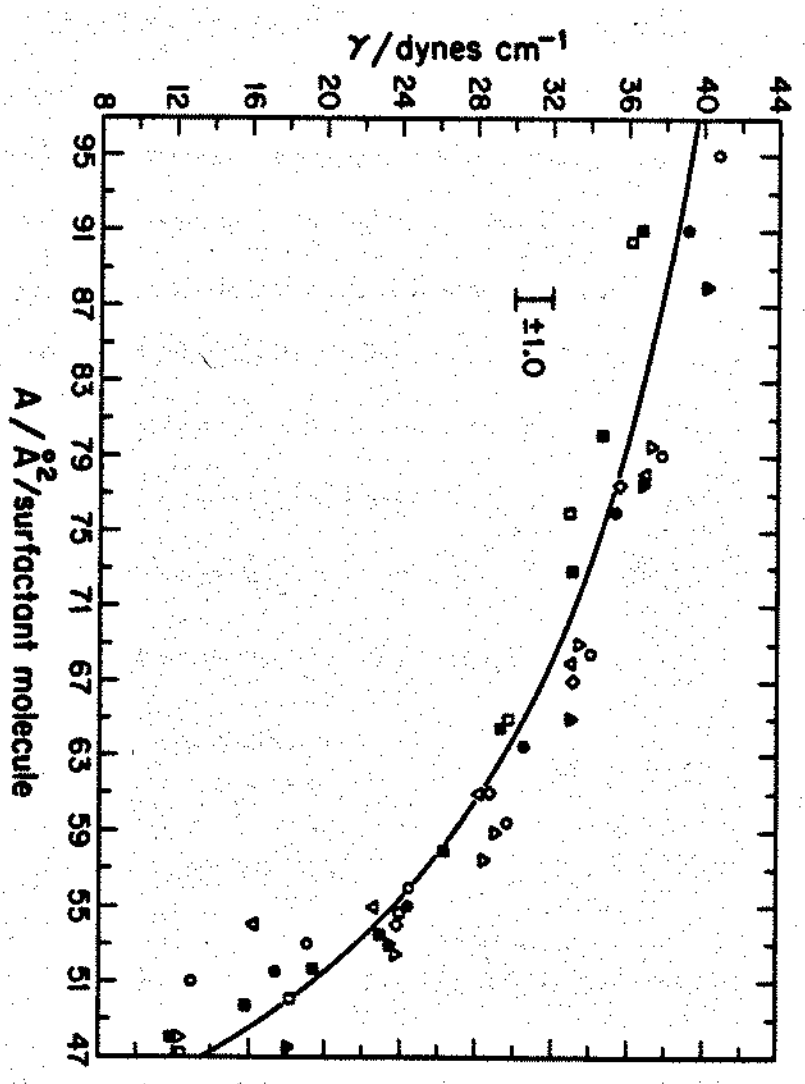
γ/dynes cm⁻¹
8
12
16
20
24
28
32
36
40
44
95
91
87
83
79
75
71
67
63
59
55
51
47
A/Å²/surfactant molecule
I ±1.0

systems are essentially indistinguishable for two different organic phases, three different surfactants, and three different salt concentrations.

Recently, a monolayer model for surfactant adsorption based upon Butler's thermodynamic approach (94) has been shown to be extremely useful. The extension of this approach to the effect of the presence of adsorbed surfactant at a planar interface on the adsorption of other solutes to that interface will be described later. Equation 5.15 shows the general relation of surface mole fraction, x_1^s, to bulk mole fraction, x_1^l, of the solvent. This equation provides a basis for calculating π-A diagrams of surfactants. At the interface, for charged surfactants containing two ions, $x_1^s + 2x_2^s = 1$, where x_2^s is the surface mole fraction of the surfactant ion. Equation 5.4 shows the relationship of x_2^s to $\pi(=\gamma_o-\gamma)$

$$x_2^s = \frac{1-x_1^s}{2} = \frac{1-x_1^l \exp(-\pi a_1/RT)}{2} \qquad (5.4)$$

Here a_1 is the partial molar area of water. The area, A, of the surfactant ion at the interface in $Å^2$/charge is given by

$$A = 10^{16}/x_2^s \, n \times 6.023\times10^{23} \qquad (5.5)$$

where n is the total number of molecules at the surface,

$$n = 1/(x_1^s a_1 + x_2^s a_2) \qquad (5.6)$$

where a_2 is the partial molar area of the surfactant ion and the counterion.

Effective co-areas of homologous series of ionic surfactants at a hydrocarbon /water interface have been shown to be very similar (134). Equations 5.4 to 5.6 indicate that if a_2 values are assumed to be the same for the three homologous alkyl sulfates studied, then the same A value for all of these surfactants will be obtained for any given π. The theoretical curve in Figure 5.1 was calculated on the basis of an a_1 value of 7.62 $Å^2$ (152) and an a_2 value obtained from the fitting of equations 5.15 and 5.16 to the SDS data of Haydon and Taylor at the petroleum ether-water interface.(135) The curve gives a reasonable description of the data for these three systems. The variations in σ_o between decane and petroleum ether at varying salt concentrations are shown by this congruence of σ data to be inconsequential. The differences in σ_o for these systems are small

and, moreover, much of the surface is taken up by surfactant at this degree of coverage.

Rehfeld (58) has studied the interfacial tension of aqueous SDS solutions against various hydrocarbon liquids. He represented his interfacial tension data using an equation in terms of lnc and lnc^2. Area values derived by differentiation of fitted equations are very sensitive to the functional representation and to the range of variation of the data. For comparison between very similar sets of data which have been treated in the same manner these data are more reliable. Table 5.5 lists the interfacial tensions at surface coverages similar to those of sodium dodecyl sulfate micelles. These values are somewhat lower than those from the data of Haydon and Taylor.(135,151) The difference between these sets of data is most likely to be due to the determination of the area A from differentiation of equations expressing γ as a function of ln c. On a relative basis the data in Table 5.5 show that the interfacial tension at the same area per surfactant monomer is independent of the chain length of the hydrocarbon liquid over a wide range from hexane to heptadecane.

The above data indicate that at hydrocarbon-water interfaces containing sodium alkyl sulfates at charge densities similar to that of micelles, the

TABLE 5.5

Interfacial Tensions of Alkane/SDS Aqueous Solutions at 69.1Å^2/SDS Monomer at 25°C

alkane	γ/ergs cm^2
n-hexane	29.8
n-octane	29.5
n-nonane	29.1
n-decane	31.7
n-heptadecane	30.0

S.J. Rehfeld, J. Phys. Chem., 71, 738 (1967)

interfacial tension depends almost entirely on the value of the area per surfactant monomer and not upon the chain length of the hydrocarbon, or the surfactant, or any added electrolyte concentration. Further evidence for this comes from the study of Kling and Lange. They showed that for C_{10}, C_{12} and C_{14} alkyl sulfates against n-heptane, the data could be described by a single π-A curve. (134). Brooks and Pethica (153) have measured the interfacial tension against heptane of trimethyl ammonium surfactants.

They found that the same π/1/A curve could describe the data for the C_{12}, C_{18}, and C_{22} homologs. A significant difference, about 5 dynes cm $^{-1}$, was noted between this curve and the one describing the alkyl sulfate data at A values applicable to micellar systems. This emphasizes the importance of the nature of the specific head group ion determining the tension. At the same π (same σ) the alkyl sulfates have a lower A than the trimethyl- ammonium bromides (TABs). This means that more alkyl sulfates than TABs must go to the surface to lower σ, the TABs being more efficient at surface tension lowering. All of these data are consistent with the Butler relationship outlined earlier, which indicated that for homologs having the same co-area at the interface the same A value is expected for

any given partial molar volume regardless of the surfactant chain length.

The above findings support the validity of the assumption of the fluid model that at bulk planar hydrocarbon/aqueous surfactant solution interfaces the interfacial tension is determined primarily by the nature of the headgroup and the area available to each head group at the interface. Extending these ideas to micelles, the fluid model of the micelle describes the core as a hydrocarbon fluid.(9,23,28) The above finding that hydrocarbon chain length and surfactant chain length do not have a significant effect on interfacial tension for the systems studied supports the use of bulk planar interfacial tension data to estimate the micellar interfacial tension .

Further verifiation of these assumptions is provided by comparison with experimental Laplace pressure measurements. For the alkyl sulfates the interfacial tensions of micelles were estimated from the 20°C data in Figure 5.1. For 25°C estimates these σ values have been reduced by 0.5 dynes cm^{-1}. For DeTAB and CTAB values from the work of Brooks and Pethica were used.(153) The area per surfactant molecule in the micelle was estimated from the partial molar volume of a surfactant monomer in a micelle (154,155,156) and the micelle molecular weight from light

scattering data (15,157). On the basis of a spherical geometry for the micelle, the area per surfactant head group was calculated to be 69.1 $Å^2$ for SDS, 71.8 $Å^2$ for SDeS, 74.7 $Å^2$ for SOS, 58.7 $Å^2$ for SDS in 0.1M NaCl, 81.3 $Å^2$ for DeTAB, and 77.4 $Å^2$ for CTAB. The interfacial tensions in dynes cm^{-1} used at these surface coverages were, for SDS 33.1; SDeS 34.2, SOS 35.1; SDS in 0.1M NaCl 27.3; DeTAB 32.8; and CTAB 31.0.

The radius chosen for use in equation 5.3 must correspond to the surface of tension of the micelle. The position of this surface is not known. To a good approximation the value of the radius at the surface of tension may be assumed to be equal to the hydrocarbon radius. This approach was also recently adopted by Ericksson and co-workers (125) as a convenient choice for the hydrocarbon/water interface. It is also consistent with theoretical evidence that at high curvature the surface of tension is likely to be about 1-2Å inward of the physical surface.(158) The radius at hydrocarbon core-water interface was calculated from the micellar volume used above by subtraction of the volume of the headgroup.(154-156,159)

In Table 5.6 the values of the micellar Laplace pressure obtained in this manner from equation 5.3 are compared with those determined from gas solubilities. For SOS, SDeS, SDS and CTAB the values agree within 10%. The

TABLE 5.6

Comparison of Experimental and Calculated LaPlace Pressures, ΔP (atm)

	SOS	SDeS	SDS	SDS (0.1M NaCl)	DeTAB	CTAB
$\Delta P_{(expt)}$	615	510	440	390	580	330
$\Delta P_{(calc)}$	645	500	395	280	470	290

$\Delta P_{(calc)} = 2\delta/\text{radius}$

disagreement in the case of SDS in 0.1M NaCl may well be due to significant deviation from sphericity of these micelles, which are much larger than those in water.(153,160) If these micelles are assumed to be spherical, the calculated radius of the hydrocarbon core is 19.5Å. This is significantly greater than the 16.6Å, estimated by Stigter (161), for the fully stretched out length of the dodecyl chain. Therefore, these micelles are very likely to be non-spherical. The agreement between experimental and calculated values for Laplace pressures provides strong support for the fluid model of the micelle. It also provides a reasonable method for calculating micellar Laplace pressures.

Alternatively, the micelle may be regarded as possessing two interfaces or surfaces of tension. At the inner interface the hydrocarbon core contacts water and a tension, γ_0, equal to a hydrocarbon/water interface is present, leading to a higher Laplace pressure than produced by γ. The partial counteracting influence of π is located at the outer radius or the full micellar radius. The resulting pressure is given by

$$\Delta P = \frac{2\gamma_0}{R_{inner}} - \frac{2\pi}{R_{outer}} \qquad (5.7)$$

This assessment increases the calculated values of the Laplace pressure by

between l5 to 30 atm., about 5% of the total.

According to equation 5.7 the Laplace pressure due to γ_0 is reduced by a negative pressure originating from the π values. Stigter ascribed this outward (negative) pressure to charge effects originating from headgroup repulsion.(161) Using some older aggregation numbers available to him (161-163), and applying the Gouy-Chapman theory to micelles assumed to have spherical double layers, Stigter calculated this electrical pressure to be 10.86 dynes cm^{-2} for SDS micelles in water at 25°C. From equation 5.3, this corresponds to a π value of ll dynes/cm. Ignoring the positive γ_0 term of equation 5.7, Stigter concluded that the micelle was under this negative pressure. If a γ_0 value of 52 dynes/cm is used in equation 5.7, these calculations would indicate a higher micellar interfacial tension than that suggested by measurements on hydrocarbon-aqueous surfactant systems. However, the π for charged surfactants at bulk interfaces has been shown to be determined primarily by an electrostatic term and a nonelectrostatic term.(164) The latter term is due to the co-area of the surfactant molecules. This contribution to π was ignored by Stigter.

Stigter's results for the electrical contribution to π, 11 dyne/cm, for spherical micelles, can be compared with predictions for planar surfaces

which are also based upon Gouy-Chapman theory. Such an equation, developed by Davies (164,165), gives a value for the electrical contribution to π for a planar surface about 1 dyne/cm higher at the same surface charge density as used by Stigter for spherical SDS micelles. It is thus interesting to note that curvature of micelles may reduce the electrical contribution to π slightly.

In conclusion, the reliability of the approach employed here has been supported by the excellent agreement found between Laplace pressures estimated from the fluid model of micelles and those experimentally determined from gas solubility data. The search for compensating effects and incorrect assumptions in the model is hampered by our lack of knowledge of the precise nature of the micelle-water interface. Uncertainty with respect to the extent of fluctuation of the micellar interface raises questions about the assumption of exact sphericity. Although ignored here on the basis of experimental evidence (149), curvature effects are expected by theory (148,158) to reduce the value of σ_0 relative to the planar interface. As observed above, curvature effects may also significantly reduce the electrical contribution to π. Together these effects of curvature would tend to compensate each other at least

partly, according to equation 5.7. For highly curved surfaces, molecular theories suggest that the radius at the surface of tension is likely to be 1-2 Å less than that at the physical surface.(158) Since γ_0 and radius values are both likely to be lower than estimated, inaccuracies in each may cancel in the calculation of Laplace pressure.

In summary, the above examination of available data on micellar Laplace pressures and interfacial tensions in relation to a simple fluid model for the micelle has produced encouraging results. The model provides a means by which Laplace pressures for anionic and cationic surfactants have been calculated. Butler's equation has also been demonstrated to be a reasonable indicator of the value of interfacial tension needed for these calculations. The agreement of experimental and calculated Laplace pressure values suggests that the values of γ at hydrocarbon-aqueous surfactant solution interfaces and at the micelle-water interface are of similar magnitude. In view of the importance of micellar interfacial tension to thermodynamic descriptions of micelle formation these findings are likely to be of interest in theoretical considerations.

B. Solubilization of Interfacially Active Species and the Application of the Two State Model.

1.Background:

Much of the research on the solubilization of molecules in micelles has centered around attempts at determining the location of the solubilizate in micelles.(46-56) Results are often interpreted in terms of a single environment fro the solubilizate.(24,31,46-48) Models of solubilization have also been developed based upon a single location for the solubilizate in the micelle(166).

The work of Mukerjee and Cardinal (28,50) led to the development of a two-state model for micellar solubilization. One of the more direct evidences for the need for two or more different states was a finding by Mukerjee and Cardinal (50) that for benzene and the alkylbenzenes the micellar environment became continuously less polar as the number and size of the alkyl groups increased. The systematic variation of microenvironmental polarity was not consistent with a single environment for the solubilizate in the micelle. These workers postulated that the solubilizate in the micelle was distributed between a non-polar "dissolved"

state associated with the hydrocarbon core of the micelle and a more polar "adsorbed" state at the micelle-water interface. It was noted that a significant feature of the micelle was that it possessed an enormous interfacial area relative to its volume. If this geometrical feature is combined with high interfacial activity even small amounts of solubilizate in the micelle core can be in distribution equilibrium with considerable amounts of solubilizate at the micelle/water interface. The "adsorbed" state can thus potentially be the only state of practical significance, containing more than 99.9% of the molecules, as shown later for some solubilizates.

Pyter, Ramachandran, and Mukerjee (52) applied the two-state model to the nitroxides TEMPO and OTEMPO. These are considerably more surface active than benzene, and some of the problems raised in this study are pertinent for this discussion. They determined the micelle-water partition coefficients in several surfactant systems. The partition coefficients between dodecane and water and interfacial activities at the dodecane-water interface were also measured. The dodecane-water partition coefficients corrected for the Laplace pressure effect gave an estimate of the partitioning into the micellar core from water. The experimental

micelle-water partition coefficients were found to be 71 times higher for TEMPO and 1600 times higher for OTEMPO. On the basis of the two-state model, these values are the ratios of the nitroxides adsorbed at the micelle-water interface to that in the core. From the interfacial adsorption to bulk dodecane-water interface, the same ratio was estimated to be about 400 for TEMPO and 5300 for OTEMPO. The second method is qualitatively consistent with the first one, since both show the over-whelming importance of the adsorbed layer. However, a discrepancy by factors of 5.6 and 3.3 was noted. A possible contributory factor resulting in this relatively large discrepancy is the assumption that the adsorption to the micelle surface is the same as the adsorption to a hydrocarbon/water interface containing no polar group.

2. Scope and Aim:

Adsorption to the micelle/water interface cannot be measured directly. In terms of a model of a fluid micelle with a polar coat, an appropriate model system for adsorption of any solubilizate to the micelle/water surface is the adsorption of the same solubilizate to a bulk hydrocarbon liquid/water interface containing surfactant molecules at the same coverage as in the micelle. Such data for bulk planar surfaces are not

available. In order to use adsorption estimates to hydrocarbon/water interfaces without polar groups originating from surfactant head groups or counterions, a correction for the presence of polar groups at the micelle/ water interface is needed. A thermodynamic approach has been developed here which provides a suitable correction for the presence of such polar groups. Recently, hydrocarbon/water distribution coefficients, micelle/ water distribution coefficients, and estimates of adsorption to hydrocarbon/water interfaces for a number of highly interfacially active compounds have become available from different sources.(45,52,119,170-178) The availablity of these data, including some systems where 99.9% of the molecules are at the interface, coupled with the new approach for correcting the adsorption data, allows a searching test of the two-state model.

In this section the relationship of the two micellar states to parameters which can be measured or estimated are presented. The correction factor for adsorption in the presence of surfactant is presented. Data on the micelle/water partition coefficients of some interfacially active substances are analyzed in relation to the two-state model.

3. The Two State Model

The first state which will be examined is the dissolved state. In this state the molecules are in a hydrocarbon-like environment subject to a high Laplace pressure. Since the micelle core is essentially fluid-like,(16,150) a hydrocarbon solvent provides a suitable model for the core. For studies at infinite dilution, the hydrocarbon/water partition coefficient, $K_{h/w}$, provides a starting point for describing solubilization. If the solubilizate has a low solubility in the micelle, the two-state model at its present state of development may be used to describe micellar solubilization at saturation. Analysis of such data is presented in the next chapter. In this case the mole fraction solubility, x_h, of the solubilizate in a hydrocarbon of chain length equal to that of the surfactant monomer is used to assess the solubility in the hydrocarbon core of the micelle. As described in the last section, a high Laplace pressure, ΔP, also exists within the micelle. The mole fraction in the dissolved state, x_d, is given by:

$$x_d = x_h \exp(-\Delta PV/RT) \qquad (5.8)$$

An equilibrium exists between the dissolved and adsorbed states. The concentration in the adsorbed state, x_a, is related to the adsorptivity of the molecule and the area available for adsorption:

$$x_a = \Gamma A f \tag{5.9}$$

where Γ is the interfacial excess of a solubilizate at a hydrocarbon/water interface, f is the correction factor for the effect of the headgroup on adsorption, to be discussed in detail below, and A is the micelle/water interfacial area per mole of surfactant. Combining equations (5.8) and (5.9) gives

$$x_m = x_d + x_a = x_h \exp(-\Delta PV/RT)[1 + \Gamma A f/x_d] \tag{5.10}$$

A similar relation holds for the micelle/water partition coefficient, $K_{m/w}$

$$K_{m/w} = K_{h/w} \exp(-\Delta PV/RT)\,[1 + \Gamma A f/x_d] \tag{5.11}$$

The interfacial excess is related to the lowering of interfacial tension by:

$$\Gamma = \frac{-1}{RT}\frac{\delta\gamma}{\delta \ln a} = \frac{-x}{RT}\frac{\delta\gamma}{\delta x}\frac{1}{\frac{\delta \ln f}{\delta \ln x}+1} \qquad (5.12)$$

where f is the activity coefficient and a is the activity.

At infinite dilution the quantity $\frac{\ln f}{\ln x} = 0$, and $\Gamma = \frac{-1}{RT}\frac{\delta\gamma}{\delta \ln x}$.

This means that the quantity Γ/x_d in equations (5.10) and (5.11) can be evaluated from the relation:

$$\frac{\Gamma}{x_h} = \frac{-1}{RT}\frac{\delta\gamma}{\delta x}$$

The magnitude of A must be stressed. Light scattering (15) or other studies (41,160) can estimate a micellar molecular weight which, if the density and micellar geometry are known, can provide an estimate of the surface area of the micelles. In an SDS micelle of 62 monomers, the interfacial area per mole of surfactant monomers is $4.2 \times 10^9 cm^2$. One mole of dodecane (228 ml) divided into 0.5 million 1mm diameter spheres would have a total surface area of $1.4 \times 10^4 cm^2$, five orders of magnitude less than the micelle. One micron spheres would have a total surface area still three orders of magnitude

less than the micelle. One micron spheres would have a total surface area still three orders of magnitude less than the micelle. Thus the magnitude of the micelle's interfacial area can potentially make the second term in equation (5.7) significant and even predominant.

The presence of polar groups of the surfactant itself reduces the interface available for adsorption of nonionic solubilizates. The typical micellar surface has an area per surfactant headgroup of about 70Å^2/charge. Studies of adsorption of ionic surfactants to hydrocarbon/water interfaces report estimates of co-areas of surfactant molecules in the range of 30-40 Å^2/charge.(134) A significant portion of the interface is, therefore, unavailable for adsorption.

The competition between surfactant and solubilizate for an interface is described below in terms of a new thermodynamic approach. On the basis of a monolayer of molecules at the surface, the interfacial tension, σ, between two phases can be described by Butler's equation.(94)

$$\mu_i^s = \mu_i^{o,s} + RT \ln(x_i^s f_i^s) + \sigma a_i \qquad (5.13)$$

where μ is the chemical potential of component i, superscript s stands

for surface, superscript o stands for standard state, and a_i is the partial molar area of component i. In the bulk the chemical potential can be written as

$$\mu_i^l = \mu_i^{0,l} + RT \ln(x_i^l f_i^l) \qquad (5.14)$$

where superscript l stands for bulk (liquid). At equilibrium $\mu_i^s = \mu_i^l$. For the solvent, species 1,

$$\mu_1^{o,s} = \mu_1^{o,l} + \gamma_0 a$$

where γ_0 is the interfacial tension in the absence of any additive. If f_1^s and f_1^l are assumed to be unity, the above relationships yield equation 5.15. For surfactant component 2, a 1-1 electrolyte, and the uncharged interfacially active component 3 solubilizate, equations 5.16 and 5.17 can be derived on similar bases.

$$x_1^s = x_1^l \exp(-\pi a_1/RT) \qquad (5.15)$$

$$x_2^s = x_2^l f_\pm^l \exp(A) \exp(-\pi a_2/2RT) \qquad (5.16)$$

$$x_3^s = x_3^l \exp(B) \exp(-\pi a_3/RT) \qquad (5.17)$$

In these equations, $f_{\pm}$ is the mean ionic activity coefficient of the surfactant, π is γ_0-γ, and a_2 and a_3 are the partial molar areas of components 2 and 3 respectively. The factor of two arises in equation 5.16 since the mole fraction of a 1-1 electrolyte at the electroneutral interface is twice the mole fraction of each of the ionic species.(164) The quantities f_3^l, f_3^s, and $f_{\pm}^s$ are all assumed to be unity. Exp(A) and exp(B) are measures of free energies of adsorption of components 2 and 3, respectively. (164,167,168) Values for the terms A and B can be determined for a particular surfactant or solubilizate independently in two-component systems from experimental values of π and activity. Estimation of partial molal areas at interfaces is difficult. (99,120) Often these terms are treated as adjustable parameters.(103) In this study the parameter used for a_1 corresponds to 7.62 $Å^2$/water molecule, which was derived from the average hard sphere diameter of water for which values in the literature ranged from 2.50 - 2.93Å.(152) The a_2 parameter calculated from SDS adsorption data (135) and π-A calculation used here has been shown earlier. The same parameter has been used for all surfactants. The choice of the a_3 term, partial molal area of solubilizate, will be discussed later in

relation to individual solubilizates.

This treatment for a three component system provides a means for estimating the mole fraction of solubilizate at the micelle/water interface, x_3^s, in the presence and absence of surfactant. Equations 5.15 - 5.17 are subject to the condition $x^s + 2x_2^s + x_3^s = 1$. At infinite dilution of component three in the absence of surfactant, $\pi=0$ and in the presence of surfactant $\pi=\pi_s$. Therefore from equation 5.17

$$\frac{x_3^s(\text{surfactant present})}{x_3^s(\text{no surfactant})} = \exp(-\pi_s a_3/RT) \qquad (5.18)$$

The ratio of the number of solubilizate molecules at the surface, n_3^s, in the presence and absence of surfactant is

$$\frac{n_3^s(\text{surfactant present})}{n_3^s(\text{no surfactant})} = \frac{n_1^s + 2n_2^s}{n_1^s} \exp(-\pi_s a_3/RT) \qquad (5.19)$$

where $n_1^s = 1/a_1$ and,

$$n_1^s + 2n_2^s = 1/(x_1^s a_1 + x_2^s/a_2)$$

Equation 5.19 provides the correction factor,f, for the competitive adsorption of a solubilizate and surfactant to an interface. Since the

solubilizate is at infinite dilution, the interfacial tension lowering, π_s, is due to the surfactant only. The value of π_s determines the values of x_1^s and x_2^s from equation 5.15. Equation 5.19 shows that, since π_s is a positive quantity, n_3^s is lower in the presence than in the absence of surfactant.

The competitive adsorption of a surfactant and simple non-electrolytes to an oil/water interface has not been studied extensively. Some experimenal data by Jho and King (169) allow for a test of equation 5.19 for bulk interfaces. These workers measured the adsorptions of dimethyl ether to the hexane/water interface in the presence and absence of sodium dodecyl sulfonate (SDSO). From published diagrams of the surface excess of dimethyl ether as a function of pressure of the gas at three fixed concentrations of surfactant, the relative values of the surface excess at low pressure of dimethyl ether determined from values of $(-\delta\sigma/\delta P)_{P\to 0}$ have been estimated.

Table 5.7 shows the large effect of the surfactant. As indicated in the table the adsorptivity $(-\delta\sigma/\delta x)$ of solubilizate in the presence and absence of surfactant decreases by a factor of six from 40 ergs cm^{-2} atm^{-1} in the absence of surfactant to 6.7 in the presence of the highest concentration of

TABLE 5.7

Effect of Sodium Dodecyl Sulfonate on the Adsorption of Dimethyl Ether at the Heptane-Water Interface (Data of Jho and King, 1981)[a]

Concentration of Sodium Dodecyl Sulfonate moles/l	$-\frac{\delta\gamma}{\delta p}$ (ergs $cm^{-2}atm^{-1}$) ($p\to 0$) (exptl)	$-\frac{\delta\gamma}{\delta p}$[b] ($p\to 0$) (calc)
0	40.0	—
.002	9.5	9.9
.003	7.7	7.7
.004	6.7	6.2

a. ref. 168

b. 18.1 $Å^2$/ molecule used,

$V^{2/3}N^{1/3}$ calculation gives 24 $Å^2$

surfactant. Jho and King gave a qualitative explanation for this effect based upon competitive adsorption.(169) In order to test the applicability of equation 5.19 to these data, we have assumed that the partial molal area of sodium dodecyl sulfonate and sodium dodecyl sulfate are identical. The values for $-\delta\sigma/\delta x$ in the presence of surfactant determined on the basis of values calculated for the left hand side of equation 5.19 are tabulated. Using a mean area of 18.1Å^2 for the area of dimethyl ether, a nearly quantitative agreement is obtained from the three surfactant concentrations studied. This value of the mean area which produces this agreement with theory is reasonable although somewhat lower than the value which would be expected from $(V/N)^{2/3}$, 24Å^2/molecule (169), a commonly used approximate estimate of molar area.(103,108) An overcorrection of f from 35-50% over the experimental range would result from the use of 24Å^2/molecule. The effect of the surfactant polar head groups may be overcorrected somewhat by the use of $V^{2/3}$ estimates. The assumption of a value of unity for the activity coefficients in the monolayer model (equations 5.15-51.7) is also likely to influence the magnitude of the effective area value which produces fit to the data. The agreement between experiment and theory using a single reasonable value

for the area term provides support for the extension of the use of equation 5.19 to micelles.

Preferred orientations of molecules at an interface must be taken into account in the estimation of partial molar areas. At interfaces some asymmetrical molecules are likely to be oriented. For such molecules the commonly used $V^{2/3}$ are unrealistic. In the subsequent analysis of micellar solubilization, amphipathic molecules which would be expected to be strongly oriented at the interface, such as alcohols, ketones and amides, were assigned an area of 20.5Å^2, which corresponds to the closest packing for hydrocarbon chains.(4,119,99)

4. Data Analysis On the Basis of the Two-State Model:

The success of the two-state model in describing the micelle/water partition coefficients for interfacially active solubilizates is demonstrated in Table 5.8. In this table data from the literature for the partitioning into SDS micelles of alkanols, ketones, and nitroxides is compared with values calculated on the basis of the two-state model. (45,52,172) Also displayed are the hydrocarbon/water partition coefficient $K_{m/w}$,(170,171) along with its correction for micellar Laplace pressure, the value of $-\delta\sigma/\delta x$, (119,171) and the term $\Gamma Af/x$ of equation

TABLE 5.8

Comparison of SDS Micelle/Water Partition Coefficients, $K_{m/w}$, From Experimental Measurements and From the Two-State Model For Several Interfacially Active Compounds

	$K_{h/w}$	$K_{h/w}\exp(-\Delta PV/RT)$	$\frac{d\gamma}{dx} \times 10^{-3}$	$\frac{\Gamma A f}{x}$	$K_{m/w}$ (calc)	$K_{m/w}$ (expt)
1-Butanol	1.4[a]	0.27	20[b]	990	270	300[c]
1-Pentanol	6.2[a]	0.87	15[b]	740	650	720[c]
1-Hexanol	20.8[a]	2.2	19[b]	930	2000	2250[c]
1-Heptanol	91.7[a]	7.1	15[b]	730	5200	6220[c]
2-Butanone	4.6[d]	0.92	2.6[d]	130	120	140[e]
2-Pentanone	22[d]	3.2	1.6[d]	78	250	270[e]
2-Heptanone	260[d]	20.2	3.0[d]	150	3070	2300[e]
TEMPO	280[f]	12.4	2.4[f]	120	1490	1750[f]
OTEMPO	2.7[f]	0.09	32[f]	1600	150	290[f]

a. ref. 170 b. ref.119 c. ref.45 d.ref.171 e. ref.172 f. ref.52

5.11, which is the estimated ratio of adsorbed to dissolved molecules on the basis of the two-state model. Competitive adsorption (equation 5.19) was used to estimate the amount of the solubilizate at the interface. The π value used was 19 dynes/cm on the basis of interfacial tension data at surfactant coverage similar to that found in the SDS micelle.(135,151)

We can see from the overall agreement between $K_{m/w}$(calc) and $K_{m/w}$(expt) that the two-state model including Laplace pressure and competitive adsorption is capable of describing the solubilization of three classes of interfacially active molecules - alkanols, ketones and nitroxides. Analysis of the data begins with the interaction of the solubilizate with hydrocarbon as indicated by the $K_{h/w}$. The $K_{m/w}$ values are all much larger than the $K_{h/w}$ values. However, as the initial indicator of interactions between the solubilizate and the micelle, trends in $K_{h/w}$ are reflected in trends of micelle/water partition coefficients for compounds within the same class, having the same interfacial activity. The molecules with the higher $K_{h/w}$ have the higher $K_{m/w}$. For example $K_{h/w}$ increases continuously from butanol (1.4) to heptanol (91.7) as does $K_{m/w}$ (300 -

6220). However, when molecules of different types which do not have the same interfacial activity are compared, this trend is not seen. For example, 2-butanone has a higher $K_{h/w}$ (4.6) than butanol (1.4) yet the $K_{m/w}$ of 2-butanone (140) is about one-half that of butanol (300).

The effect of Laplace pressure, an intrinsic feature of the micelle due to its structure,(18) must be taken into account. This pressure has been demonstrated to influence the micellar solubility of hydrocarbon gases (23,126-131) and will influence the partitioning into micelles of all solubilizates.(23,52) The Laplace pressure corrected $K_{h/w}$ is shown in the second column of Table 5.8. The magnitude of the trends in this value for molecules of similar interfacial activity is much closer to that of the experimental $K_{m/w}$ than is the trend in $K_{h/w}$. For example, a 21-fold increase in $K_{m/w}$ and a 26-fold increase in the Laplace pressure corrected $K_{h/w}$ is seen in going from butanol to heptanol, while the $K_{h/w}$ shows a 65 fold increase. The molar volume effect, which is accounted for by Laplace pressure, is indicated by the above comparison.

The major factor influencing the micellar solubilization of the compounds listed in Table 5.8 is their interfacial activity. There is little

question that these molecules will expose themselves to water when solubilized in a micelle.(9,23,179) They contain polar groups which can act as hydrogen bond donors or acceptors. In this way they are amphipathic just as are the surfactants which have aggregated to form the micelle. It is thus quite reasonable to expect that nearly 1000 times as much butanol is at the surface of the micelle as that in the core. The amount in the core cannot be neglected in determination of $K_{m/w}$. Only through reasonable assessment of the amount in the core, based upon interactions between the solubilizate and the hydrocarbon chains and a knowledge of micellar structure, can an estimate of $K_{m/w}$ be achieved.

Recently some experimental values for the micellar partitioning of some amides and long chain alcohols in alkyl sulfates have been published.(173) These values were determined through the cmc decreasing ability of the solubilizate. They are likely to be subject to somewhat greater errors than other methods because amphiphatic molecules are known to achieve high levels in the micelle near the cmc.(8,23,180) The data, however, are likely to be reliable to within an order of magnitude. Table 5.9 lists the experimental values along with those calculated by the present model, the hydrocarbon/ water partition coefficient, the Laplace pressure correction

TABLE 5.9

Comparison of Micelle/Water Partition Coefficients For n-Amides and n-Alkanols From Experimental Measurements and From the Two-State Model

Solubilizate	Surfactant	$K_{h/w}$[a]	$K_{h/wexp}(-\Delta PV/RT)$	$-\delta\gamma/\delta x$[a]	$\Gamma Af/x$	$K_{m/w}$ (calc)	$K_{m/w}$[b] (expt)
Amides							
C_3	SDeS	4.8×10^{-4}	1.07×10^{-4}	15.8×10^{6}	8.7×10^{5}	93	200
C_4	SDeS	2.1×10^{-3}	3.5×10^{-4}	16.5×10^{6}	9.1×10^{5}	310	280
C_5	SDeS	5.7×10^{-3}	7.0×10^{-4}	16.2×10^{6}	8.9×10^{5}	630	525
C_3	SDS	4.8×10^{-4}	1.32×10^{-4}	15.8×10^{6}	7.9×10^{5}	104	180
C_4	SDS	2.1×10^{-3}	4.42×10^{-4}	16.5×10^{6}	8.2×10^{5}	360	270
C_5	SDS	5.7×10^{-3}	9.37×10^{-4}	16.2×10^{6}	8.1×10^{5}	760	540
Alcohols							
C_4	SDeS	1.4[c]	.20	2.0×10^{4}	1100[d]	220	1077
C_8	SDeS	300[c]	10.7	1.48×10^{4}	820[d]	8760	9940
C_{10}	SDeS	4300[c]	75.6	1.44×10^{4}	795[d]	60200	27900
C_{10}	SDS	4300[c]	132	1.44×10^{4}	720[d]	95200	24600

a. ref.171 b. ref.173 c. ref.170 d. ref.119 e. C_x stands for x number of carbon atoms in these straight chain molecules.

and the interfacial adsorption using a 20.5 $Å^2$ molecular area of the solubilizate.

The experimental $K_{m/w}$ values in table 5.9 were determined at 43.8°C. The $K_{h/w}$ and $-\delta\sigma/\delta x$ parameters in the literature have been determined at 20 or 25°C. Therefore, the results on the alcohols are included to show the general order of magnitude agreement which is attained when the lower temperature parameters are used.

The amides have much lower $K_{h/w}$ values than those compounds discussed earlier. On the other hand their interfacial adsorptivity ($-\delta\sigma/\delta x$) is about 1000 times higher than that seen for the alcohols, ketones, or nitroxides. The adsorbed to dissolved ratios $\Gamma A f/x$ indicate that only about one part in one million of the molecules in the micelle are in the core out of contact with water. The adsorbed state might be considered to be the only state of practical interest. However, it is only through the proper evaluation of the dissolved state that an assessment of the adsorbed state is possible. The major result to be stressed here is that a reasonable value of the micelle/water partition coefficient in two different surfactants has been recovered from an assessment of the distribution of solubilizate between

adsorbed and dissolved states on the basis of experiment and theory.

The micelle/water partitioning at infinite dilution of benzene by two different surfactants, SOS and SDS, is shown in Table 5.10. Two-state model calculations are also shown. The hydrocarbon/water partition coefficient (1650) is seen to be larger than that of the micelle/water partition coefficient in each type of micelle (560 SOS, 950 SDS). (174,175) This compound is much less interfacially active ($-\delta\sigma/\delta x = 33$) than the alcohols, ketones, amides or nitroxides. It is important to note, however, that even this mild interfacial activity of benzene leads to a predominant fraction of solubilized molecules at the micellar surface. The value of the adsorbed to dissolved ratio calculated without consideration of competitive adsorption, $f=1$, is shown first for each compound. As seen for nitroxides by Pyter, Ramachandran and Mukerjee,(52) this value of the adsorbed to dissolved ratio (5.99 for SOS) is higher by a factor of about three than that which is determined from the experimental $K_{m/w}$ ((560-175)/175 = 2.2).

In order to estimate the effect of competitive adsorption, an area term for benzene must be estimated. Benzene does not have the amphipathic character of the other compounds studied in this section. Since no

preferred orientation is known for this compound at the micelle/water interface, the $(V/N)^{2/3}$ estimate is employed as a first approximation. This value is seen to overcorrect for the effect of competitive adsorption. A somewhat low calculated $K_{m/w}$ results, although even this value is of the order of magnitude found experimentally.

As discussed in the preceding chapter, aromatic molecules are hydrogen bond acceptors. An orientation of the aromatic ring lying parallel to the interface provides the most favorable position for hydrogen bonding across the interface.(83-86) The hydrogen bonding of aromatics is not strong enough to make this orientation the only one feasible, however. From data of Kiselev (181,182) on adsorption of benzene to graphon, the area of the benzene ring is 40Å^2. This provides an approximate upper limit to a reasonable interfacial area for benzene. The vanderWaals thickness of the π system is 3.7Å^2. Using these molecular dimensions a perpendicular orientation of the aromatic at the interface, which may be considered to be feasible for the asymmetric alkylbenzenes at the hydrocarbon/water interface, is 23.4Å^2.

In Table 5.10 the value of benzene area which produces agreement between the theory and experiment is found to be 18Å^2/molecule in SOS

TABLE 5.10

Solubilization of Benzene

Micellar System	$K_{h/w}$ x exp(-ΔPV/RT)	$\frac{\Gamma A f}{X}$	f	Area Å^2	$K_{m/w}^{calc}$	$K_{m/w}^{exp}$
$Na^+C_8SO_4^-$	175	5.99	1.00		1224	560[b]
$K_{h/w}$ = 1650	175	2.26	.367	18.0	560	560
$-\delta\sigma/\delta x$ = 33	175	1.45	.242	28.0[a]	430	560
$Na^+C_{12}SO_4^-$	330	5.54	1.00		2160	950[c]
$K_{h/w}$ = 1650	330	1.88	.339	17.4	950	950
$-\delta\sigma/\delta x$ = 33	330	1.83	.329	18.0	932	950
(decane/water)	330	1.15	.208	28.0	710	950

a. $(V/N)^{2/3}$ estimate

b. ref. 174

c. ref. 175

and 17.4 $Å^2$ in SDS. As shown for SDS, the difference in these two values results in little change in the calculated $K_{m/w}$ (i.e. 950 with 17.4$Å^2$ and 932 with 18.0$Å^2$). The agreement of these values using experimental data from three sources (174,175,present work) lends support to this analysis. The magnitudes of the values are also reasonable. The analysis of the data of Jho and King (169) in the previous section showed that an area term for dimethyl ether which was 75% lower than the $(V/N)^{2/3}$ approximation was required to fit the newly formulated Butler monolayer competitive adsorption model. The area values found to fit the experimental micellar data here are about 62-64% lower than the $V^{2/3}$ estimate. The need for a lower effective area at the micelle/water interface as compared with a bulk planar interface will require examination of more systems and more detailed theory. Constraints on molecular moton at the micellar interface may be important in regulating the interfacial activity of solubilizate. For benzene the $K_{h/w}$ and $K_{m/w}$ values are quite similar. Some investigators (183,184) have reasoned that such behavior indicates a non polar location for such molecules in micelles. This reasoning neglects the large Laplace pressure of the micelle, which reduces, relative to hydrocarbon, its ability to solubilize molecules. When Laplace pressure is considered, the amount

exposed to the surface becomes evident.

Figure 5.2 compares log $K_{m/w}$ (calc) and log $K_{m/w}$ (expt) in SDS to log $K_{h/w}$. The solubilizates included are those in Table 5.8, benzene in SDS and SOS, the hydrocarbon gases at one atm. pressure in SDS and cyclohexane at saturation in SOS. The straight line is the equation $K_{m/w} = K_{h/w}$. There are solubilizates on either side of this line. This demonstrates the need for a model which can address $K_{m/w}$ values both lower than and greater than hydrocarbon/water partition values. The triangles indicate the Laplace pressure correction of the hydrocarbon/water partition coefficient of the alcohols. On the basis of this degree of partitoning into the core, the amount at the interface can be determined from experimental and theoretical assessments to recover the total.

The compounds shown here have $K_{h/w}$ values ranging over five orders of magnitude. Inclusion of the amides in Table 5.9 would extend this to eight orders of magnitude. The $K_{m/w}$ values for the compounds considered span two orders of magnitude. Consistent treatment of partitioning and interfacial tension data and a model which accounts for micellar Laplace pressure and competitive adsorption to the micellar interface is seen to be

working well from these results.

Figure 5.2 log $K_{m/w}$ plotted as a function of log $K_{\substack{\text{hydrocarbon} \\ \text{alkane/water}}}$

O experimental

• calculated

Δ $K_{h/w}$ exp(-ΔPV/RT)

1. butanol
2. pentanol
3. hexanol
4. heptanol
5. OTEMPO
6. TEMPO
7. 2-butanone
8. 2-pentanone
9. 2-heptanone
10. methane
11. ethane
12. propane
13. butane
14. pentane
15. benzene SDS
16. benzene SOS
17. cyclohexane

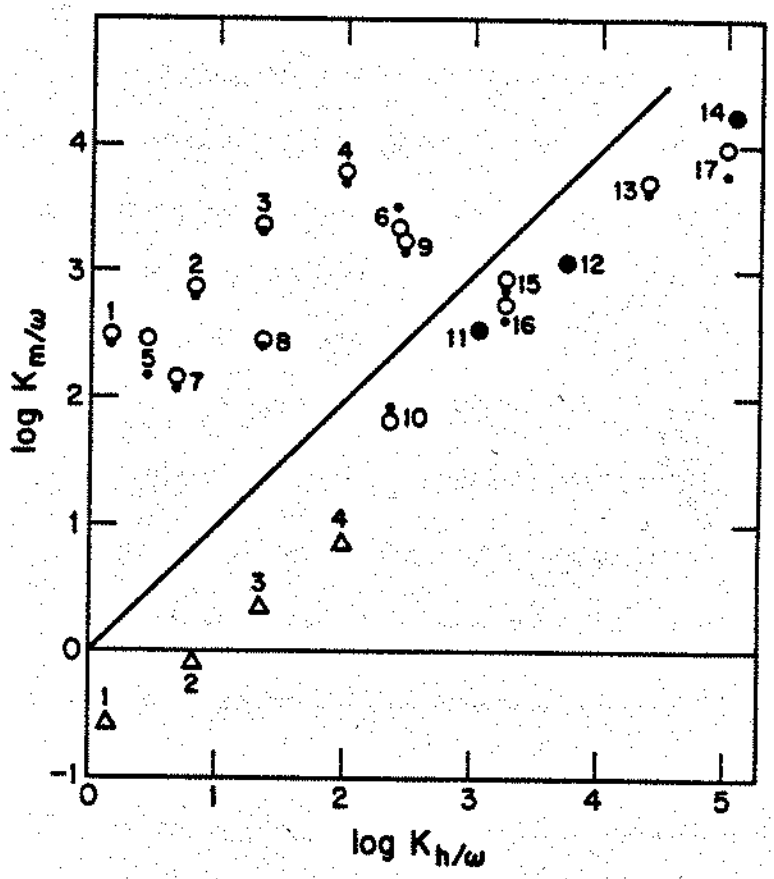
log $K_{m/\omega}$
log $K_{h/\omega}$
0
1
2
3
4
5
−1
14
17
13
6
9
12
15
16
11
10
8
7
5

C. Assessment of Head Group Effects: Comparison of Solubilization by SDS and CTAB Micelles

A complete understanding of micellar solubilization requires consideration of effects due to the surfactant polar groups on the "adsorbed" fraction of the solubilizate over and above the role of π.(eq.5.19) In the model presented above, such effects are reflected in activity coefficient terms which were ignored in the formulation of the ideal Butler model. These effects, suggestive of specific head group effects, are small in comparison with the effects arising from interfacial activity itself. As shown before, $K_{m/w}$ values can differ from $K_{h/w}$ values by a factor of 10^5 , beacuse of interfacial activity. In comparison, specific head group effects may affect $K_{m/w}$ values by factors of one to three in typical cases. In general, cationic micelles have been shown to be capable of providing a greater degree of solubilization than anions for many types of solubilizates.(35,30) For example, the mole fractions of benzene in lauryl pyridinium bromide micelles and in SDS micelles differ by 25%, although these micelles are of similar size. (35) Studies of the microenvironmental polarity of pyrene in anionic and tetraalkylammonium micelles have been performed by Almgren and coworkers (29) and Lianos

and coworkers (187). The results indicated that pyrene experiences a more polar environment in cationic micelles. These workers attributed this effect to a weak interaction between pyrene and the cation, arising from the weakly basic character of pyrene. Also the study of Jacobs and Anacker (36) on C_1 - C_4 trialkylammonium decyl bromides showed an increasing solubilization of Orange OT as the headgroup of the micelle became larger.

In this work we present an approach to the understanding of such polar group effects. Our reasoning was based upon the well-known effect of electrolyte on the aqueous solubility of nonelectrolytes(188). Essentially, the empirical relationship between solubility (S) or activity coefficient (f) of nonpolar molecules and the concentration of electrolyte in solution (C_s) has been shown to be

$$\log(S_o/S) = \log (f/f_o) = k_s C_s \qquad (5.20)$$

where k_s is a constant whose value depends upon the chemical nature of the electrolyte and the nonelectrolyte, and the subscript o refers to the solution in the absence of electrolyte. This relationship is called the Setschenow equation. A positive value of k_s indicates that the salt will decrease the solubility of the nonelectrolyte in water, which is called

salting out. Most inorganic ions cause salting out of nonelectrolytes from aqueous solutions. However, large organic ions, such as tetraalkyl ammonium salts, enhance the aqueous solubility of nonelectrolytes. Hydrophobic interactions may be involved in this effect (193), which is known as salting in or hydrotropy. These salts have negative values of k_s.(186) The molecular interactions involved in the salting-in in bulk solution are likely to exist to some extent at the micelle-water interface. This gives a qualitative explanation of the head group differences discussed. An additional fact of some interest is that Deno and Spink (185) have noted a rough proportionality between k_s and the molar volume of the nonelectrolyte. They demonstrated this relationship in both sodium sulfate and tetramethylammonium bromide solutions for a group of aromatics and alkylaromatics ranging in molar volume (V) from 89 to 177 ml/mol and for benzene and a number of polar solutes, alcohols, ethers, ketones, and aldehydes in ammonium sulfate solutions. The theory of Long and McDevit (186), which has been the most successful in qualitatively describing both salting out and salting in, also contains this proportionality.

In this preliminary investigation of the effects of head groups on micellar solubilization, we have attempted to determine the extent to

which the known ability of quaternary ammonium ions to enhance the aqueous solubility of aromatics containing no polar groups can account for the greater solubility of these compounds in cetyl trimethyl ammonium bromide micelles (CTAB) than in SDS micelles after appropriate account is made of the differences in the Laplace pressures of CTAB micelles (330 atm.) and SDS micelles (440 atm.), referred to earlier. Table 5.11 lists the mole fraction solubilities of benzene, naphthalene, biphenyl, anthracene , and pyrene in SDS and CTAB micelles, along with the molar volume of the solubilizate. The ratio of the solubility of these molecules in these two micelles is also indicated. Figure 5.3 is a plot of the natural logarithm of the ratio of the micellar mole fractions of these solubilizates as a function of the molar volume of the solubilizate. Clearly, these molecules dissolve to a greater extent in the cationic micelles. Unfortunately, there are major differences in the reported data on some systems. For example, the x_{CTAB}/x_{SDS} ratios for anthracene and pyrene differ by factors of two to three, when results of two different investigators are compared. This disagreement demonstates some of the experimental problems involved in the measurement of solubilization capacities (Chapter VI).

The data in Table 5.11 and Figure 5.3 show the general trend that the

TABLE 5.11

Mole Fraction Solubility of Benzene, Naphthalene, Anthracene, Biphenyl, and Pyrene in SDS and CTAB Micelles

Solubilizate	V ml/mol^{-1}	X_{SDS}	X_{CTAB}	X_{CTAB}/X_{SDS}
Benzene	89[a]	0.48[b]	0.78[c]	1.64
Naphthalene	123[a]	0.080[b,c]	0.25[c,d]	3.12
Anthracene	150[a]	0.00145[c]	0.0096[c]	6.62
		0.0016[e]	0.0051[e]	3.19
Biphenyl	163[f]	0.046[c]	0.22[c]	4.7
Pyrene	175[f]	0.016[c]	0.108[c]	6.75
		0.006[e]	0.015[e]	2.5

a. ref. 91
b. present work
c. ref. 29
d. ref 191
e. ref. 190
f. calculated on the basis of a 10% increase from that calculated on the basis of the solid density as indicated for naphthalene by the molar volume given in ref. 91

Figure 5.3 Natural logarithm of the ratio of the mole fraction of listed compounds in CTAB micelles to that in SDS micelles plotted as a function of the molar volume of the solubilizate.

1. Benzene
2. Naphathalene
3. Anthracene*
4. Biphenyl
5. Pyrene*

o Experimental

— $\frac{(\Delta P_{SDS} - \Delta P_{CTAB})}{RT} V$

□ Equation 5.21

Δ Equation 5.22

-- Trend indicated by Equation 5.22

* a. data of reference (29)
  b. data of reference (190)

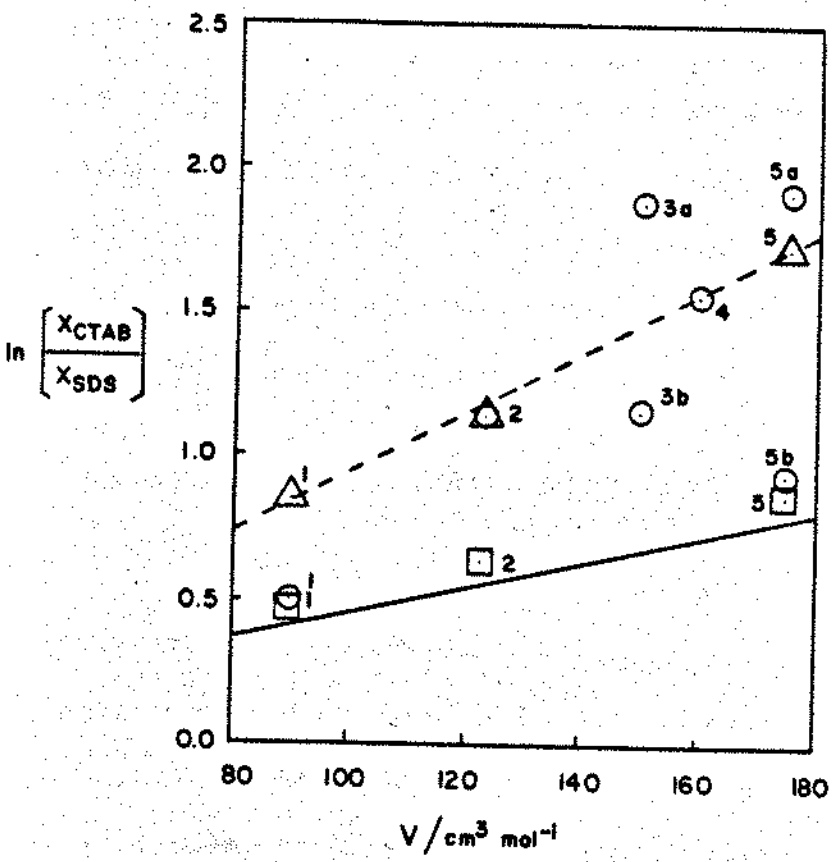
2.5
2.0
1.5
1.0
0.5
0.0
80
100
120
140
160
180
$\ln \left[\frac{x_{CTAB}}{x_{SDS}}\right]$
$V/cm^3\ mol^{-1}$
1'
2'
3a
4
5
5a
3b
5b
1
2
5

solubilizates having larger molar volume favor CTAB over SDS to a greater extent than the smaller solubilizates on a relative basis. Figure 5.3 also shows the calculated $\ln(x_{CTAB}/x_{SDS})$ values for benzene, naphthalene and pyrene when these solubilizates are at infinite dilution in micelles. The calculations are based on equation 5.10, which follows from the two-state model (equation 5.11) without any additional account being taken of specific head group effects.

$$\ln \left(\frac{X_{CTAB}}{X_{SDS}}\right) = (\Delta P_{SDS} - \Delta P_{CTAB})\frac{\overline{V}}{RT} + \ln \frac{1+A_{CTAB} f(\delta\sigma/\delta x)/RT}{1+A_{SDS} f(\delta\sigma/\delta x)/RT} \qquad (5.21)$$

The correction factor f here is based on molar areas of 23.4 $Å^2$ for the polycyclic hydrocarbons. The calculated effect of Laplace pressure alone (the first term on the right hand side of equation 5.21) is shown as the solid line. It is seen that the Laplace pressure term is the dominant term in equation 5.21 and uncertainties in the calculation of the second term are of little consequence. These calculations show that a major part of the higher solubility in CTAB than in SDS is due to the Laplace pressure effects, which also show the expected trend with molar volume. However, these effects do not provide a full explanation of the experimental data.

Equation 5.21 is expected to work better for those compounds which are at low mole fractions in the micelles, that is the larger molecules shown in Table 5.11. Structural and interfacial tension changes occurring at high loading of the micelle, particularly for benzene, are expected to be significant, and have not been incorporated into the theory calculations (equation 5.21). The deviations of experimental data points in Figure 5.3 from calculations based in equation 5.21 are larger for the larger solubilizates. The overall qualitative conclusion is that specific salting in type short range effects caused by the organic head groups in CTAB are significant and probably increase with molar volume of the solubilizate.

In order to examine if these residual salting-in effects are compatible with those observed in bulk solutions, we have introduced the factor S/S_o (>1) from equation 5.20 into the adsorption term of equation 5.21 to account for the interaction between the solubilizate and the quaternary ammonium head group. The resulting expression is

$$\ln \left(\frac{X_{CTAB}}{X_{SDS}}\right) = (\Delta P_{SDS} - \Delta P_{CTAB}) \frac{\bar{V}}{RT} + \ln \left[\frac{1+A_{CTAB} f(S/S_o)(\delta\gamma/\delta x)/RT}{1+A_{SDS}\, f(\delta\gamma/\delta x)/RT}\right] \qquad (5.22)$$

Salting in effects depend upon k_s and C_s. The concentration of head

groups at the micelle surface, C_s, has been estimated from the spacing between them to be about 3M.(248) The experimental value of k_s for benzene in aqueous solutions of tetramethyl ammonium bromide is -.0149 (189). Values of k_s for naphthalene and pyrene can be estimated from the volume ratios.(185) The dotted line in Figure 5.3, calculated using one-half of the estimated solution k_s values, gives a reasonable description of the data. The lower k_s values needed indicate that the full effect of the quaternary ammonium ion is not expressed at the micelle-water interface, as might be expected.

The overall conclusions noted presently are in line with the observations of Almgren and coworkers (29) and Lianos and coworkers (187) that a specific effect between aromatics and the cationic head group accounts for the greater polarity of the environment of aromatics in cationic micelles than in anionic micelles. It is also consistent with the greater solubility of benzene seen in tetradecyl tripropyl ammonium bromide (TTPAB) micelles than in tetradecyl trimethyl ammonium bromide (TTMAB) micelles by Venable and Nauman.(35) The TTPAB micelles, having the larger head group, solubilize more benzene. These micelles were found

to be smaller in size than TTMAB micelles (35), so that Laplace pressure effects act in the opposite direction to the observed solubilization effect. It is known that for bulk solubilities of benzene the absolute magnitude of k_s values for quaternary ammonium ions increases with the size of the alkyl chains attached to the nitrogen. (185)

In summary, we have shown from literature data on the solubilities of a number of aromatics in CTAB and SDS micelles that the ratio x_{CTAB}/x_{SDS} increases with molar volume of the solubilizate. The major portion of this increase is explained by the Laplace pressure effect, which is also dependent on molar volume. Deviations from theory were found to be compatible with a specific short range interaction between the aromatic solubilizate and the polar group of CTAB. The magnitude of the effect was found not to be as large as noted from bulk solution data at head group concentrations similar to those found at the surface of micelles. Careful experiments at dilute concentrations of aromatics in micelles would provide data to allow a quantitative examination of these effects. Accurate solubilization data for slightly soluble compounds would also facilitate further analysis. In the next chapter a new method for determining solubilization capacities is presented which can expedite

such measurements.

SOLUBILIZATION CAPACITY OF MICELLES AND A NEW METHOD FOR ITS DETERMINATION

A. Background:

One of the most important properties of micelles is that their presence allows for the enhanced solubility of most organic molecules in aqueous solution.(23,24,31) In many applications of micellar solutions, such as formulation technology, the maximum amount of solubilizate which can be introduced into solution due to the presence of the surfactant is of greatest interest.(32,33) As discussed in the introduction and preceding chapters, the enhancement of solubility is due to an association of solubilizate molecules with micelles.(23,24,33) Therefore, the ratio of the number of moles of solubilizate in the micelle to moles of surfactant in the micelle is referred to as the solubilization capacity of the micelle.(23) As with micelle-water partition coefficients discussed in the last chapter, solubilization capacity of simple solubilizates in micelles of well defined surfactants provides insight into the nature of the hydrophobic interaction and the factors which control micellar solubilization.

A review of the literature indicates that solubilization capacity measurements can be quite variable. Table 6.1 lists solubilization capacity

TABLE 6.1

Reported Values of Benzene Solubility in Aqueous SDS solutions at 25°C

Reference	SDS Concentration	Micellized Solubilizate/ Micellized Surfactant
Almgren (29)	0.05	0.57[a]
Brady & Huff (175)	0.1	0.88
	0.25	0.96
Rehfeld (47)	0.254	0.90
Chaiko et. al. (44)	0.1	1.68

a. 21±1°C

values from the literature for benzene in aqueous sodium dodecyl sulfate (SDS) solutions at concentrations above the cmc.(29,175,47,44) A threefold difference is noted between the highest and lowest values. In the hands of this investigator, two methods for determining solubilization capacity of liquids in micellar solutions proved unsatisfactory. In the turbidity method, which has been used by many workers,(24,30,37,194) known amounts of solubilizate were shaken vigorously with the aqueous surfactant solution and the turbidity of the sample was measured on a UV spectrophotometer. At concentrations greater than the solubilization capacity, turbidity is expected to increase dramatically. Turbidity measurements were not reproducible. The level of turbidity was found to decay very rapidly with time after agitation was stopped, making its determination difficult. The other method employed involved layering of the organic liquid onto the aqueous solution in long culture tubes with teflon lined screw caps. The tubes were then laid in a water bath to create the greatest surface area of contact between the phases without formation of droplets. The tubes were gently rolled intermittently. Samples of the aqueous phase were taken by syringe and analyzed spectrophotometrically in an alcohol solution as described in the introduction. The solubilization capacity results by this

method varied by ± 14%. In view of these difficulties in the determination of solubilization capacity, it was decided that a new approach should be attempted.

General considerations regarding the measurement of solubility also indicate that in certain systems conventional solubility determination methods and phase separation techniques are likely to cause complications. (196,197) The level of solubility determines the extent to which such complications will be significant. Very low solubilities, such as dodecane in water, have not as yet been determined precisely.(88) When solubilities are measured two condensed phases are usually placed in contact. A separation of these phases is required before the solubility can be measured. This is often accomplished by centrifugation or filtration. Suspended droplets or particles generated by handling or thermal convection between interfaces can usually be cleared from the phase of interest by centrifugation. If the solubility is high enough the presence of any remaining particles will not cause significant variation in measured solubility values. However, small particles or droplets which are not easily centrifuged may contain amounts of material which are large in relation to the solubility of poorly soluble compounds. Even after centrifugation,

handling in preparation for the final measurement can cause the formation of microparticles. Filtration, the other commonly used separation technique, may cause loss of material from solution due to adsorption on the filter. Some of the above problems are made even more severe by the presence of surfactant in solution. Surfactants stabilize and promote the formation of fine suspensions.(33,180) Vapor transfer, a method which avoids condensed phase contact and associated problems of the interface, is limited to use with highly volatile compounds.

In the present study a new method for determining solubility in solution is used. In this method a membrane separates a pure liquid or a concentrated suspension of a solid from the solution in which solubility is measured. Suspended particles or droplets do not cross over into, or form on, the side of interest due to the presence of the membrane. Adsorption to the membrane does not change the activity of the compound being dissolved since a large reservoir of it is present in the form of a pure liquid or concentrated suspension on one side.

Benzene, toluene, ethylbenzene, naphthalene and Orange OT were studied. SDS, SDS in NaCl aqueous solution, and sodium perfluorooctanoate (SPFO) were the surfactant systems used. For numerous reasons explained in the

introduction, the interaction of aromatic compounds with surfactant micelles is of interest in various fields. These molecules are potential carcinogens and their interactions with micelles provide a model for the interactions with physiological membranes.(66) The nature of the interaction between perfluorocarbon surfactant and nonelectrolytes is likely to be of interest in the preparation of perfluorocarbon emulsions as blood substitutes.(147) The perfluorocarbons are distinctly different from hydrocarbon alkanes in their interactions with aromatics and alkanes, large miscibility gaps being noted.(198) Work with perfluorocarbon surfactants provide a test for the two state micellar solubilization model in a different type of micelle.(199)

Orange OT is very slightly soluble in water (about 10^{-7} molar)(27) and has been used as a tag for micelles and for the determination of the cmc.(200) Its solubility in SDS micelles is low, causing little perturbation of the micelle. Therefore, it provides an excellent indicator of effects of changes in micellar structure on solubilization. Such changes from spherical to rod like structure of micelles have been noted at high salt concentrations above 0.4 M.(40,201-203) Studies of Orange OT solubility in SDS at high salt concentrations were performed and analyzed in terms of

the effect of shape changes on uptake into micelles. Orange OT is a more complex molecule than the others studied, containing 3 aromatic rings, an alcohol and an azo group. It serves as a model for complex drug molecules or other molecules of biological or technological interest for which association with lipid assemblies is of interest. Another reason for interest in Orange OT is that it has a micellar solubility in SDS similar to its hydrocarbon solubility.(27,199) This has been used to indicate that it is dissolved in a hydrocarbon environment in the core of the micelle. Since it contains a phenolic hydroxyl group, Orange OT might be expected to be somewhat interfacially active at a hydrocarbon water interface. In Chapter 4, Figure 4.14 and Table 4.13, the results of the studies of interfacial tension vs composition of Orange OT at the decane/water interface are displayed. The initial slope of that curve is approximately 2150 dynes/cm as compared with phenanthrene (63 dynes/cm), which also contains three aromatic rings, or butanol (20000 dynes/cm). Butanol was found in the last chapter to be nearly 1000 times more concentrated at the surface of SDS micelles than in the bulk. It is reasonable to conclude that a significant portion of Orange OT is also at the micellar surface. The present study addresses this point.

B. Scope and Aim:

A new experimental method for determining the solubility of molecules in surfactant solutions is presented. The method involves the use of a membrane to separate the test solution from either the pure liquid or a concentrated suspension of solid whose solubility is being measured. No phase separation is needed in this method. The membrane method is validated against a vapor transfer method for which an apparatus has been developed as described in the experimental section. These methods have been used to measure the solubilization capacity of three liquids and two solids. Experimental measurements of the solubility of benzene, toluene, ethylbenzene, napthalene, and Orange OT in SDS micelles with and without added electrolytes are presented. Measurements on benzene and toluene in SPFO micelles are also presented. These results are examined in relation to the two-state model of micellar solubilization discussed in the preceding chapter.

C. Results

1. Method testing and validation.

a. Liquids: As described in the experimental section, porous cellulose

membranes with a 12,000-14,000 MW cut off and 24Å diameter pores were used in these experiments. Cellophane membranes have been shown to be impermeable to SDS micelles (195), and therefore were not used. The membranes were kept wet at all times by filling the cells to the top or shaking constantly. This prevented the drying of the membrane, which could lead to stress on the membrane, transfer of organic liquid through the vapor, or wetting by the organic liquid. Stainless steel cells described fully in the experimental section were constructed for use with the liquids studied here.

Passage of liquids of low interfacial tension through porous membranes is known to occur.(204) In the present studies with aromatic liquids on one side of the membrane and SDS solution at concentrations above the cmc on the other side, the interfacial tension is expected to be about five dynes/cm.(58) Experimentally it was found that aqueous SDS solution did penetrate into the benzene side. About 0.1 ml of aqueous solution was at the bottom of the benzene side when samples were taken. This effect was not seen when benzene was placed against water. The passage of aqueous surfactant solution onto the organic side is likely due to the flow of surfactant solution along the organic side of the membrane driven by the

low surface tension between the surfactant solution and the organic liquid.(4)

On the aqueous side, however, penetration of fluid benzene was shown to be small. Turbidity measurements at 400 nm, where benzene does not absorb, were performed on samples of 0.1M SDS solutions which had been saturated with benzene by this dialysis method. The adsorbances measured in three different experiments were 0.004, 0.005, and 0.017. A number of other turbidity sources as well as instrumental inaccuracies could be responsible for such low absorbances. If they are ascribed to the presence of benzene alone, results from the turbidity method, which was described in the introduction to this chapter, can be used to make a rough estimation of the amount of benzene present as droplets. An approximately linear relationship between turbidity at 350 nm and benzene concentration above saturation had been obtained. Correcting these values for wavelength differences between 350 nm and 400 nm, an absorbance of 0.01 is about 0.2% of the saturation solubility of benzene in this SDS solution. Such a low value is insignificant in these experiments where the overall error is about 1-2%.

Validation of the membrane method was accomplished by comparison

with results from the vapor transfer method, which was described in the experimental section. Comparisons of solubility of benzene in water and 5 mM SDS solution, which is below the cmc of SDS aqueous solution in equilibrium with pure benzene,(47,58) are shown in Table 6.2.

The average values of the benzene concentration in water of 0.0226M and 0.0224M by dialysis and vapor transfer respectively indicate that the two methods agree within experimental error. These values are in good agreement with the literature average of 0.0228M given in a review by Mackay,(88) and employed later by Abraham.(87) In a recent review by Abraham, benzene values in water were found to range from 0.0206M to 0.0233M.(87) Good agreement is also found in the 5mM SDS solution with average values of 0.0232M and 0.0229M for dialysis and vapor transfer methods respectively. The presence of surfactant at a concentration high enough to lower the interfacial tension between the benzene and aqueous phases to 7 dynes/cm (58) has not altered the validity of the dialysis method. These results also indicate that the presence of SDS below the cmc is not significantly changing the solubility of benzene in aqueous solution.

Table 6.3 shows the solubility of benzene in SDS solutions by concurrent dialysis and vapor transfer experiments. Average values of the two

TABLE 6.2

Benzene Solubility In Water and In 5mM SDS at 25°C by Dialysis and Vapor Transfer Methods

Solvent	Benzene mol/l	Method
Water	0.0227	Dialysis
	0.0221	
	0.0222	
	0.0235	
Water	0.0222	Vapor Transfer
	0.0224	
	0.0227	
5mM SDS	0.0232	Dialysis
	0.0232	
5mM SDS	0.0224	Vapor Transfer
	0.0230	
	0.0227	
	0.0233	

TABLE 6.3

Benzene Solubility in SDS Solution in Concurrent Experiments Performed By Dialysis and Vapor Transfer at 25°C

[SDS] (M)	Benzene M	Method
0.0969[a]	0.121	dialysis
"	0.121	dialysis
"	0.122	vapor transfer flask method
0.1003[b]	0.124	dialysis
"	0.125	dialysis
"	0.126	vapor transfer flask method
0.105[c]	0.129	dialysis
"	0.132	dialysis
"	0.131	vapor transfer 6-port cell, 48 hrs
"	0.131	vapor transfer 6-port cell, 48 hrs
"	0.131	vapor transfer 6-port cell, 125 hr
"	0.131	vapor transfer 6-port cell, 125hrs

a. BDH as received - 1 dyne/cm min.
b. BDH -6 recrystallizations
c. BDH - pre 1979 lot, purified (no min. in surface tension vs conc. plot)

methods agree within ±1%. This agreement on three different occasions is a strong validation of the dialysis and vapor transfer methods. The other point noted in Table 6.3 is the equivalence of the SDS batches of different purity with respect to solubilizing power at high concentrations. The influence of small amounts of impurities is diluted out at high surfactant concentrations.

In summary, agreement between the two methods at three different concentrations of SDS above and below the cmc is noted. This confirms the validity of both methods. The results of either method are reliable to ± 2% as shown by the primary data in Tables 6.2 and 6.3.

b. Solids: As described in the experimental chapter, the solid material to be studied was placed on one side of the dialysis cell and surfactant solution of the same surfactant concentration was placed on both sides of the cell. Polycarbonate membranes of 500Å diameter pore size were used. These membranes contain capillary pores which have been cut through the membrane in contrast to the meshwork found in the cellulose membranes. Micelles of the surfactant studied are expected to be able to pass through 500Å diameter capillary pores. (40) To test this, a micellar solution containing the dye Orange OT was placed on one side of this membrane. On

the other side the surfactant solution at the same concentration without dye was placed. Orange OT is practically insoluble in water, the best estimates of its aqueous solubility being 10^{-7} molar.(27) Therefore, all of the Orange OT is associated with micelles. Any transfer of Orange OT to the other side of the membrane must occur by passage of the micelles through the membrane. The dye was found to appear on the other side of the membrane, proving that micelles do cross the membrane. Similar results with Orange OT were found by Dr. R. Sharma of this laboratory using the same membranes.

In order to determine if fine particles of solid pass through the membrane two experiments were performed. A 7.5mM solution of SDS, which is below but near the cmc, was placed on each side of the membrane with solid naphthalene on one side only for 24 hours. After the solid on the side containing it was allowed to settle, samples from both sides were drawn and diluted with an equal volume of 95% ethanol. Care was taken that no solid visible to the eye was sampled. The UV absorbances at the naphthalene peak were within 1% of each other. A rough estimate of the concentration from these readings indicates that the naphthalene was 10% below the saturation level of 2.56×10^{4} mole/liter measured in later experiments.

There was thus no evidence of solid particles being sampled on either side. In the next experiment to test for fines, Orange OT was placed on one side of the dialysis cell and a 7mM SDS solution was placed on the other side of the membrane. This SDS concentration is below the cmc of 8.1mM (5) but high enough to stabilize some suspended particles. When a sample from the non-solid-containing side was diluted with an equal volume of 95% ethanol, no significant absorbance at the visible peak for Orange OT could be noted. In these experiments any fine particles of naphthalene or Orange OT could have dissolved in the ethanol solution and increased the absorbance. Since the concentration values were of the order expected in each case, there is good evidence that fine particles are not passing through the membrane.

2. Solubilization Capacity Measurements:

Table 6.4 presents the results of the solubility studies in terms of the mole fraction of solubilizate in the micelle. In these experiments the molar concentration of solubilizate in solution was determined.

The mole ratio of solubilizate to surfactant in the micelle was calculated according to

$$MR = \frac{\text{total concentration of solubilizate in solution - aqueous solubility of solubilizate}}{\text{total concentration of surfactant in solution - cmc}}$$

TABLE 6.4

Solubilization Values for Benzene, Toluene, Ethylbenzene, Naphthalene and Orange OT in Aqueous Solutions of SDS and SPFO and in Aqueous Sodium Chloride Solution of SDS at 25°C in Terms of the Mole Fraction of Solubilizate in the Micelle

	SDS ([SDS])	SDS + NaCl		SPFO
Benzene	0.548 (0.2M)	0.617	(0.1M SDS)	0.0896 (0.3M)
	0.521 (0.1M)		(0.1M NaCl)	
	0.479 (0.05M)			
Toluene	0.485 (0.2M)	0.56[a]	(0.1M SDS)	0.0531 (0.3M)
	0.444 (0.1M)		(0.1M NaCl)	
Ethylbenzene	0.352 (0.1M)	0.457	(0.1M SDS)	
			(0.1M NaCl)	
Naphthalene	0.0802 (0.1M)	0.0848	(0.14M SDS)	
			(0.1M NaCl)	
Orange OT	0.00835 (0.2M)	0.00862	(0.12M SDS)	
			(0.1M NaCl)	
		0.0138	(0.066M SDS)	
			(0.5M NaCl)	
		0.0158	(0.064M SDS)	
			(0.6M NaCl) 30°C	

a. one measurement

The cmc was adjusted for the presence of solubilizate. For benzene at saturation the cmc decreases from 8.1mM (5) to 6mM.(58) For toluene and ethylbenzene a cmc between 8mM and 6mM was used calculated on the basis of an increase in cmc proportional to the decrease from benzene in the micellar mole fraction. For all other cases the literature value of the cmc of surfactant without solubilizate was used. In the case of Orange OT at 0.5 and 0.6M salt the cmc was neglected. Estimates of the error introduced by this asumption were in no case greater than 1%.

Literature values for the mole ratio of benzene in SDS at 25°C are listed in table 6.1. The mole ratio values of benzene determined here are 0.92, 0.91, and 1.21 at 0.05M, 0.1M and 0.2M SDS respectively. These are slightly higher but in the concentration region seen by Brady and Huff (175) 0.88 at 0.1M SDS and 0.96 at 0.25M SDS and Rehfeld, 0.90 at 0.25M SDS.(47) It is interesting to note that an increase in solubility of benzene seen by Brady and Huff (175) is also seen in the present data, and also noted for toluene.

Orange OT in SDS has also been measured by several investigators. Schott determined mole fraction values of 0.0079 in SDS and 0.0076 in SDS in 0.1M NaCl.(205) His values agreed with those of Williams, Phillips and Mysels.(27) The values found here, 0.00835 in SDS and 0.00862 in 0.12M

SDS in 0.1M NaCl, are slightly higher. The readings taken here were at a higher concentrations of SDS, which was 10 times higher than used by previous workers. Slight increases with increasing concentration as seen with benzene may be the reason for this increase. Small shape changes in the micelle with increasing concentration of surfactant in solution may account for this effect.(12) Naphthalene solubility in SDS solution has also been measured by Almgren and coworkers.(29) The mole fraction of naphthalene in SDS measured by these workers was 0.079 and 0.076 in water and 0.1M NaCl respectively. Excellent agreement is seen with the value of 0.080 in water found here. The salt values are similarly close but the present value may be higher due to the higher SDS concentration used.

D. Discussion:

1. General Considerations:

Qualitative comparison of the data presented in Table 6.4 indicates some general trends. For the same surfactant system, the saturation solubility in the micelle decreases as the size of the solubilizate increases. This is consistent with the trend noted by Stearns and coworkers (37) for benzene and the alkylbenzenes in potassium laurate. The

presence of 0.1M sodium chloride increases the amount of these compounds dissolved in the micelle. Higher salt concentrations, 0.5 to 0.6 Molar, where micelles are in the form of rods,(40) produces nearly a doubling of the Orange OT concentration in the micelle. Uptake of benzene and toluene is much lower in the perfluorocarbon surfactant SPFO than in SDS.

In the preceding chapter encouraging results were found when experimental micelle/water partition coefficients at low concentrations were compared with values calculated for the two-state model. For molecules which are interfacially active at an organic liquid-water interface, this model describes the distribution of solubilizate between two states in the micelle. One state is the dissolved state in the hydrocarbon core of the micelle, the other state is at the micelle-water interface. The effect of the Laplace pressure in the micelle arising from curvature of the interface must also be considered. The resulting relationship between the mole fraction in the micelle, x_m, and the parameters pertinent to the two-state model is reproduced below for convenience.

$$x_m = x_h \exp(-\Delta PV/RT)\left[1 + \frac{\Gamma A f}{x_d}\right] \qquad (5.1)$$

All of the parameters are experimental quantities except for f, the factor which accounts for the competitive adsorption of surfactant headgroups and solubilizate to the micellar interface. A new thermodynamic approach to this competition was presented in the preceding chapter. The factor f is related to the partial molar area of the solubilizate at the interface. This parameter cannot be measured experimentally but rather must be estimated. Analysis of published data on the adsorption of dimethyl ether to the interface between hexane and an aqueous solution of sodium dodecyl sulfonate indicated that a mean area of dimethyl ether of 18.1$Å^2$ described the data (Table 5.7) to within a mean error of 4%.(169) In the micelle other effects not noted at planar interfaces may be operative, including restrictions on interfacial orientations, packing problems, and restriction on the flexibility of hydrocarbon chains.(13,17,23,166) The micellar effects have been accounted for in the work by basing the area parameter for a particular aromatic compound on the effective area parameter for benzene, which produced agreement with the dilute solution two-state model.

Benzene is the only aromatic for which dilution solution data are

available. The effective area for the benzene molecule in the SDS micelle was found to be 17.4Å^2, in SOS 18.0Å^2. For the alkylbenzenes, some microenvironmental evidence to be presented in the next chapter indicated that no particular orientation of the alkylbenzenes at the micelle - water interface was favored. p-Xylene was found to have the same average micellar microenvironmental polarity as ethylbenzene.(50) These molecules also have the same interfacial tension against water,(50) suggesting similar interfacial activity. p-Xylene's symmetrically oriented methyl groups thus do not hinder its ability to approach the surface. Any ability of ethylbenzene to orient at the interface with its alkyl group away form water does not make this compound any more interfacially active than p-xylene. From these results we conclude that for the alkyl benzenes no specific orientation with the phenyl ring at the interface is favorable. The total area of the molecule must be taken into consideration. This was done by using the $V^{2/3}$ convention of assessing the area from the molar volume. Micellar effects were accounted for by dividing the $V^{2/3}$ value by the same factor which was found to give agreement for benzene in SDS, 1.61 (=28.03/17.4), for SDS micelles. In the smaller SPFO micelles the factor 1.56 (=28.03/18.0), from benzene data in SOS, was employed. Naphthalene

has been found to be oriented at the micelle/water interface in unpublished work in this laboratory by Mukerjee and Williams.(206) If naphthalene is hindered from free movement at the micelle/water interface then the larger molecule pyrene must also have a preferred orientation. Orange OT has a phenolic hydroxyl group which controls its interfacial activity. These larger molecules where orientation is likely are modelled as having an interfacial area the same as that of the effective value for benzene in SDS. In each of these series these estimates allow for relative comparisons.

2. Aromatic Liquids at Saturation in SDS.

As seen in Table 6.4 the amount of benzene, toluene and ethylbenzene taken up by micelles is high in relation to the number of surfactant molecules in the micelle. The structure of micelles saturated with these molecules is certainly influenced dramatically by the presence of such a large quantity of solubilizate.(23,207) Comparison with theory based upon a micelle with a very dilute concentration of solubilizate is not expected to be quantitative. Qualitative trends suggested by the two-state model are noted by the observation that the saturated concentration is lower for larger solubilizates. This is in line with both the greater effect of Laplace

pressure on larger molecules as well as the lower interfacial activity of the alkylbenzenes as chain length increases.

Table 6.5 lists the hydrocarbon-water partition coefficient, $K_{h/w}$, its correction for the Laplace pressure effect, exp(-ΔPV/RT), the value of $-\delta\gamma/\delta x$, the adsorbed to dissolved ratio, ΓAf/x, and the calculated micelle/water partition coefficient at infinite dilution, $K_{m/w}^{\infty}$, along with the experimental $K_{m/w}$ at saturation. In addition to results from the present study, the experimental results of Klevens (30,38) on the solubility of benzene, ethylbenzene, and butylbenzene in 0.5M potassium laurate, KC_{12}, are presented. Model calculations for butylbenzene shown are based upon the available SDS structural parameters and the infinite dilution activity coefficient of butylbenzene in decane calculated on the basis of regular solution theory.(91) The potassium laurate values are lower than the SDS values for benzene and ethylbenzene by about 20% in mole fraction. This is likely related to a somewhat higher Laplace pressure for these micelles since their hydrophobic chain actually contains 11 carbons, not 12 as in SDS.

TABLE 6.5

Comparison of Micelle/Water Partition Coefficients for Benzene, Toluene, Ethylbenzene and Butylbenzene from Experimental Measurements at Saturation and from the Two-State Model at Infinite Dilution.

Solubilizate	$K_{h/w}$	exp $(-\Delta PV/RT)$	Kh/w exp $(-\Delta PV/RT)$	$-\delta\gamma/\delta x$	$\Gamma Af/x$	∞ $K_{m/w}$ (calc)	(sat) $K_{m/w}$ (SDS)	(sat)[a] $K_{m/w}$ KC_{12}
Benzene	1650	.201	330	33	1.88	950	1260	1070
Toluene	6100	.147	895	30	1.54	2270	3620	
Ethylbenzene	20900	.110	2290	28	1.32	5300	9780	8220
Butylbenzene	412000	.060	24700	22	0.87	46100		92800

a. ref. 38

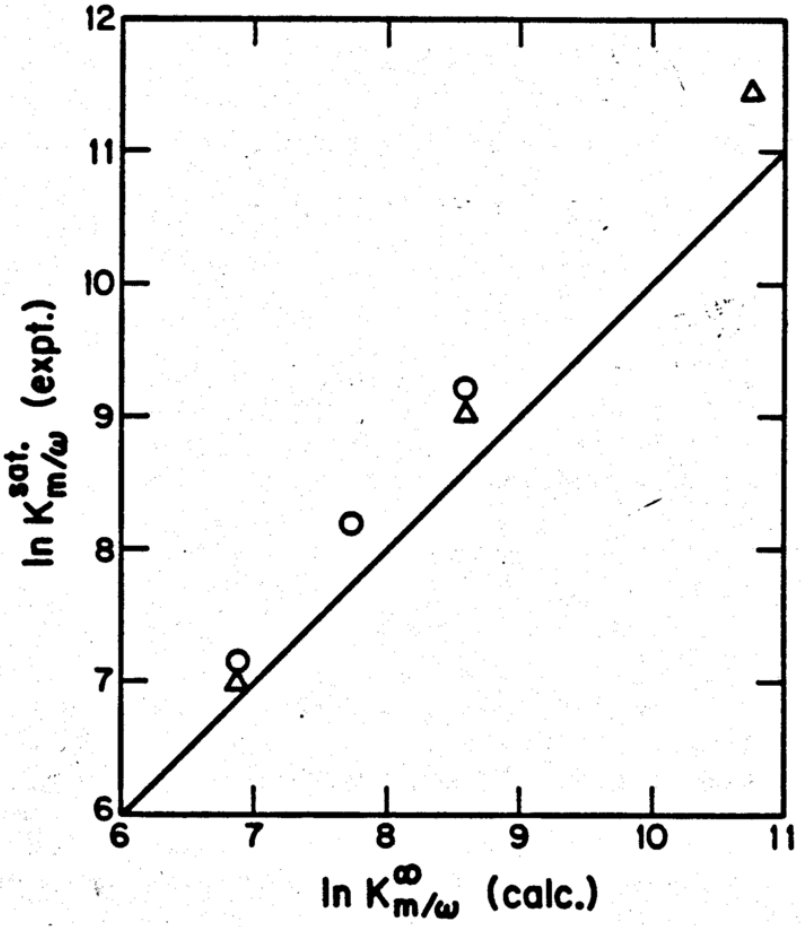
12
11
10
9
8
7
6
6
7
8
9
10
11
ln $K^{sat.}_{m/\omega}$ (expt.)
ln $K^{\infty}_{m/\omega}$ (calc.)

It is first noted that $K_{h/w}$ is greater than $K_{m/w}$ .The value of $K_{h/w}$ is seen to increase with the size of the molecule due primarily to the diminished water solubility as the alkyl chain length increases. The Laplace pressure correction decreases with the size of the solubilizate and adsorbed to dissolved ratio also decreases due to reduced interfacial activity as the alkyl chain length increases. The result is that while $K_{h/w}$ increases by 250 times from benzene to butylbenzene and 13 times from benzene to ethylbenzene, the calculated increase in $K_{m/w}$ at infinite dilution is 48 times from benzene to butylbenzene and 5.6 times from benzene to ethylbenzene. The trends in the experimental results for the micelle/water partition coefficients at saturation reveal that the increase in micelle/water partition coefficient as chain length increases is better reflected by the model than by the hydrocarbon /water partition coefficient. The $K_{m/w}$ at saturation in potassium laurate from benzene to butylbenzene increases by 87 times and in SDS from benzene to ethyl-benzene increases by 7.8 times, much closer to the calculated values.

The values of the calculated $K_{m/w}$ from the infinite dilution two-state model theory, are expected experimental values at saturation . Two primary

parameters in the calculated infinite dilution values are certain to change in the direction of higher solubility in the micelle as micellar uptake increases. The $K_{h/w}$ will increase as the compositions of aromatic in the organic phase increases, as seen in Chapter Three, due to a decrease in the activity coefficient.(79) The Laplace pressure will also decrease due to the reduction of interfacial tension caused by adsorption of interfacially active solubilizate and increase in the micellar radius upon introduction of solubilizate molecules.(207) Compensating effects due to decreases in adsorptivity with increasing solubilizate composition have a much smaller influence in these systems.

Although the calculated values are lower as expected, the ability of the model to describe the magnitude of the trends better than $K_{h/w}$ as seen above suggests its usefulness in correlating solubilization capacity data. Figure 6.1 shows the ln of the micelle-water partition coefficients at saturation plotted as a fraction of the ln of the calculated value from the infinite dilution two-state model. The 45° line of equality is shown for reference. A linear relationship between $K_{m/w\ sat}$ and $K_{m/w}^{\infty}{}_{(calc)}$ for solubilization data in both SDS and potassium laurate is noted. The trends

are nearly parallel for the SDS and potassium laurate, which is due to the consistently lower values in potassium laurate by about 20% in mole fraction. The linearity indicates that the dilute solution two-state model in association with these data provides a correlation for extrapolating and interpolating to other systems. The observed linearity for the different micellar systems indicates the general applicability of the model. This correlation can be used in conjunction with other methods presented in this work for estimates of Laplace pressure from calculable values of σ and radius and interfacial adsorption from work of adhesion on pure systems. It is expected to be useful to the practical scientist interested in a reliable estimate of solubilization capacity who lacks the time or resources for experimentation.

3. Solubility of Solids in Micelles of SDS.

Table 6.1 lists the two-state model parameters and micellar solubilities for naphthalene, pyrene, and Orange OT in SDS at 25°C. The pyrene solubilization data from two literature sources is listed. (29,190) Unlike the alkylbenzenes these compounds have a decreasing solubility in hydrocarbon with decreasing size. Therefore, the Laplace pressure correction acts in the same direction as the hydrocarbon solubility. On the

TABLE 6.6

Comparison of Micellar Solubility for Naphthalene, Pyrene and Orange OT from Experimental Measurements at Saturation and from The Two-State Model at Infinite Dilution

	x_h	$x_h \exp(-\Delta PV/RT)$	$-\frac{\delta\gamma}{\delta x}$	$\frac{\Gamma A f}{x}$	(calc) x_m	(exp) x_m
NAPHTHALENE	0.15[a]	0.0165	41	2.41	0.056	0.0802
PYRENE	0.017[b]	7.2×10^{-4}	72	4.25	3.82×10^{-3}	0.0145[b] 0.0060[c]
ORANGE OT	0.0056[d]	6.28×10^{-5}	2150	126.2	7.99×10^{-3}	0.00835 0.0079[e]

a. ref. 208 b. ref. 29 c. ref. 190 d. ref. 43 e. ref. 205

other hand, interfacial activity of these compounds increases with molecular size. The increase in the number of double bonds and the enhanced ability for hydrogen bonding which accompanies this has been shown in Chapter Four as the reason for the increase in interfacial activity of the polycyclic aromatic. Orange OT has a phenolic hydroxyl group which certainly influences the interfacial activity relative to other polycyclic aromatics and controls the orientation of this molecule at a hydrocarbon-water interface.

In general the model reproduces the data to within better than an order of magnitude. In each case the direction of change from $K_{h/w}$ to $K_{m/w}$ is reproduced, lower for naphthalene and pyrene, slightly higher for Orange OT. This is accomplished by taking account of both Laplace pressure-volume effects and interfacial activity effects, for each molecule in a consistent manner. No ad hoc disregard of either effect has been attempted to achieve a better fit. As with the alkylbenzenes the calculated values are lower than experimental because an infinite dilution model is being used.

The use of the hydrocarbon solubility as a model for hydrocarbon-solubilizate interactions in dilute solution is justified in the case of pyrene and Orange OT because of its low, <0.02, mole fraction. For

naphthalene the higher hydrocarbon (decane) solubility value used, 0.15, can best be described as a rough estimate of the dilute solution interactions with hydrocarbon liquid. Experimental hydrocarbon-water partition coefficients are not available for naphthalene. Estimates on the basis of regular solution theory give a calculated $K_{m/w}$ of 1.2×10^4. Work of Dr. N. Williams of this laboratory indicated a $K_{m/w}$ for naphthalene in dilute SDS solution of 1.35×10^4.(206) Again reasonable agreement is seen. For pyrene the experimental values in the literature disagree by more than a factor of two. Uncertainties such as these cast doubt on each value. Some support for the lower value, 0.006, (190) is seen in comparison with the work of Klevens on solubilization in potassium laurate.(38) As noted in the preceding section, an approximately 20% higher mole fraction of the aromatics in SDS than in potassium laurate is noted. For naphthalene the increase is about 30%. The lower literature value for pyrene is consistent with this effect, giving a 33% higher value in SDS. The question of the f factor for pyrene is difficult to resolve with the present data. Ignoring the competition of surfactant for the interface (f=1) gives an x_m^{calc} for pyrene in SDS of 9.8×10^{-3}; this is higher than the experimental pyrene solubility

value of 0.006, which is expected to be more reliable. If orientations are random and the total volume of pyrene at the interface is considered as in the case of the alkylbenzenes, then the calculated value for pyrene is 1.64×10^{-3}, much lower than 0.006. The hindrance of such a large molecule to free movement at the micelle/water interface due to packing problems suggests that it is reasonable to assume that its interfacial area is about the same as that of benzene.

For Orange OT the agreement between experiment and theory is excellent. This molecule has been widely studied and its analysis in solution is straightforward. The concentration of the molecule in hydrocarbon at saturation is very small (27) and provides a good model for hydrocarbon interactions for use in this dilute solution theory. Also, the interfacial activity is quite high, making its determination more precise. The results are consistent with all of the data of other systems presented in this chapter and the preceding chapter in confirming the validity of the two-state model. In the case of pyrene the result begins to suggest the need for better experiments.

The two-state model also reveals the distribution of solubilizate between the two states of greatest interest to the solution chemist, the

ratio of molecules in the adsorbed state (in contact with water) to the dissolved state (out of contact with the continuous phase). As noted this ratio ($\Gamma Af/x$) is greater than two for these compounds, indicating that a significant fraction is in contact with water. For Orange OT the same model, which predicts the solubility within error, also states that only one in 126 molecules out of contact with water. The agreement between hydrocarbon solubility and micellar solubility might be used as an indicator that Orange OT is in a hydrocarbon-like environment in SDS. Similar reasoning has been used for benzene on the basis of the free energy of transfer to the micelle from vapor.(183,184) The two-state model results indicate that agreement of thermodynamic properties is not a predictor of environment in the micelle. By taking into account Laplace pressure, which reduces the amount in the core relative to hydrocarbon, the influence of the interfacial activity of the molecule is revealed.

4. Effect of Added Electrolyte on the Solubilization Capacity of Micelles.

As seen in Table 6.4 the solubilities of the compounds studied here increase with the addition of sodium chloride. For the liquids which are highly soluble, the increase upon addition of 0.1M NaCl is about 20-30% while for naphthalene the increase is much smaller and for Orange OT it is

within experimental error.

Experiments of Hoskins and King have shown that up to 0.6M NaCl no change in the solubility of ethane in SDS micelles occurs.(127) This indicates that Laplace pressure is not changing with salt concentration, even in the region where rods are formed.(40,201-203) The average value of the Laplace pressure found by analysis of Wishnia's data for SDS micelles in 0.1M NaCl was 390 atm.(64) From the data of King, in the absence of NaCl the value was found to be 440 atm.(128-130) These estimates are within the range of experimental error of the gas solubility method.

The spherical model has been shown to be inappropriate at 0.1M NaCl. The stretched out hydrocarbon chains (16.6 Å) (161) cannot account for the larger radius (19.5Å) the spherical model would predict at 0.1M NaCl. (15,160) However, long rods for which the Laplace pressure can be written as σ/r are not seen at 0.1M NaCl. (40,201) The geometry of the intermediate structure present at this NaCl concentration is unknown and difficult to estimate.

The present data at 0.1M NaCl are consistent with these considerations. The very small change in Orange OT solubility upon addition of 0.1M NaCl is consistent with no change in Laplace pressure and no overall change in

adsorptivity. The more highly soluble molecules have perturbed the micellar structure greatly at saturation. As in the no added salt case, this leads to a reduction in interfacial tension and, therefore, probably a reduction in Laplace pressure. The higher solubility in the presence of salt indicates that these effects are expressed to a greater extent in the presence of 0.1M NaCl than in its absence.

As noted in the introduction, Orange OT was also studied at much higher salt concentrations, 0.5 and 0.6M NaCl, where rod-like micelles have been shown to exist. Missel et al showed that in 6.9mM SDS and 0.6M NaCl at 30°C micelles have a mean hydrodynamic radius of 63Å and average aggregation number of about 400.(40) This is compared to the micellar hydrodynamic radius of about 25Å and aggregation number of 60 in the absence of salt.

The results indicate an almost two-fold increase in the mole fraction solubility of Orange OT in these micelles. Other workers have seen sharp increases in the solubilization capacity of dodecyltrimethylammonium halides at salt concentrations above the sphere to rod transition.(209,210) The values of Orange OT in SDS are still low enough to consider the Orange OT as a nonperturbing probe of the micelle. Interpretation of this result

requires a knowledge of the Laplace pressure of the rod like micelle and some indication of its geometry. The Laplace pressure of a long rod is γ/r, where γ is the interfacial tension and r is the radius. For the Laplace pressure of a rod to equal that of a sphere ($\Delta P = 2\gamma/r$),(42) the interfacial tension must increase or radius of the rod decrease relative to that of the sphere. On the basis of the fluid model of the micelle, micellar interfacial tension is related to the area per head group of the surfactant monomers. Figure 5.1 shows the relationship between γ and A for sodium alkyl sulfates at hydrocarbon-aqueous surfactant solution interfaces. These values have been used in Laplace pressure calculations and found to produce good agreement with experimentally determined Laplace pressures. Using the relationship between γ and A shown in Figure 5.4, a consistent set of parameters ΔP, r, π and A were determined. The set of parameters which produces agreement between the Orange OT solubility value at 0.6M salt and the two-state model calculations is $\Delta P = 420$ atm., $\gamma = 38$ dynes/cm, $\pi =$ 15 dynes/cm, $A = 85\text{Å}^2$ and $r = 9.0\text{Å}^2$.

These results strongly support the findings of Hoskins and King that ΔP at 0.6M NaCl does not change significantly from that in water ($\Delta P = 440$

atm.).(42) Since Orange OT has a molar volume about four times that of ethane, it is more sensitive to Laplace pressure changes, yet no change is noted. Relative to the sphere, the interfacial tension of the rod is larger by about 5 dynes/cm and the radius decreases by about 45%. Smith and Alexander have commented that rod like micelles are likely to be thin.(60) Verification of this marked thinning requires further investigation.

E. Solubilization of Benzene and Toluene in Sodium Perfluorooctanoate Micelles.

The data presented in Table 6.4 are the first reported attempts at determination of the solubilization capacities of perfluorocarbon micelles. Clearly, these micelles are solubilizing much smaller mole fractions of benzene, 0.0896 and toluene, 0.0531, than are SDS micelles, 0.521 and 0.444, respectively. The benzene value in SPFO is even lower than that found in sodium octylsulfate micelles, 0.26, which forms smaller micelles than SDS.(15) These results indicate that the interactions between these aromatic compounds and SPFO micelles are quite different from their interactions with hydrocarbon surfactant micelles. It is thus interesting to analyze these interactions on the basis of the two-state model .

Table 6.7 lists the dilute solution micelle-water partition coefficients

determined experimentally (174-176) and according to the dilute solution two-state model for benzene in SPFO, SDS, and SOS. The saturated solution value of $K_{m/w}$ for benzene in SPFO determined here, 220, is in agreement with the dilute solution value reported by Carlfors and Stilbs, 230 ± 10. (176) Also listed in Table 6.7 are the two-state model parameters. The values of $K_{f/w}$ and $-\delta\gamma/\delta x$ have been presented in Chapters Three and Four. It is noted that the perfluorohexane-water partition coefficient is eight times lower than the decane-water partition coefficient for benzene. This provides the initial indication of the reason for the lower solubility of benzene in SPFO as compared to SDS or SOS micelles. Benzene has a much higher activity coefficient indicating a much more non-ideal interaction with perfluorocarbon alkanes than with hydrocarbon alkanes. However, an eight fold difference is not noted in the $K_{m/w}$. The $K_{m/w}$ of SOS and SDS are between 2 to 4 times the SPFO value. The two-state model shows why this occurs. Comparison of the $-\delta\gamma/\delta x$ values indicates that benzene is much more surface active in perfluorohexane than in decane. The adsorbed to dissolved ratio for benzene in SPFO is more than four times that in the alkyl sulfates. In SPFO, for every benzene molecule in the core 9 molecules

TABLE 6.7

Comparison of Micelle/Water Partition Coefficients for Benzene in SPFO, SDS and SOS From Experimental Measurements and From the Two-State Model at Infinite Dilution

Surfactant	$K_{o/w}$	$K_{o/w}\exp(-\Delta PV/RT)$	$\delta\sigma/\delta x$	$\Gamma Af/x$	$K_{m/w}$ (calc)	$K_{m/w}$ (expt)
SPFO	205	16.1(ΔP=697atm.)	107	9.07	162	230[a]
	205	22.8(ΔP=600atm.)	107	9.07	230	230[a]
SDS	1650	330	33	1.88	950	950[b]
SOS	1650	175	33	2.20	560	560[c]

a. ref. 176
b. ref. 175
c. ref 174

are at the interface, while in the case of SOS or SDS only about 2 are at the interface for each one in the core. This indicates that the average environment of a benzene molecule in SPFO is much more polar than in SDS. Contact between water and other components of the aqueous phase and benzene occurs to a greater degree in SPFO than SDS. This analysis shows how the adsorbed to dissolved ratio, $\Gamma Af/x$, can help the investigator who is interested in enhancing or retarding contact between a solubilizate and water. The determination of $\Gamma Af/x$ requires only a knowledge of interfacial activity and an estimate of the A value. A knowledge of Laplace pressure is not necessary.

In the present case the value of A, $6.16 \times 10^9 cm^2$/mole SPFO, was determined from unpublished NMR data from this laboratory.(211) The value of π, 18.35 dynes/cm, used to calculate f (eq. 5.19) was obtained from unpublished interfacial tension data also from this laboratory. (212) The area term, a_2 (eq. 5.19), used for the alkyl sulfates was also used for SPFO. The benzene area used was $18.0 Å^2$, which was that which produced agreement between the dilute solution experimental and calculated $K_{m/w}$ for benzene in SOS.

A rough Laplace pressure calculation was made on the basis of the NMR and interfacial tension work cited. (211,212) As indicated in Table 6.7 using this value of 697 atm. for the Laplace pressure a $K_{m/w}$ which is about 30% lower than the experimental is calculated. To achieve quantitatively exact agreement with the $K_{m/w}$, a ΔP of 601 atm. is required. The above ΔP estimates are all of reasonable magnitude, since the ΔP of SOS, which has the same carbon chain length and, therefore, probably a similar radius, is 615 atm. The reasonable picture of solubilization of benzene in SPFO produced by the two-state model is an encouraging indication that the model can be extended to micelles of many types of surfactants, and can form the basis of a general solubilization model.

It must again be stressed that an inappropriate conclusion would be drawn if the similarity of the free energy of transfer from water to perfluorocarbon and from water to micelle were taken to indicate a location for benzene in the core of the SPFO micelle . The Laplace pressure effect for these micelle is large, reducing the solubilizing power of the core to 10% of that of perfluorohexane. The high interfacial activity of benzene and larger surface area of these micelles places about 90% of the

molecules at the interface.

The experimental value for toluene in SPFO can be analyzed in relation to that of benzene. Comparison with SDS data shows the differences between these micelles. The ratio of the mole fractions at saturation for benzene and toluene in SDS is 1.17. This can also be considered as the ratio of the micelle to oil ratio for each of these compounds since at saturation the mole fraction in the oil is unity. At infinite dilution the ratio

$$\frac{x_m \text{ Benzene in SDS}/x_o}{x_m \text{ Toluene in SDS}/x_o}$$

was calculated from the micelle-water and oil-water partition coefficients at infinite dilution and found to have a value of 1.55. This infinite dilution value is the highest value this ratio can be expected to take for SDS and the saturation value, 1.17, the lowest. This ratio is greater than one mainly due to the Laplace pressure effect which allows smaller molecules to dissolve in micelles to a greater extent than large molecules. For SPFO, the ratio of the mole fractions at saturation for benzene and toluene is 1.69. This is even higher than the infinite dilution value in SDS. If the adsorption terms of benzene and toluene in SPFO are similar, as they are in SDS, then this ratio is a measure of the Laplace

pressure effect. It indicates a higher Laplace pressure for SPFO than SDS, since at saturation the smaller solute is favored to a greater degree than in SDS at infinite dilution.

In conclusion, the new dialysis method of solubilization capacity determination has been shown to be working for two types of surfactant micelles. Analysis of data indicates that the two-state model is consistent with partitioning of the compounds studied between SDS and SPFO micelles. The model provides insight into the distribution of molecules in the micelle from experimentally determinable physical properties.

MICROENVIRONMENTAL POLARITY STUDIES IN SDS AND SPFO MICELLES

A. Review of Previous Work:

In the preceding chapters a two-state thermodynamic model of micellar solubilization was presented. It provided an indication of the extent to which molecules associated with micelles are exposed to the aqueous medium. When molecules are exposed to water, their environment is certainly more polar than when they are embedded in the hydrocarbon core of the micelle. Estimates of the polar nature of the environment of molecules are attainable through various types of spectroscopic studies. (46-56) In this study we will use UV spectroscopy.(46-52)

Certain features of the UV absorption spectra of benzene, naphthalene, and some alkylbenzenes have been used to determine the polarity of the molecule's environment in solution.(47,50,213) Benzene exhibits a solvent-induced band about 3.6 nm to the red of the first prominent band.(49) This peak is absent in the vapor spectrum.(213) The ratio of the intensity of the solvent induced band to that at the first peak, ϵ_s/ϵ_p , was found by Cardinal

and Mukerjee (49) to increase in a nearly linear manner with the solvent dielectric constant for the series of solvents, heptane, 2-propanol, 95% ethanol, 50% methanol/water, 70% methanol/water, and water. For this series of solvents, the dielectric constant was also found to correlate with a parameter H, defined as the ratio of the molar concentration of dipoles in a solvent to the dipole concentration in water (55.4 moles/l). H is essentially a measure of the degree of hydrophilic character of the solvent.

Mukerjee, Ramachandran, and Pyter (57) demonstrated that the bulk dielectric constant was related to the H value for 28 solvents including one alkane, six n-alkanols, water, and methanol or ethanol/water mixtures. A linear correlation ($r = .999$, $SD = 0.957$) was noted. In an attempt to explain this relationship, these workers reasoned from the Kirkwood-Frohlich equation for hydrogen bonded liquids

$$\frac{(D - n^2)(2D + n^2)}{D(n^2 + 2)^2} = \frac{4\pi N_1 \mu_g^2 g}{9kT} \qquad (7.1)$$

where D is the dielectric constant, n is the refractive index, N_1 is the

number of molecules per unit volume, μ_g is the dipole moment of the molecule in the gas phase, k is the Boltzmann constant, T is the absolute temperature and g is a correlation parameter arising from the mutual interaction of dipoles. For hydroxylic solvents D is large compared to n, and the left quantity $(D-n^2)(2D+n^2)/D$ is approximately 2D. In addition, g, μ_g and n likely show only small or mutually conpensatory variations within the reference solvent series. This makes D primarily dependent on N_1, which is proportional to H, since $H = N_1/N_w$, where w stands for water. A monotonic variation of ϵ_s/ϵ_p with H was also seen for the series. Structurally complicated alkanols and molecules which contain different numbers or kinds of polar groups do not fit into the same correlation. For example, CCl_4, D=0, has a value of ϵ_s/ϵ_p, nearly equal to that of water, D=78.(213)

Cardinal and Mukerjee also found other spectral parameters which showed a monotonic decrease with dielectric constant in this series.(49) A series of solvent-induced peaks is responsible for raising the height of the valley between the permanent peaks. For benzene the ratio of the absorbance at the higher wavelength major peak to the absorbance at the

valleys between that peak and the next major peak, R_{pv}, was found to vary continuously between 5.4 for heptane to about 2 for water. A fixed wavelength ratio, R_c, of absorbances near the peak and valley was also found to decrease with increasing solvent polarity. Similar parameters which varied monotonically with dielectric constant were found for seven other aromatic compounds studied.

Mukerjee and Cardinal then dissolved these aromatic compounds in aqueous micellar solutions and determined the value of the above spectroscopic parameters.(49,50) UV spectroscopy gives a weighted sum of the parameter for all the states the molecule encounters. Solubilizate molecules are distributed between the micellar and the aqueous phase. Therefore, the value of the spectroscopic parameter was measured at increasing concentrations of surfactant. At the highest surfactant concentrations more than 88% of the solubilizate was associated with the micelle . The value of the parameter for the solubilizate molecules associated with the micelle was determined by extrapolation to zero concentration of water. The R_c parameter was found to be particularly suitable for micellar studies as will be shown later. However, this

parameter was sensitive to spectral shifts occurring due to factors, such as refractive index differences, other than polarity. Due to refractive index differences in the reference solvent series, the spectra of benzene and the other compounds studied showed a shift to longer wavelengths (red shift) for the absorption peaks as the solvent became less polar. From water to heptane the total shift was usually less than 1nm. In SDS and CTAC micellar solutions the spectra of the compounds studied were found to be red-shifted by about 0.1-0.3 nm compared to heptane. This was consistent with the increase in refractive index with chain length of the aliphatic, which is associated with a red shift of about 0.4 nm in the benzene spectrum. Corrections for this spectral shift on R_C in micellar solutions were calculated by estimating the effect of such a shift on the solvent of appropriate polarity. These corrections were found to be small, changing the effective dielectric constant by 1-3 units. Studies on the spectra of benzene in 2.2N $NaSO_4$ (213) and 3M CTAC (50) indicated that the high concentrations of polar groups at the micelle-water interface were not likely to affect the polarity estimates. The microenvironmental polarity in the micelle, H or effective D, was determined by comparison with the

calibration curves of the reference solvents. H values or effective dielectric constants of solubilizate in micelle were found to decrease with increasing alkyl substitution.

D. Scope and Aim:

In the present work UV absorption spectroscopy was used to determine the microenvironmental polarity of aromatic molecules dissolved in surfactant micelles. Particular attention was drawn to the relationship betwen the results found here and those determined from the two-state model for micellar solubilization presented in previous chapters.(50)

In the first section a reference solvent calibration curve for toluene and microenvironmental polarity results for this compound in SDS micelles are presented. The average environmental polarities of benzene, toluene, ethylbenzene, butylbenzene , and p-di-tert-butylbenzene determined spectroscopically are compared on the basis of their interfacial adsorptivity and the two-state model .

Use of the UV technique to determine the effective environmental polarity of benzene in SPFO required a new approach. A difference method was developed based upon the experimental values of the micelle-water partition coefficient.(176) The polarity estimate is discussed relative to

that of benzene in SDS.

In the final section, preliminary data on the microenvironmental polarity of benzene and p-xylene in aqueous SDS solutions also containing n-hexanol, a zwitterionic surfactant (Zwittergent 3-12), or tetrabutylammonium bromide are presented. The results are discussed in relation to the effect of the additive on uptake and distribution in the micelle.

C. Results and Discussion

1. Microenvironmental Polarity of Toluene in SDS and the Relationship of Microenvironmental Polarities of Aromatics to Interfacial Adsorptivity at the Micelle-Water Interface.

Studies discussed in the preceding chapters have focused on the physical properties and micellar solubilization of benzene, toluene and ethylbenzene. Thermodynamic properties of these compounds, such as their hydrocarbon-water partition coefficients, $K_{h/w}$, micelle-water partition coefficients, $K_{m/w}$, adsorptivity to a hydrocarbon-water interface, $-\delta\gamma/\delta x$, and the fraction of molecules at the micelle-water interface have been examined. The relationship between these values and their microenvironments in micelles is certainly of interest. It was first necessary to

complete the micellar microenvironmental studies by examining toluene, which had not been studied previously. Toluene was found to give values for the thermodynamic properties listed above which were intermediate between benzene and ethylbenzene. It is therefore of interest to see where the polarity of the micellar microenvironment of toluene lies.

In order to develop a polarity-indicating calibration curve, a polarity-sensitive change in the UV spectrum of toluene was established. A peak at 264.8 nm in hexane, associated with a valley at 263.8 nm, was not found in water. The ratio of the absorbance of toluene at 264.8 nm to that at 263.8 nm decreased in a continuous manner as the dielectric constant of the solvent increased. Figure 7.1 shows a plot of the R_c ratio of toluene absorbances at 263.4 nm/263.8 nm. The spectroscopic parameters used by Cardinal and Mukerjee (49,50) for ethylbenzene involved the same peak. The monotonic decrease of the R_c ratio for ethyl benzene at the fixed wave-lengths 264.4 nm/263.3 nm as a function of H is also plotted in Figure 7.1. The toluene and ethylbenzene calibration curves are found to be parallel, indicating that the spectroscopic change occurring is similar for these two molecules.

of

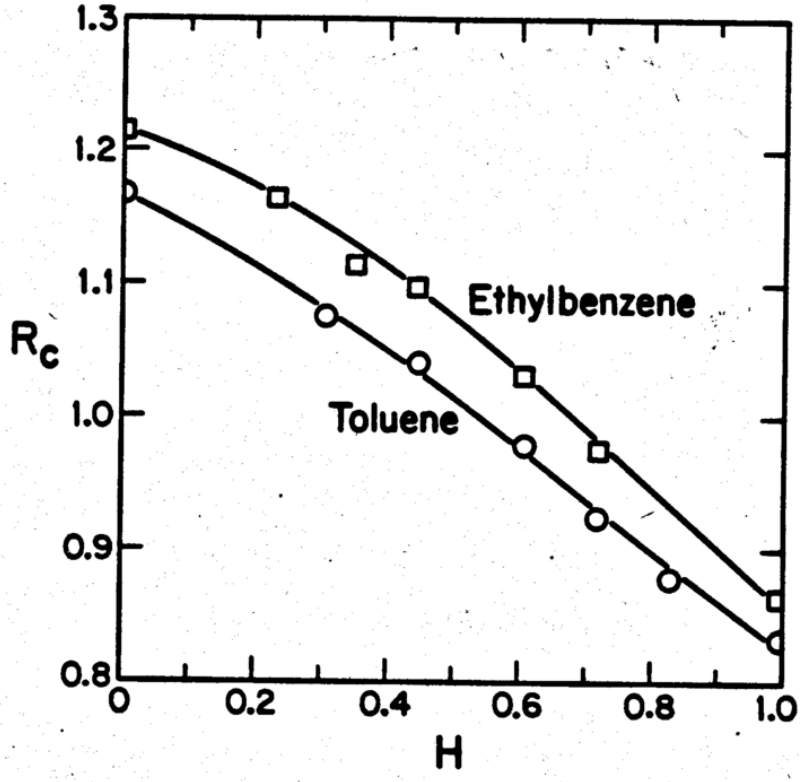

As discussed in the introduction, solubilizates dissolved in micellar solutions are distributed between the micellar and aqueous phases. Therefore, the spectroscopic parameter read is an average quantity. The R_c parameter is most useful for the determination of the value of the ratio for solubilized molecules. The total concentration of solubilizate, C, can be expressed as

$$C = C_m \Phi_m + C_a \Phi_a \qquad (7.1)$$

where C_m is the concentration of solubilizate in the micelles (in molecules/l of micelles),

C_a is the concentration of the solubilizate in the aqueous phase,

Φ is the volume fraction and

subscripts m and a stand for micellar and aqueous phases.

The ratio

$$R_c = A_1/A_2 = \frac{\epsilon_{1,m} C_m \Phi_m + \epsilon_{1,a} C_a \Phi_a}{\epsilon_{2,m} C_m \Phi_m + \epsilon_{2,a} C_a \Phi_a} \qquad (7.2)$$

where ϵ is the molar absorptivity,

A is the absorbance, and

subscripts 1 and 2 stand for wavelengths 1 and 2.

From the definitions

$$K_m = C_m/C_a \tag{7.3}$$

$$R_{c,m} = \epsilon_{1,m}/\epsilon_{2,m} \tag{7.4}$$

$$R_{c,a} = \epsilon_{1,a}/\epsilon_{2,a,} \tag{7.5}$$

equation 7.6 can be derived from equations 7.1-7.5.

$$R_c = R_{c,m} - \frac{\epsilon_{2,a}}{\epsilon_{2,m}} \frac{(R_c - R_{c,a})\Phi_a}{K_m \Phi_m} \tag{7.6}$$

It is noted that a plot of R_c against $(R_c - R_{c,a})\,\Phi_a / \Phi_m$ is linear with an intercept of $R_{c,m}$, the value of R_c for the micellar state.

Figure 7.2 is such a plot for toluene in SDS at 25°C. The extrapolation to $R_{c,m}$ is small in terms of solubilized toluene since about 90% is in the

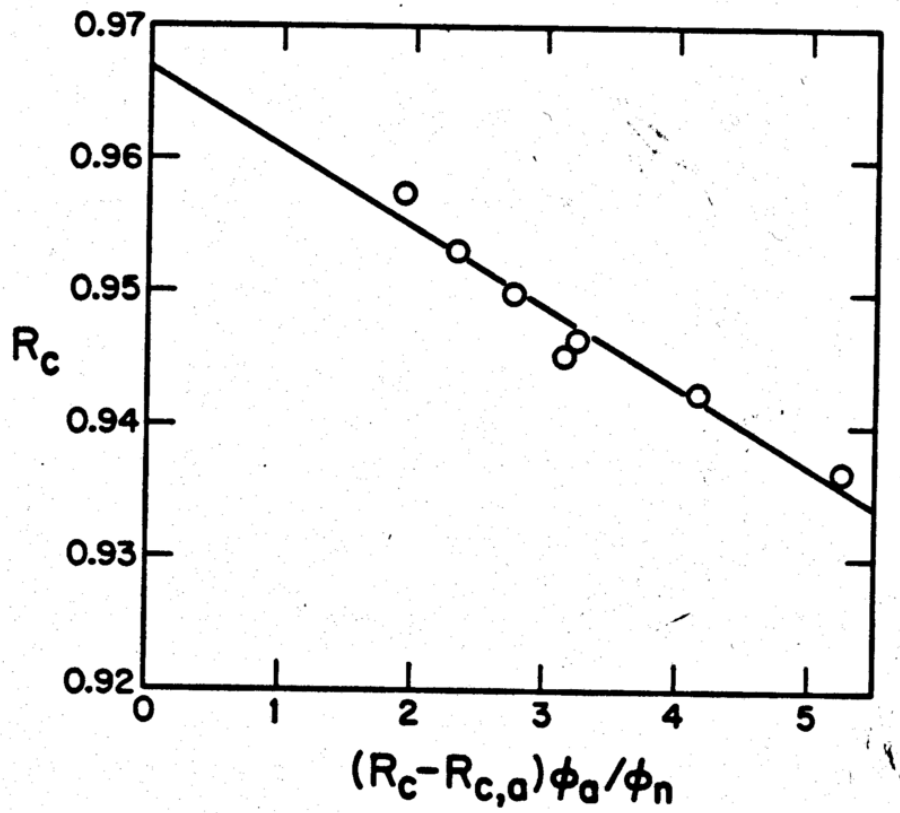

Figure 7.2 R_c of toluene in aqueous solutions of SDS plotted as a function of $(R_c-R_{c,a})$ Φa/Φm.

micelle at the highest surfactant concentration used. The ordinate intercept gives a $R_{c,m}$ of 0.967. Before determining the value of the microenvironmental polarity from the calibration curve, this $R_{c,m}$ value must be corrected for any spectral shift associated with solubilization in the micelle.(49,50) The effect of this spectral shift on the R_c of a reference solvent of similar dielectric constant was used as a correction. This correction was found to produce about a 1% increase in $R_{c,m}$. The effective H value in the micelle was found to be 0.61.

In Table 7.1 the H parameters for toluene are listed along with those of benzene and three alkyl benzenes studied by Mukerjee and Cardinal.(50) It is noted that toluene follows the trend of decreasing H value with increasing alkyl substitution, fitting in between benzene and ethylbenzene.

The H parameter varies from zero for pure hydrocarbon to one for water. Therefore, the value of H gives an indication of the degree of exposure to water over the sum of all molecules in the micelle. The two-state model provides a thermodynamic estimate of the fraction of molecules exposed to water. For benzene upon correction of the $K_{h/w}$ for Laplace pressure effects, the estimated distribution between the SDS micellar core and the

TABLE 7.1

Comparison of the H Parameter and the Fraction of Solubilizate at the Micelle-Water Interface From the Two-State Model For Benzene and Four Alkylbenzenes in SDS Micelles

Solubilizate	H[a]	Fraction at SDS micelle surface[b]	$\frac{\Gamma Af/x}{1+\Gamma Af/x}$
Benzene	0.65	0.65	
Toluene	0.61	0.61	
Ethylbenzene	0.55	0.57	
Butylbenzene	0.49	0.47	
p-di-tert-Butylbenzene	0.18	0.44	
		0.17[c]	

a. Ref. 50

b. Area per molecule = $(V/N)^{2/3}/1.61)$

c. Area per molecule = $(V/N)/(3.7\text{Å} \times 1.61)$

aqueous phase is 330. The experimental $K_{m/w}$ is 950.(175) From these values the calculated fraction at the surface is 0.65 (= (950 - 330)/950), which is the same as the H value for benzene in SDS. Although the exactness of the agreement may be accidental, it indicates that the spectroscopic H parameter is mainly determined by the fraction of molecules at the micellar surface.

As noted in the preceding chapters, benzene is the only molecule for which dilute solution micelle/water partition coefficient data are available in SDS. It is the only molecule for which the above comparison can be made on the basis of experimental $K_{m/w}$, $K_{h/w}$, and Laplace pressure effects. The factor 1.61, which corrected the benzene $V^{2/3}$ area value to produce agreement between experimental and calculated $K_{m/w}$ values in SDS, was used in calculating the areas of the alkylbenzenes.

This procedure is likely to be appropriate based upon the following observation. Ethylbenzene and p-xylene exhibit the same interfacial tension against hydrocarbon liquid. These molecules are thus likely to have similar interfacial activities at the hydrocarbon-water interface. The H parameters of these compounds in SDS micelles were found to be the

same.(50) Thus the ability of ethylbenzene to orient at the micelle-water interface with its phenyl ring at the interface and alkyl group toward the micellar core does not enhance its interfacial activity in the micelle, relative to p-xylene for which such an orientation is not as favorable. This indicates that orientation is not important for these molecules. If no orientation is evident, then the full area of the molecule must be considered. This is accomplished by using the $V^{2/3}$ parameter. This value has the advantage of being known quite precisely.

Adjustment of the $V^{2/3}$ value by a factor of 1.33 has been found to produce agreement of the monolayer model for competitive adsorption with interfacial adsorptivity data of dimethyl ether at the hexane/aqueous sodium dodecyl sulfonate solution interface.(169) One reason this correction is needed is that the activity coefficients have been taken to be unity in the present competitive adsorption model. (Chapter 5) As noted the correction factor which produced agreement between experimental and calculated micelle-water partition coefficients for benzene in SDS is 1.61. This factor is presently taken to account for activity coefficients, and various micellar effects such as packing effects, hindrance of chain movement, and curvature.(13,17,23,166) In this way all molecules are

treated in a consistent manner.

Table 7.1 lists the fractions of the other alkylbenzene molecules at the SDS micelle-water interface on the basis of the two-state model and the new monolayer model for competitive adsorption. Nearly quantitative agreement between the fraction at the surface and the H parameter is seen for benzene and three alkylbenzenes. It must be stressed that these values arise from two very different approaches, one spectroscopic and the other thermodynamic modelling. This cross check based upon consistent values of molecular parameters provides strong support for the two-state model. It clarifies the meaning of the parameter in micelles as an indicator of the fraction of molecules of the micelle surface. The above results give evidence that 65% of benzene and nearly 50% of butylbenzene molecules are in contact with water. This high fraction at the interface is not detected by thermodynamic measurements which compare free energies of transfer from micelle to water and from hydrocarbon to water.(183,184) Spectroscopic results are consistent with a model which takes into account the high surface area of the micelle, the interfacial activity of the solubilizate, competition for adsorption, and the Laplace pressure of the micellar core. However, it is important to point out here, as in the previous

chapter, that the fraction at the interface can be determined in two independent ways.(52) First, partitioning into the micellar core can be determined from the $K_{h/w}$ and the Laplace pressure effect. Using the experimental $K_{m/w}$ the surface fraction is obtainable as in the above example with benzene. The second way is through the interfacial adsorptivity corrected for the competitive adsorption with surfactant headgroups.

p-Di-tert- butylbenzene may have orientational problems at the micelle-water interface. Exposure of a t-butyl group to water is highly unfavorable, the free energy of transfer from hydrocarbon to water being 2100 cal mol^{-1} for the CH_3 group as compared to 825 Cal mol^{-1} for the $-CH_2$ group.(1,4) The random orientation of this molecule with bulky t-butyl groups is much less probable than for the smaller alkylbenzenes. This molecule is much larger than the others studied here. Its molar volume has been estimated from that of benzene and t-butylbenzene to be about 222 ml mol^{-1}. Problems of packing this molecule at the micelle-water interface are much more severe. A reasonable orientation of p-di-tert- butylbenzene at the micelle-water interface is with its aromatic ring lying

perpendicular to the micelle-water interface to minimize the overall area of contact. Based upon this geometry, the molecular volume was divided by 3.7Å, the vanderWaals thickness of the π system of the aromatic ring (182), to give an appropriate area for this box-like molecule. This value was corrected by the benzene area factor,1.61 for SDS micelles. Use of this effective area produced agreement between the two-state model calculation and the H-parameter. The much lower fraction at the surface for these molecules is due to the restrictions on orientation and packing of this molecule, which contains two large, inflexible and highly hydrophobic groups.

In conclusion, excellent agreement is seen between H and the fraction at the surface from the two-state model using consistent and reasonable parameters. In this way the meaning of the micellar H value is elucidated. The present construction of the two-state model is further supported by spectroscopic measurements, which are able to indicate average polarities of the solubilizate environments.

2. Microenvironmental Polarity of Benzene in SPFO Micelles.

Certainly perfluorocarbon surfactant micelles provide an interesting

system in which to study the solubilized environment of hydrocarbons. The antipathy of interaction between perfluorohexane and hydrocarbons is well documented.(69,100,198,199) Extreme nonideality has been noted in the interaction of benzene and perfluorocarbon in this work. An activity coefficient of approximately 11 for benzene in perfluorohexane was reported from partitioning experiments in Chapter Three. These high nonidealities also give rise to a much higher interfacial adsorptivity of benzene to the perfluorocarbon/water interface than to the decane/water interface. As pointed out in the preceding chapter, the value of the fraction of benzene at the SPFO micelle/water interface is expected to be higher than that found in hydrocarbon micelles. Calculations based upon this interfacial activity and competitive adsorption to the micelle/water interface indicated that in dilute solution 90% of solubilized benzene molecules in SPFO are at the micellar interface compared to 65% in SDS and 69% in SOS. A spectroscopic determination of the degree of association with water of benzene molecules solubilized in SPFO is certainly of interest.

An attempt was made to estimate the effective dielectric constant or H parameter (49,50) of benzene in SPFO micelles. The method of

extrapolation of the polarity sensitive parameter to pure micellar phase has been demonstrated in the preceding section. This method is not useful for benzene in SPFO. The partition coefficient of benzene between the micelle and water is much smaller than in SDS, the values being 230 in SPFO (176) and 950 in SDS.(175) Even at the highest SPFO concentration possible at room temperature only 65% of the total benzene in solution is in the micelles. Extrapolation of any polarity sensitive parameter to pure micellar phase would thus be quite long.

A new method for the determination of the spectroscopic parameter of interest was required. A difference method was developed. A 0.253 molar SPFO solution (37.3 wt%) containing a known concentration of benzene was prepared. Its UV spectrum was determined and corrected for the absorbance due to SPFO. The fraction of benzene not solubilized was calculated from the volume fractions of the micellar , Φ_m, and aqueous , Φ_a, phases and the distribution coefficient of benzene between these phases, K.(176) The volume fraction of micellar phase was calculated from the molar volume of SPFO and the aggregation number determined by unpublished NMR work of this laboratory. (211) The molar absorptivity of benzene in water over the relevant spectral region had been previously determined. The absorbance in

the micellar solution due to unsolubilized benzene was calculated, and subtracted from the total absorbance. The remaining absorbance divided by the concentration in the micelle gives the molar absorptivity, ϵ, of benzene in the micelle . The resultant spectrum is shown in Figure 7.3. The ϵ_s/ϵ_p value of 0.235 ± 0.010 was determined. The uncertainty of the ϵ_s/ϵ_p value is based upon the reported errors in K values (±5%).

Interpretation of the ϵ_s/ϵ_p parameter required a new approach, due to the nature of the UV spectrum of benzene in the perfluorocarbon alkanes. (214,215) These solvents have very low refractive indices. For example, perfluorohexane has a refractive index of 1.2514 while that of n-hexane is 1.375, and vacuum is 1.00.(213) The low refractive index produces a spectrum more similar to vacuum than the compounds of the reference solvent series.(216,217) Figure 7.4 is a comparison of a portion of the UV spectrum of benzene in perfluorohexane and in water. The solvent induced band is not as prominent. The ϵ_s/ϵ_p ratio for benzene in perfluorohexane is 0.0515, which is significantly lower than in hexane, 0.142.

The series of solvent-induced peaks which are responsible for raising of the valleys between the peaks is also much less evident in this spectrum.

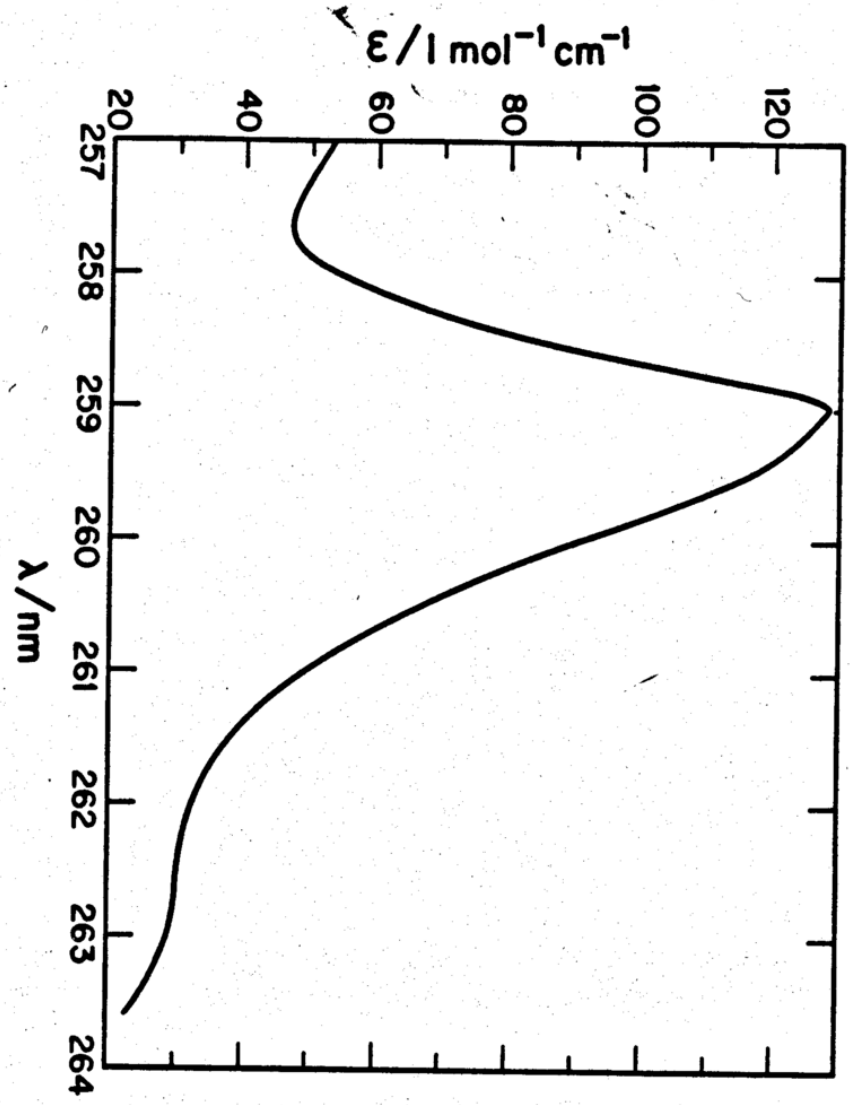

Figure 7.3 Difference spectrum of benzene in SPFO micelles.

Figure 7.4 UV spectra of benzene in perfluorohexane and in water. (Relative absorptivities of benzene in perfluorohexane and water not indicated.)

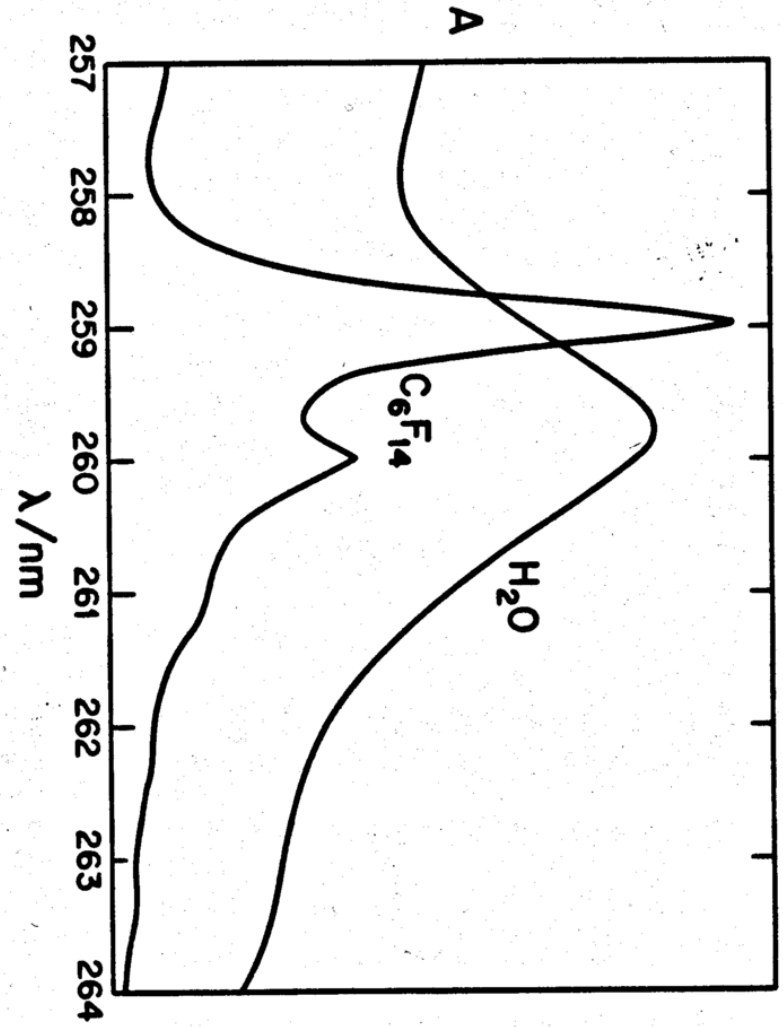

The R_{pv} value of benzene is 14 in perfluorohexane, nearly three times that found in heptane. The low refractive index of the perfluorocarbon compounds causes a spectral shift compared to other molecules of the same dielectric constant. For example, the λ max of benzene in perfluorohexane is at 253 nm, and in n-hexane at 254.3 nm. Therefore, the R_c parameter ($A_{260.4}/A_{259}$) which had been used by Cardinal and Mukerjee (49) has a value of 0.22 in perfluorohexane, while that in water is about 2 and in heptane about 5.2. In view of the above, the calibration procedures based upon a reference solvent series of hydrocarbon alkanes, n-alkanols and n-alkanol/water mixtures is not applicable for perfluorocarbons.

An assessment of the nature of the microenvironmental polarity of benzene in SPFO can be made by comparison with the values for ϵ_s/ϵ_p in SDS found by Mukerjee and Cardinal.(50) Table 7.2 lists the ϵ_s/ϵ_p values for benzene in heptane, SDS micelles, and in water, found by Mukerjee and Cardinal.(50) Also listed are the ϵ_s/ϵ_p values for benzene in perfluorohexane, SPFO micelles, and water found in this work. The values for water agree considering the use of two different instruments and

TABLE 7.2

ϵ_s/ϵ_p Ratios For Benzene

SOLVENT	
p-heptane	0.142[a]
perfluorohexane	0.0515[b]
water	0.292,[b] 0.302[a]
SPFO micelle	0.235 ± 0.01[b]
SDS micelle	0.232[a]

a. Mukerjee and Cardinal (ref. 50)

b. present work

possible differences in instrumental settings such as slit width. This indicates that comparison of the parameters from the two sets of data is allowable. As noted above, the value of ϵ_s/ϵ_p in perfluorohexane is much lower than that found in heptane. However, in spite of the low refractive index contribution to the spectrum of benzene molecules in the SPFO micelle, the absolute values of ϵ_s/ϵ_p for benzene in SDS and SPFO micelles are the same. Indeed the difference between the perfluorocarbon value and that in the SPFO micelle, 0.184, is greater than the change in the value of the parameter seen in going all the way from heptane to water, 0.16. The benzene parameter in SPFO is much further away from the non-polar organic liquid parameter than it is in SDS.

A linear interpolation of the ϵ_s/ϵ_p parameter between organic liquid and water gives a rough indication of the fraction of polar character of the average micellar microenvironment of benzene. In SDS this results in a value of 0.56, and in SPFO, 0.76. The actual H parameter in SDS was shown to be 0.65.(50) Some increase in the SPFO value is also likely. Benzene molecules associated with SPFO micelles are in an environment which is

much more polar than a perfluorocarbon environment.

These results are then consistent with the estimate of the two-state model that a high fraction of benzene molecules are at the SPFO micelle surface. The model has also shown that this fraction is considerably larger than that found in SDS.

3. Effects of Additives on the Microenvironmental Polarity of p-Xylene and Benzene in SDS Micelles

Considering the importance and usefulness of micellar solubilization, the ability of an additive to enhance or retard the uptake or partitioning into micelles is certain to be of interest. In the preceding chapter the effect of sodium chloride on the solubilization capacity of the micelles was examined. The effect of additives on the location and orientation of solubilized molecules is also of concern. The solubilizate may need to react or be protected from reaction with compounds confined to the aqueous phase.(11,218) Furthermore, biological lipid assemblies, for which micelles are simple models, are composed of numerous additives such as cholesterol and proteins.(219) The effect of additives on interactions of solubilizates with micelles provides a better understanding of the processes regulating uptake into such membranes.

One particular class of additives which has gained much attention are the C_4-C_8 medium chain length alcohols.(207,179,220-222) As shown in Chapter 5 these compounds partition into micelles to a high degree. These additives have been used extensively in solutions of micellar surfactants to form microemulsions which are capable of solubilizing large quantities of alkanes. Tertiary oil recovery processes are based upon such systems. (34) The effects of alcohols on micellar systems has thus received much attention. Alcohols have been shown to decrease the cmc and aggregation numbers of micelles, indicating that they stabilize micelle formation. (45,179,221) Some recent studies on the location and distribution of molecules within micelles have indicated that solubilizates experience a more non-polar environment and are not as able to interact with the aqueous phase when alcohols are added to micellar solutions. For example, Whitten and coworkers (220) have studied the association constant of the doubly charged aromatic acid methylviologen (MV^{2+}) with a series of surfactant stilbenes. MV^{2+} is concentrated in the headgroup region of anionic micelles. Solubilizates which associate with MV^{2+} must have some degree of surface exposure. The complexation constant between a solubilizate and MV^{2+} is higher as greater association between these

molecules occurs. In SDS micelles the complexation constant between MV^{2+} and the stilbenes was reduced significantly when 1-heptanol was added. Recently this group has also reported that complexation between MV^{2+} and pyrene in SDS micellar solutions was reduced in the presence of 1-heptanol.(221) The polarity of the microenvironment of pyrene can be measured by its fluorescence intensities.(56) A decrease in the polarity of the average pyrene environment upon addition of heptanol to SDS micelles was noted by this method.(221)

As discussed in the preceding chapter, counterions have also been shown to influence the solubilizing power of micelles. The addition of counterions causes size and shape changes which affect solubilization. (40,201,203) Changing the counterion also produces micelles with different properties. These effects are particularly noteworthy when hydrophobic counterions are employed.(192) For example the cmc of SDS is 8.1mM at 25°C. The cmc of tetrabutylammonium dodecyl sulfate is 1.2mM and that of tetramethyl- ammonium dodecyl sulfate is 5.4mM at the same temperature.(192)

The cmc decreases with addition of each carbon to the chains of the tetraalkylammonium counterions. Hydrophobic interactions between these

counterions and the micelle stabilize the micelle and reduce the cmc.(192) The effect of these counterions on solubilization has not been reported.

The work reported here is a preliminary study of the effect of hexanol, tetrabutylammonium bromide, and a zwitterionic cosurfactant, Zwittergent 3-12, on the microenvironmental polarity of benzene and p-xylene in SDS micelles. The polarity sensitive parameter used was R_{pv}. This parameter increases with decreasing polarity of the environment. R_{pv} for benzene ranges from 5.2 in heptane to 1.85 in water. For p-xylene it decreases to 3.6 in heptane and 1.9 in water. In SDS micelles with no additive Mukerjee and Cardinal found values of R_{pv} for benzene of 2.78 and for p-xylene of 2.72.(49,50)

Table 7.3 lists the R_{pv} values in the systems studied, including SDS aqueous surfactant solutions with and without additive. The R_{pv} values here report a complicated weighted sum of both solubilized and non-solubilized benzene or p-xylene. As the concentration of SDS increases without additive, the R_{pv} value increases due to increase in the volume fraction of micelles in solution. Comparison of the R_{pv} values in the

TABLE 7.3

Microenvironmental Polarity of Benzene and p-Xylene Aqueous Solutions of SDS and SDS + Additive

SDS (M)	ADDITIVE (M)		Rpv	SOLUBILIZATE
0.0685	———		1.91	Benzene
0.0652	Hexanol	0.038M	2.03	Benzene
0.245	———		2.35	Benzene
0.235	Hexanol	0.207M	2.61	Benzene
0.050	Tetrabutylammonium Bromide	0.052M	2.34	Benzene
0.0404	———		2.23	p-Xylene
0.200	———		2.60	p-Xylene
0.201	———		2.60	p-Xylene
0.200	Hexanol	0.209M	2.87	p-Xylene
0.109	Zwittergent 3-12	0.109M	2.68	p-Xylene
0.050	Tetrabutylammonium Bromide	0.052M	2.80	p-Xylene

presence and absence of additives at similar SDS concentrations shows that in each case the additive has caused an increase in R_{pv}. This indicates a more hydrophobic environment. The p-xylene values are particularly striking. Upon addition of hexanol or tetrabutylammonium bromide to SDS solution the R_{pv} values for p-xylene have exceeded the micellar values found by Mukerjee and Cardinal.(50) The averge polarity of all of the p-xylene in solution, including that in the aqueous phase, is lower than that of p-xylene associated with SDS micelles without additive. The micro-environmental polarity of p-xylene in the micelle must be much lower or the partitioning into the micelle must be greatly enhanced by the presence of additive. A combination of these effects may also be responsible for the decreased polarity in the presence of additive.

The additives studied here are associated with the micelles in solution. Hexanol has a $K_{m/w}$ for SDS micelles of over 6000.(45) Electrostatic and hydrophobic forces keep tetrabutylammonium bromide at the micelle-water interface.(192) Zwittergent 3-12 is itself a surfactant with a cmc of 3.6mM. These compounds are not influencing the polarity of the benzene or p-xylene molecules outside the micelle.

The decrease in the overall polarity of the aromatic compounds is consistent with a decrease in interfacial tension of the micelle in the presence of the additives studied. Hexanol is known to be highly interfacially active at hydrocarbon-water interfaces.(119) In Chapter 4 the micelle-water partition coefficient of hexanol was shown to be related to its interfacial activity in the micelle. Organic solutions of tetrabutyl-ammonium dodecyl sulfate form spontaneous emulsions when placed on water due to the exceedingly low interfacial tension caused by this surfactant .

As discussed in Chapter 4, the magnitude of the micellar interfacial tension determines the Laplace pressure of the micelle. As the interfacial tension decreases the Laplace pressure of the micelle decreases and the micelle-water partition coefficient of solubilizate increases. A lower interfacial tension also acts to increase the fraction of solubilizate in the micellar core out of contact with water. Therefore, the average environment of the solubilizate is less polar than in the absence of solubilizate in the micelle. This occurs in two ways. First, the reduction in Laplace pressure of the micellar core increases the solubilizing power of the core. Second, the lower interfacial tension increases the value of π.

This reduces the driving force for competitive adsorption of solubilizates to the micellar interface effectively reducing the f factor of Equation 5.19. Since less solubilizate is in the adsorbed state, a greater fraction is in the micellar core and the overall polarity of the environment is reduced.

The effect of a lower interfacial tension on the solubilization of alkanes has been shown by other workers. Chaiko, Nagarajan and Ruckenstein,(44) studied the solubilization of mixtures of benzene and hexane by several ionic surfactants. They found that the mole ratio of hexane in the micelle did not decrease linearly with mole fraction. Rather, the amount of hexane solubilized stayed the same or increased at low composition of benzene and then declined gradually. The benzene mole ratio showed a linear increase with mole ratio across the whole composition range. On the basis of the one-state model used by these workers agreement of theory with this synergistic effect of benzene on hexane solubilization could only be accounted for if the benzene was near the interface, thereby lowering the interfacial tension. The two-state model shows that, for compounds which are not interfacially active, reduction of interfacial tension reduces the Laplace pressure, thereby increasing uptake

into the micelle.

DETERMINATION OF ACID DISSOCIATION CONSTANTS OF PERFLUOROCARBOXYLIC ACIDS AND CRITICAL MICELLE CONCENTRATIONS OF THEIR SALTS BY UV SPECTROSCOPY

A. Background

Perfluorocarbon compounds are of interest and importance in a variety of fields. They are highly hydrophobic, which has made them useful in lubrication and materials technology.(79,223) Liquid perfluorocarbons are able to dissolve high concentrations of oxygen.(147) Emulsions of these liquids are currently being tested as blood substitutes.(147) On the molecular level perfluorinated compounds are also quite interesting. Perfluorinated alkanes exhibit low refractive indices (213), low cohesive energy densities (91), and low surface tensions against air.(100) These properties indicate the weakness of the intermolecular forces between these molecules. Mixtures of perfluorocarbon alkanes and hydrocarbon alkanes are also highly non-ideal.(100,198) For example, n-heptane and perfluorohexane exhibit a miscibility gap between 0.1 and 0.8 mole fraction heptane at 25°C.(100) Perfluorinated surfactants are much different than hydrocarbon surfactants, exhibiting a higher interfacial activity and lower cmcs.(69) The nonidealities between perfluorocarbon

and hydrocarbon have been found to carry over into the surface chemical and micellization behavior of mixtures of these types of compounds. (69,100,199,224)

Aside from their uses as surfactants, perfluorinated acids are also moderately strong organic acids. The acid dissociation constant of trifluoroacetic acid has a dissociation constant close to unity. (225,226) This property is attributable to the electron withdrawing ability of the fluorine atoms. The extent to which additional $-CF_2$ groups enhance this effect has not been examined.

In view of the above, perfluorinated compounds are certainly important and their physical properties are of interest. In this work the UV spectrum of perfluorinated carboxylic acids has been examined and exploited to advance the research of these compounds and to determine two of their important physical properties, namely the pK_a and cmc. Association of these moderately strong acids with protons and micellization of these compounds are expected to be reflected in their UV spectra. Micellization of fatty acids effects a change in the environment of the carbonyl chromophore. In the monomer state in aqueous solution, the C=0 bond being surrounded by water. The micelle surface provides a much different

environment, containing a high concentration of headgroups and counterions. No investigation has been reported on the use of the UV spectrum of carboxylic acids for cmc determinations.

In the region of 200 nm, the vacuum spectra of aliphatic carboxylic acids show absorption maxima with molar absorptivities of about 50 l mol^{-1} cm^{-1}. (227,228) These absorption bands have been shown to be due to the $n \rightarrow \pi^*$ transition.(227,228) At 160 nm an absorption band having molar absorptivity on the order of 2500-4200 l mol^{-1} cm^{-1} is noted. This band is attributed to $\pi \rightarrow \pi^*$ transitions. (227,228)

In solution the $n \rightarrow \pi^*$ transition is also seen. For example, acetic acid in 0.01M H_2SO_4 shows a peak at 205 nm with a molar absorptivity of 38 l mol^{-1} cm^{-1}.(229) For general $n \rightarrow \pi^*$ transitions of carbonyl groups, a blue shift on increasing solvent polarity has been known for some time. (216,230) In hydroxylic solvents hydrogen bonding stabilizes the ground state of the lone pair n electrons. In the excited state hydrogen bonding is not possible since one of the n electrons is promoted to a higher energy anti-bonding π^* orbital. The energy of the transition is therefore higher in hydroxylic solvents. The classical example, acetone, then shows a blue shift of 14.5 nm between hexane and water. This corresponds to a five Kcal

mol^{-1} hydrogen bond.(230)

Some experimental evidence that the $n \rightarrow \pi^*$ transition of carboxylic acids is shifted to longer wavelength with increasing solvent polarity has been noted. (228,231) For example, Rusoff and coworkers found that in heptane myristic acid had a λ of 205 nm and molar absorptivity (ϵ) of 63 l mol^{-1} cm^{-1}, while in 95% ethanol the λ max was 210 nm and ϵ = 50 l mol^{-1} cm^{-1}. On the other hand extensive work of Clousson and coworkers on the $n \rightarrow \pi^*$ transition of carboxylic acid esters showed a blue shift of about 7 nm upon changing the solvent from isooctane to water. (232) A blue shift for ethyl acetate was also noted upon decreasing the ethanol concentration in a series of ethanol-water mixtures. (233) The overall shift was about 5 nm. This group found no systematic change in molar absorptivity upon change in the solvent in any of their studies.(232-234)

Increase of the chain length of aliphatic carboxylic acids has been shown to be accompanied with a small shift in the $n \rightarrow \pi^*$ transition to longer wavelengths and a small increase in molar absorptivity.(231-235) For example Rusoff and coworkers saw a slight difference in the molar

absorptivity between acetic acid (40 l mol^{-1} cm^{-1}) and caprylic (C_8) or myristic (C_{14}) acids (63 l mol^{-1} cm^{-1}) in heptane. (231) Clousson and coworkers have shown red shifts of about three nm and increase in molar absorptivity on the order of 20 l mol^{-1} cm^{-1} in changing from acetate to isobutyrate methyl ester. (232) The length of the chain was not found to materially affect the molar absorptivity of the series formic, acetic, butyric, caproic, caprylic, lauric, myristic, palmitic and stearic acids between the wavelengths 200 nm and 255.5 nm. (235) No investigation of the effect of chain length on the UV spectrum of perfluorinated acids has been reported.

In the anionic form the $n \rightarrow \pi^*$ transition often appears as part of the $\pi \rightarrow \pi^*$ peak.(227,228) For example, for acetate anion in 5×10^{-2}M phosphate buffer no peak is noted near 204 nm and the molar absorptivity is about 100.(229) This compares with acetic acid in 0.01M H_2SO_4,where a peak is seen at 204 nm and the ϵ = 38 l mol^{-1} cm^{-1}.(229) Szyper and Zuman (228) have investigated the spectra of several carboxylic acids as a function of pH. They have described the difference in the spectra of the free acid and anion forms. In general, the free acid forms showed an absorption band (ϵ=

33 for acetic acid) at 205 to 210 nm and a weak shoulder between 220 and 250 nm, (ϵ = 4 for acetic acid). For the anion the shoulder at 225 nm was absent, with the longer wavelength peak relatively unchanged. These workers used these differences in absorptivity to determine acid dissociation constants for a number of carboxylic acids. For formic and acetic acids they measured pKa values which were stated to agree with literature values (3.75 and 4.75 respectively).

Of particular interest to this study, Szyper and Zuman (228) found that trifluoroacetic acid showed a strong absorption below 195 nm (ϵ >100), a shoulder at 210 nm (ϵ≈30) and a weaker shoulder at 225 nm. The anion was found to have a higher absorbance (ϵ > 200) below 195 nm, no change at 210 nm, but no shoulder at 225 nm. These workers attempted to measure the pK_a of this compound using this spectroscopic change by titration with sulfuric acid. The half-titration point corresponded with a pK_a of about -0.92 (K_a = 8.3) on the H_o acidity scale. However, the H_o function was found to be inadequate in describing the observed change in absorbance with acid concentation for this compound.

Others have also found the question of the pK_a of trifluoroacetic acid to be interesting.(225,226,242-245) As a moderately strong acid this compound stretches conventional methods for determining pK_a, such as conductance, to their limits. (225,226) High concentrations of acid are needed to achieve association. NMR and Raman spectroscopic studies yielded a range of values for K_a between 4 and 8. (226) The refractive index method used by Grunwald and Haley did provide a rather precise value for $K_a = 1.07 \pm 0.25$, ($pK_a = -0.029 \pm 0.10$).(225) About 50% of the error cited by Grunwald and Haley arose from uncertainty of the activity coefficient of trifluoroacetic acid. In the present work the spectral change due to dissociation of trifluoroacetic acid and perfluorobutyric acid was examined. The dissociation constant was determined by use of the activity coefficients based upon HCl.

B. Scope and Aim

This study is an attempt to employ the UV spectrum of perfluoro-carboxylic acids to obtain the values of physical properties of these compounds which are difficult to determine by other methods. In this

study the cmc of perfluorooctanoate micelles was determined by observing the change in the UV absorbance of these compounds with concentration. The sodium and tetraethylammonium salts were studied. Also, a preliminary study was made of the lithium salt at 1M added salt. The pK_as of trifluoroacetic acid and perfluorobutyric acid were measured by observing the change in UV absorbance upon addition of HCl. A new method of determination of the acid dissociation constant was used applying activity coefficients from HCl, the titrating acid. A distinct chain length effect on the absorptivity of the perfluorocarboxylic acids was also noted.

C. Results and Discussion

1. Chain Length Dependence The UV spectra of the perfluorocarboxylic acids and their salts studied here exhibit a shoulder at 210 nm in water. This was also seen by Szyper and Zuman (228) as discussed in the introduction.

Table 8.1 lists the molar absorptivity at 205 nm of trifluoroacetic acid (HPFA), sodium perfluorobutyrate, (SPFB), sodium perfluorooctanoate

TABLE 8.1

Chain Length Effect on the Absorptivity of Aqueous Solutions of Perfluorocarboxylic Acids and Their Salts at 205 nm.

	ϵ/l mol^{-1}cm^{-1}
Trifluoroacetic Acid	58[e] ± 3
Na Perfluorobutyrate	253[e] ± 2
Na Perfluorooctanoate	354.5[a,c] ± 0.5 337.7[b] ± 3
Perfluorooctanoic Acid	331.3[b,d] ± 1

a. Acid purified by recrystallization from CCl_4 before salt formation.

b. Acid used as recieved.

c. Beer's Law plot shown in Figure 8.1.

d. Beer's Law plot shown in Figure 8.2

e. Acids distilled prior to reading

(SPFO) and perfluorooctanoic acid (HPFO) in water at 205 nm. Beer's Law behavior below the cmc was noted for SPFO and HPFO. The typical plots are shown in Figures 8.1 and 8.2. The other readings in Table 8.1 are single concentration determinations. The commercial source of HPFO used here has been shown by previous workers in this laboratory (69) to be free of detectable impurities and of uniform chain length. The reason for the higher absorbance of the SPFO made from HPFO which had been recrystallized from CCl_4 is uncertain.

An increase in the molar absorptivity of 280 l mol^{-1} cm^{-1} from HPFA to HPFO is seen. This change is far greater than that seen with the hydrocarbon acids and esters. For example, an increase of 20 l mol^{-1} cm^{-1} was noted upon extending the chain length from acetic to myristic (C_{14}) acid.(231) This result indicates that the intensity of the transition is affected by addition of $-CF_2$ groups distant from the carbonyl chromophore. Such an effect was not seen with the addition of $-CH_2$ groups.(231) The electron- withdrawing $-CF_2$ groups enhance the $n \rightarrow \pi^*$ transition

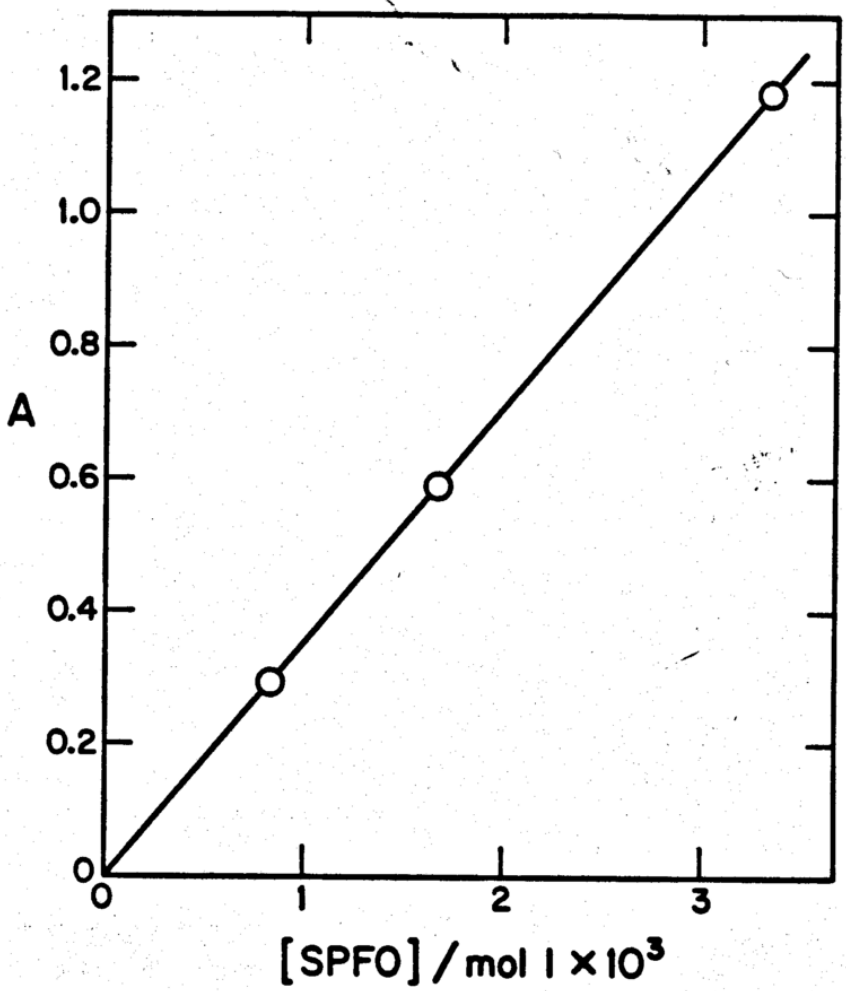

Figure 8.1 UV absorbance of SPFO at 205 nm plotted as a function of the molar concentration of SPFO in water.

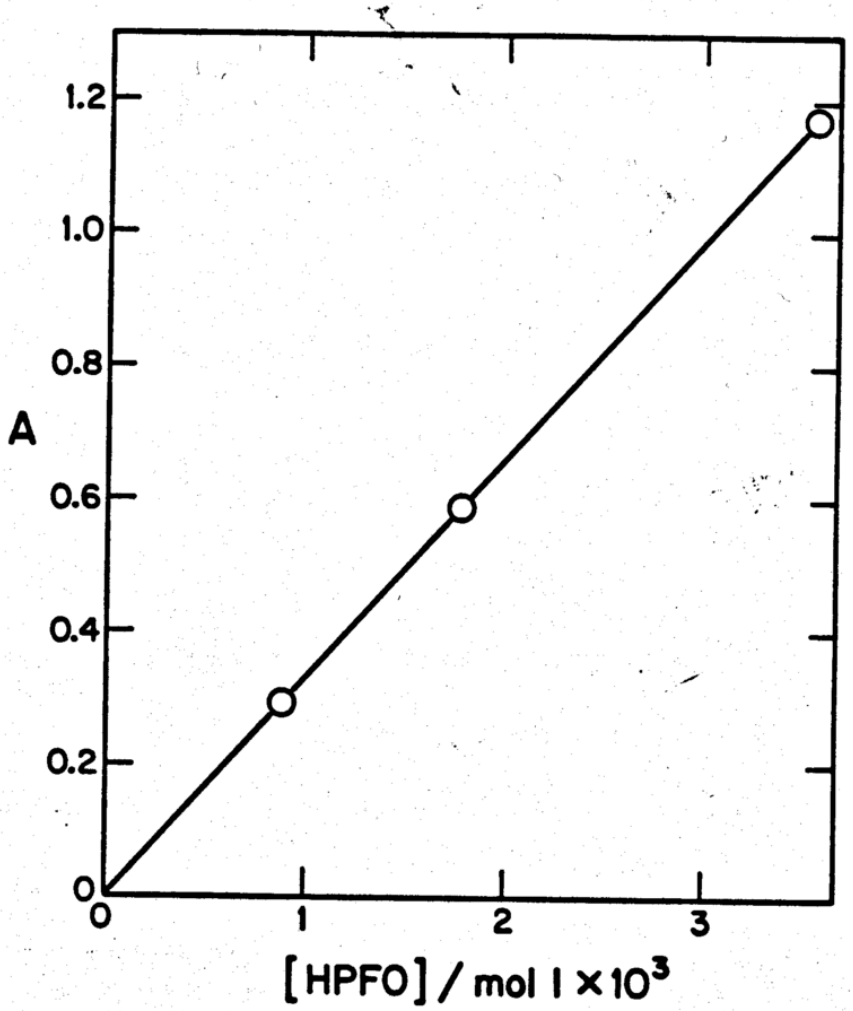

Figure 8.2 UV absorbance of HPFO at 205 nm plotted as a function of the molar concentration of HPFO in water.

probability. Increased delocalization of the n electrons by additional -CF_2 groups is likely to be responsible for this effect. The increase in molar absorptivity reflects the influence of additional -CF_2 groups on the ground state properties of the carboxyl group.

2. Approach toward determination of dissociation constants for perfluoroacids.

Substitution of a halogen onto the alkyl group of a carboxylic acid is well known to increase its acid strength. For example, the pK_a of acetic acid (4.75) is higher than that of monofluoroacetic acid (2.6) or monochloroacetic acid (2.9).(236) This effect is due to the electron-withdrawing ability of the halogen, which stabilizes the anion formed by dissociation. The effect is evident, although much reduced, even at a distance of four carbon atoms from the carbonyl. For example, butyric acid has a pK_a of 4.8 ($K_a = 1.52 \times 10^{-5}$) while that of ω- chlorobutyric acid is 4.5 ($K_a = 2.96 \times 10^{-5}$), and ß-chlorobutyric acid is 2.9.

Addition of more than one halogen results in a stronger acid.(228,236) Trichloroacetic acid and trifluoroacetic acid are known to be moderately strong acids.(226) For this reason their acid dissociation constants are

difficult to measure precisely. Conventional methods for determination of dissociation constants are at the borderline of precision in this acid region.(226) One major difficulty in the measurements is that association of the acid occurs only at high acid concentration where the activity coefficients are difficult to estimate. Dilute solution theories are not reliable at acid concentrations in the region of 5N H_2SO_4 where Szyper and Zuman estimated the half-titration point of HPFA. As discussed in the introduction, Covington and coworkers (226) have reviewed the K_a values reported for HPFA and trichloroacetic acid. A compilation of results from conductance (242), coulometric measurements (243), NMR (244), Raman spectroscopy (226) and refractometry (225) gave values for HPFA which varied from 0.588 to 8.(226) Using differential refractometry Grunwald and Haley arrived at the rather precise value of 1.07 ± 0.25 for the dissociation constant of HPFA. Much of the uncertainty reported in this value was due to uncertainty of the activity coefficient.(225)

The UV spectroscopic approach used here is based upon the difference in absorptivity of the acid and anion forms of the carboxylic acids trifluoroacetic acid (HPFA), and perfluorbutyric acid (HPFB). As had been noted by Szyper and Zuman for HPFA,(228) the absorbance at a fixed

wavelength in the region 220 nm to 250 nm increased as the inorganic acid concentration increased. This was shown not to be a general medium effect. Lithium chloride at 5.2 molal was found to have about a 3% effect on the absorbance of sodium perfluorobutyrate at 230 nm, relative to water. In comparison a 2.6 molal HCl solution increased the absorptivity of HPFA by 85% relative to water. For HPFB absorptivity rose from 16.2 l mol^{-1} cm^{-1} in water to 23.75 l mol^{-1} cm^{-1} in a 2.1 molal HCl solution. This increase is due to the higher absorptivity of the free acid in this wavelength region. The absorbance measured can be expressed as

$$A = \epsilon_{HA} C_{HA} + \epsilon_{A^-} C_{A^-} \qquad (8.1)$$

where ϵ is the molar absorptivity,

C is the concentration,

and subscripts HA and A^- stand for free acid and anion respectively.

The degree of association of the acid, α, that is, fraction of acid in the free form, can be introduced into equation 8.1, which becomes

$$\alpha = \frac{C_{HA}}{C} = \frac{(A/C) - \epsilon_{A^-}}{\epsilon_{HA} - \epsilon_{A^-}} \qquad (8.2)$$

where c is the total concentration of carboxylic acid.

The ϵ_{A^-} was determined using the sodium salt of these acids, (ϵ_{SPFA} = 4.52, ϵ_{SPFB} = 16.21 l mol^{-1} cm^{-1} at 230 nm). The ϵ values for HPFB and SPFB in water were found to be equal. The absorbances of 0.2 molar HPFA solutions or 0.06 molar HPFB solutions were measured at seven wavelengths between 250 and 220 nm in a series of solutions of increasing HCl concentration. The value of ϵ_{HA} could not be determined from the data at high acid, since the apparent ϵ value did not approach an asymptote. This was probably due to protonation of the carbonyl oxygen. (237) In the case of HPFB, micellization at high acid concentration may also occur. For this reason only the lower acid concentrations up to about 2 molal total acid will be considered further in this discussion. Over this region the change in absorptivity of HPFA and HPFB was large enough that a pK_a could be determined.

The dissociation constant, Ka, of the acid at low levels of association where the activity of the free form is close to its concentration is given by:

$$K_a = \frac{m_{H^+}\, m_{A^-}\, \gamma_{\pm}^2}{m_{HA}} = m_{H^+}\, \gamma_{\pm}^2\, \frac{(1-\alpha)}{\alpha} \qquad (8.3)$$

where $\gamma_{\pm}^2$ is the mean ionic activity coefficient of the carboxylic acid, and m_{H^+} is the molality of hydrogen ion,

$$m_{H^+} = m_{HCl} + (1-\alpha)\, m_{HPFA} \qquad (8.4)$$

Substituting equations 8.2 and 8.4 into equation 8.3 gives

$$K_a = (m_{HCl} + [1 - \frac{((A/c) - \epsilon_{A^-})}{\epsilon_{HA} - \epsilon_{A^-}}]\, m_{HPFA})\, (\frac{(\epsilon_{HA} - \epsilon_{A^-})}{(A/c) - \epsilon_{A^-}} - 1)\, \gamma_{\pm}^2 \qquad (8.5)$$

The first estimate of the value of $\epsilon_{HA} - \epsilon_{A^-}$ was that which gave the most nearly constant value of K_a as a function of HCl concentration. As in previous studies of the dissociation of these strong organic acids, (225, 226) an estimate of the $\gamma_{\pm}$ of the carboxylic acid must be made. This quantity cannot be measured since the carboxylic acid is partially associated. Furthermore, the system contains a mixture of two electrolyte components, HCl and the organic acid. An estimate of the mean ionic activity coefficient of the carboxylic acid in the mixture requires some theoretical

consideration. Work is currently underway to assess the $\gamma_{\pm}$ on the basis of modern mixture theories.(238,239)

In this analysis we will use an approach based upon known trends seen in mixtures of electrolytes. When two electrolytes A and B possessing a common ion are mixed, the activity coefficient of A in the mixture tends toward that of B and vice versa.(240) Harned and coworkers (240) developed a rule based upon numerous experimental observations of mixtures of electrolytes. The rule states that in a mixture of electrolytes A and B the activity coefficient of component B, γ_B, is given by

$$\log \gamma_B = \log \gamma_{B(o)} - \delta_B m_A$$

where δ_B is a function of the total molality and

$\gamma_{B(o)}$ is the activity coefficient of B in the absence of electrolyte A but at the same total molality as the mixture.

On this basis the value chosen as a first approximation for $\gamma_{\pm}$ of the surfactant in this system was that of aqueous solutions of HCl at the same molal concentration as the total electrolyte of the mixture. Since it is

unknown whether the activity coefficient of the surfactant alone in solution is higher or lower than that of HCl at the same concentration, the choice of the HCl activity coefficient at the same total acid concentration as the mixture provides a value which is necessarily intermediate between these two possibilities. The value of the activity coefficient $\gamma_{\pm}$ ranges between 0.75 at the lowest total acid concentration up to unity at the highest concentration. The acid solutions necessary to achieve association of the carboxylic acid are much higher and far more nonideal than usually observed in K_a measurements. In this region of acid concentrations, the differences in the mean ionic activity coeffficients of the strong acids HCl, $HClO_4$ and HBr are not large. (240) At 2 molal, the highest concentration used in this study, the $\gamma_{\pm}$ of HBr is 1.168 while that of HCl is 1.009. The slightly weaker acid HNO_3 has a $\gamma_{\pm}$ of 0.793. At lower concentrations the differences are much smaller. For example, at 1 molal the $\gamma_{\pm}$ of HCl is 0.809 while that of HNO_3 is 0.724. If the perfluoroacids are acting like other acids with respect to their activity coefficients, the error of using the HCl values for the mixtures of HCl and the perfluoracids will certainly be small.

Linear plotting of equation 8.3 allows for determination of the pK_a. Equations 8.2 - 8.4 can be rearranged to

$$\frac{m'_{H^+}\,\gamma_{\pm}^2}{((A/c) - \epsilon_{A^-})} = \frac{m'_{H^+}\,\gamma_{\pm}^2}{(\epsilon_{HA} - \epsilon_{A^-})} + \frac{K_a}{(\epsilon_{HA} - \epsilon_{A^-})} \qquad (8.6)$$

where $m'_{H^+} = (m_{HCl} + (1 - \alpha)\, m_{HPFA(B)})$.

Figures 8.3 and 8.4 are plots of the left hand side of this equation as a function of $m'_H\, \gamma_{\pm}^2$, for HPFA and HPFB respectively at 230 nm. The linearity of the data indicate that over this region of acid concentration other processes such as micellization or cation formation are not occurring. At high acid concentration deviations from linearity begin to be seen. The lines drawn through the data are unweighted least-squares linear regressions. This plotting form has the advantage of placing most of the experimental error in the y value and little experimental error in the x value.

Figure 8.3 demonstrates an important point regarding the choice of $\gamma_{\pm}$. Five of the six lowest points are solutions of HPFA containing no HCl. In these solutions no more than 15% of HPFA is free acid. Overall agreement of these data with the trend established by the solutions containing HCl is

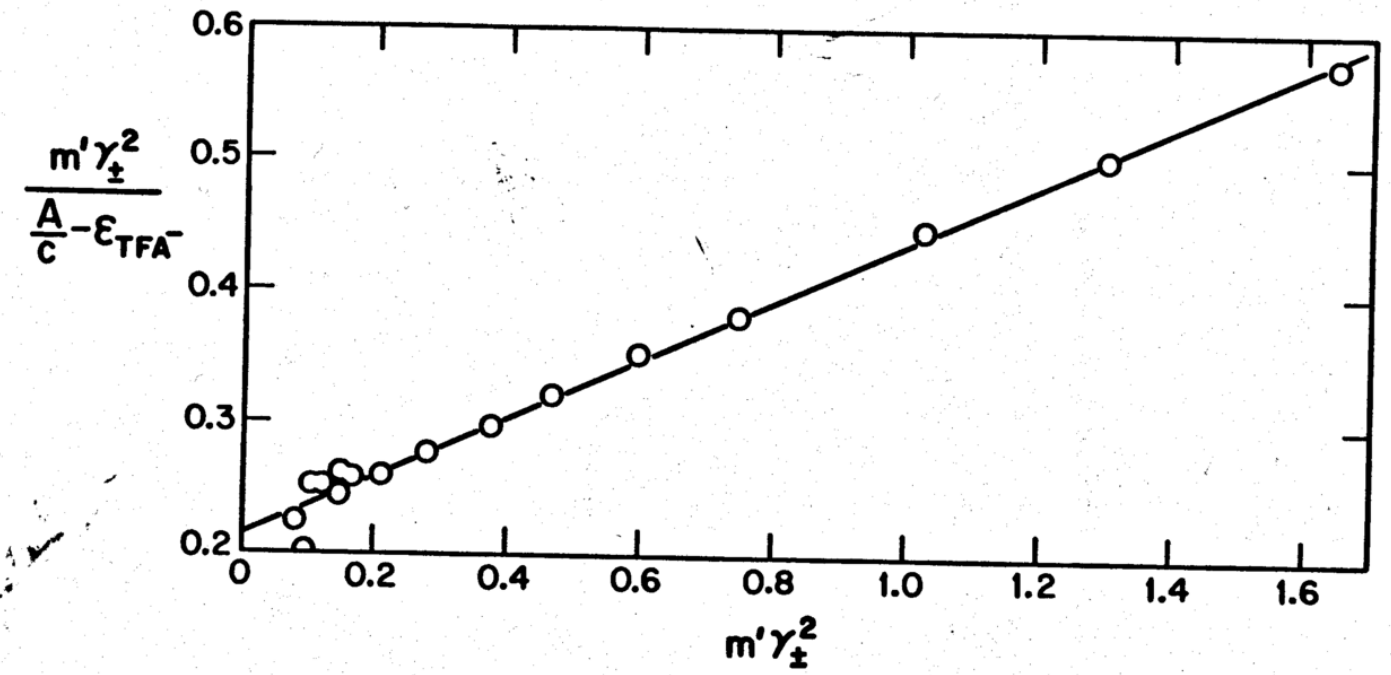

Figure 8.3 Linear plotting form (equation 8.6) for determination of K_a of trifluoroacetic acid at 25°C.

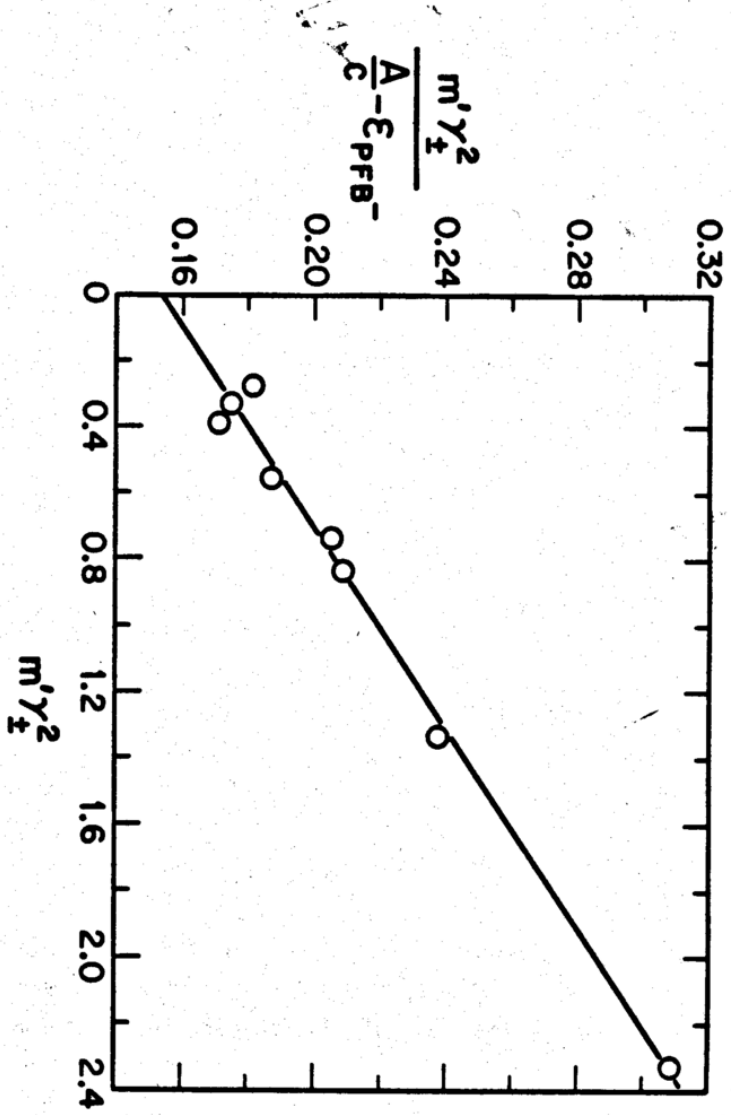

Figure 8.4 Linear plotting form (equation 8.6) for determination of K_a of perfluorobutyric acid at 25°C.

noted. The solutions containing only HPFA are described by the HCl activity coefficient in a manner which is consistent with the other data. This provides evidence that the use of the HCl activity coefficient is reasonable.

The reciprocals of the slopes of Figures 8.3 and 8.4 give the value of $\epsilon_{HA} - \epsilon_{A^-}$. The resulting values for the free acid HPFA and HPFB are 9.00 l mol^{-1} cm^{-1} and 31.45 l mol^{-1} cm^{-1} . It is interesting to note that for both of these compounds the ϵ_{HA} is nearly double that of the anion form ϵ_{HA^-}. The values of $\epsilon_{HA}/\epsilon_{A^-}$ are 1.99 and 1.94 for HPFA and HPFB, respectively. This result is reasonable since it suggests that the enhanced probability of a spectroscopic transition is affected by protonation to the same degree in each of these molecules. In other words those factors which were responsible for the magnitude of ϵ_{A^-} for each of these molecules are influenced by protonation in a proportional manner. The thermodynamic analysis above which yielded this result is thus further supported.

The K_a values for HPFA and HPFB are given by the ratio of the intercept to the slope in Figures 8.3 and 8.4. The resulting pK_a value for HPFA is 0.016 ± 0.03 and for HPFB, -0.37 ± 0.03. The errors given are 95% confidence intervals on the basis of the standard deviations of the intercept and slope.

The uncertainty of the accuracy of these values is certain to be greater. The pK_a value for HPFA is in good agreement with that of Grunwald, -0.029 ± 0.10. The overall error of the present analysis is likely to be of the same order as that seen by Grunwald. As noted by Grunwald, the largest contribution to inaccuracy arises from the uncertainty of the activity coefficient.

The pK_a of HPFB (-0.37) is certainly significantly lower than that measured for HPFA (0.016). Comparison of this result with the nearly equal and much higher pK_a's of acetic and butyric acid (4.75 and 4.8 respectively) (236) indicates the electron-withdrawing effect of additional $-CF_2$ groups. This first reported measurement of the pK_a of HPFB demonstrates the ability of this method to extend to quite strong acids.

Further work on this subject is currently underway in this laboratory by Dr. Mukerjee and Mr. Chan.(241) The primary objective is the determination of the suitable mean ionic activity coefficient. Modern mixture theories such as those of Pitzer are being examined.(238) Some further work on establishing the extent of the medium effect on the spectra is being conducted. Analysis of the data at all the wavelengths measured is needed

to establish the congruency of the results. The results reported here are certainly encouraging. The method provides values of dissociation constants which agree with the most precise values so far reported. The technique can be extended to larger chain perfluoro acids with reasonable precision.

3. Determination of the CMC of Salts of Perfluorocarboxylic Acids by UV Spectroscopy

The micellar and free forms of some surfactants have different absorption spectra.(246,247) At suitable wavelengths, changes in absorptivity produce slope changes in plots of absorbance vs. concentration. Extrapolation of the linear portions of these plots gives the cmc value. This method has been used for alkyl pyridinium halides (247), which undergo a change in their charge transfer spectra upon micellization. The cmc of Triton X-100, which contains a phenolic group between an alkyl chain and a polyoxyethylene chain, has also been obtained in this manner. (247)

In general, micellization places the head group of a surfactant at a dielectric interface and in a region containing a high concentration of headgroups and counterions. This region has been shown to be associated

with a lower effective dielectric constant than water.(249,250) Studies on dissociation constants show a higher pK_a at the micellar surface than in bulk aqueous solution. (250) Also investigation of solvent effects on the charge transfer spectra of long-chain pyridinium iodides have indicated that upon micellization the head group of these surfactants is transferred to a low dielectric constant region, (approximately 36). (249)

Previous studies have shown that for hydrocarbon micelles this region is associated with a small red shift in the spectra of hydrocarbon solubilizates in comparison with hydrocarbon solvents.(49,50) A large red shift in comparison with water is seen. This is expected since water has a lower refractive index (1.333) than the long chain hydrocarbons (1.4 -1.43) which make up the micellar core. Increase in the refractive index is known to contribute to a red shift in absorption spectra.(216,217)

Fluorocarbons have lower refractive indices (1.25 for C_6F_{14}) than water.(213) However, a red shift of the $n \rightarrow \pi^*$ transition of the perfluorocarbon carboxylate salts is expected upon micellization. This is due to the low polarity of the headgroup region as reflected by the low dielectric constants measured there. As has been discussed in the introduction, decreasing the polarity of the solvent resulted in a red shift

with respect to water of the $n \rightarrow \pi^*$ transition.(230) A red shift of the 210 nm shoulder upon micellization would cause an increase in molar absorptivity with respect to the monomer in water. The changes found experimentally were large enough to permit determination of the cmc by UV absorption spectroscopy.

Determination of the cmc was facilitated by a difference plotting form obtained in the following manner. The perfluorooctanoate salts studied were found to obey Beer's Law above and below the cmc. Therefore equation 8.7 applies above the cmc where surfactant is in monomer and micellar form.

$$A = (\epsilon_1 c_1 + \epsilon_m c_m)\, l \qquad (8.7)$$

where A is absorbance due to the surfactant

l is the path length of the spectrophotometric cell

ϵ is the molar absorptivity

c is the molar concentration and

1 and m stand for monomer and micelle respectively.

Therefore, since c_1 = cmc and $c = c_1 + c_m$ above the cmc,

$$A/l = \epsilon_1 cmc + \epsilon_m(c\text{-}cmc) \quad (8.8)$$

or

$$(A/l) - \epsilon_1 c = (\epsilon_1 - \epsilon_m)\, cmc + (\epsilon_m - \epsilon_1)c. \quad (8.9)$$

The left hand side of equation 8.9 is a linear function of c with x-intercept equal to the cmc. This form clearly indicates the breakpoint in change in absorptivity .

Figure 8.5 is a difference plot of the UV absorbance data for SPFO in water at 25°C. The cmc determined in this manner is 0.0314 molar (S.D. 0.0007). This value is in good agreement with previously reported values from Krafft point determinations (0.036 molar at 8°C), (251) NMR (0.032 molal at 25°C (7), and conductivity (0.032 molal at 25°C) (252). The present method provides a simple technique for determining cmcs of perfluorocarbon carboxylic acid surfactants. It is limited only by the limitations of absorbance measurements. For example, compounds which interfere with UV absorption in this region could not be used. The present method requires no additive and, therefore, does not disturb the micelle at all. Dye solubilization or dye partitioning techniques have been found to be

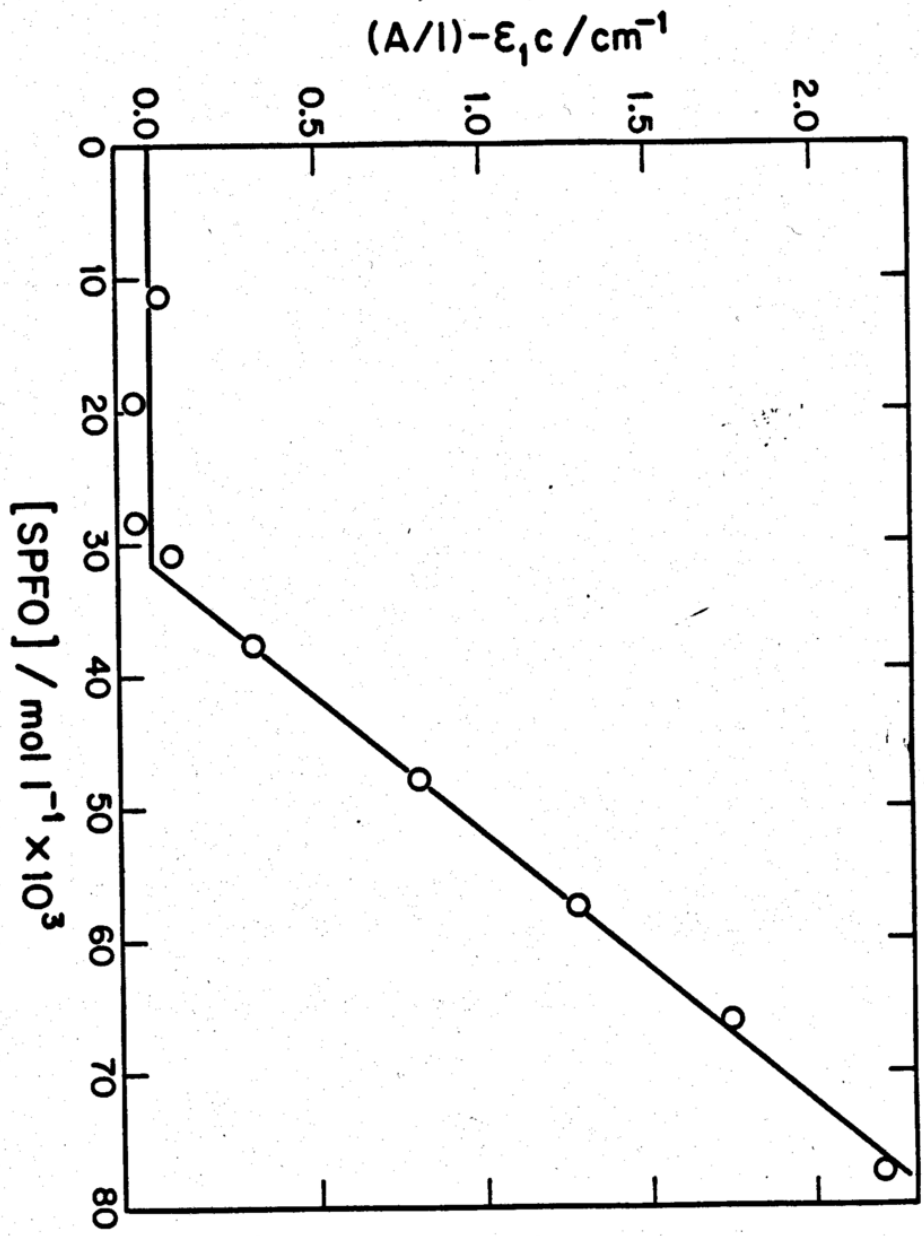
(A/l)−ε1c / cm−1
0.0
0.5
1.0
1.5
2.0
[SPFO] / mol l−1 × 10³
0
10
20
30
40
50
60
70
80

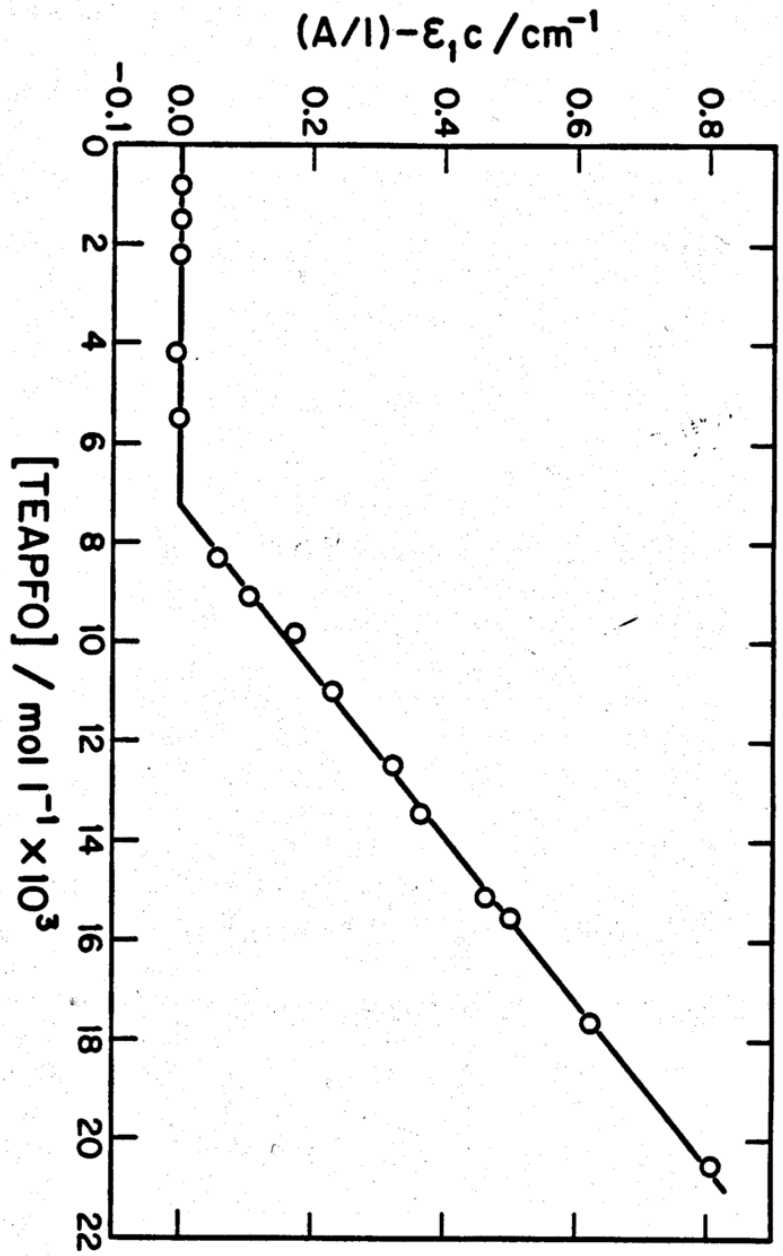
(A/l)−ε1c /cm−1
−0.1
0.0
0.2
0.4
0.6
0.8
0
2
4
6
8
10
12
14
16
18
20
22
[TEAPFO] / mol l−1 × 10³

inadequate for cmc determination of perfluorocarbon surfactants.(24) The large predominantly hydrocarbon dye molecule does not partition in most perfluorocarbon micelles to a great enough degree to permit cmc determination.

The present method was tested further to determine the effect of change of counterion on the absorption characteristics as well as the cmc. In this case tetraethylammonium perfluorooctanoate was used. This hydrophobic counterion is known to reduce the cmc of hydrocarbon surfactants.(192) The stabilization of the micelle imparted by this counterion has been attributed to its ability to interact with the hydrocarbon core of the micelle.(192) Interestingly, evidence has also been found that such counterions reduce the cmc's of perfluorocarbon surfactants. Hoffman (253) found that tetraethylammoniumperfluoro-sulfonate had a lower cmc than the corresponding sodium salt. This effect is quite interesting since perfluorocarbons and hydrocarbons are known to exhibit a mutual antipathy.(69,100,198) In the proximity of these counterions, it is of interest to see if an increase in UV absorbance on micellization is again seen. The difference in the magnitude of the effect also gives an indication of any specific counterion contribution of the

absorbance of the surfactant.

Figure 8.6 is a difference plot of the absorbance at 205 nm of tetra ethylammoniumperfluoroctanote (TEAPFO) as a function of the concentration in aqueous solution at 25°C. The characteristic breakpoint is again noted. The cmc value of 0.00721 molar (0.00010 S.D.) is in good agreement with that found by Mr. Chan of this laboratory (0.0071) molar using a fluorescent dye partitioning technique.(241) The UV method is thus shown to be applicable independent of the counterion. The spectroscopic changes are about the same as noted for SPFO. The molar absorptivity at 205 nm was found to increase by about 14% for SPFO and by about 18% for TEAPFO. Both salts are seen, in Figures 8.5 and 8.6, to obey Beer's Law above the cmc. This indicates that any structural changes and intermicellar interactions above the cmc are not influencing this spectroscopic transition.

The above results are encouraging in showing that the method has a wide application and is quite precise. The overall error in the cmc values is of the order of 5%. One area in particular where this method is expected to be useful is the measurement of cmc at high electrolyte concentrations. Conductivity measurements are extremely difficult at high salt.(254)

Methods which require measurement of the spectral changes of dyes have also been shown to be ineffective under such conditions.(241)

A preliminary study at high electrolyte concentrations has indicated that the UV method is appropriate. Lithium perfluorooctanoate (LiPFO) in the presence of one molar lithium chloride was measured. Results obtained indicated that the UV method was suitable for detecting a cmc. The breakpoint occurred at a reasonable concentration. However, experimental difficulties due to Cl^- absorption and instrumental irregularities prevented precise measurement of the cmc. Building upon these studies, the experiment was redesigned so that the difficulties encountered would be minimized. Mr. Chan of this laboratory has recently conducted this study. A precise value of the cmc of LiPFO in 1M LiCl was obtained by this method. Further work at low and high salt concentration is under way. An initial goal for extension of this work is the determination of limits of the mass action relationship (1)

$$\log \text{cmc} = A - B \log [\text{counterion}]$$

for these surfactants.

In summary, a method of cmc determination has been devised and validated. It employs the change in UV spectrum upon micellization of

perfluorocarboxylate salts to determine the cmc of these compounds. This noninvasive method has been found to be precise to ± 5%. It is much simpler to use than surface tension methods and requires instrumentation availlable in most laboratories. The method has been shown to extend to high salt concentration where other methods, such as conductivity, have serious drawbacks.

REFERENCES

1. Mukerjee, P., Adv. Coll. Interf. Sci., 1, 241 (1967).

2. Tanford, C., "The Hydrophobic Effect", John Wiley, N.Y. (1973).

3. Hartley, G.S. in "Micellization, Solubilization, and Microemulsions", p. 23, K.C. Mital, ed., 1, Plenum, New York (1979).

4. Adamson, A.W., "Physical Chemistry of Surfaces", Fourth edition, John Wiley, New York (I982).

5. Mukerjee, P., and Mysels, K.L., "Critical Micelle Concentrations of Aqueous Surfactant Systems", NSRDS-NBS 36, U.S. National Bureau of Standards, Superintendent of Documents, Washington, D.C. (1971).

6. Mysels, K.J. and Mukerjee, P., Pure and Applied Chem., 51, 1083 (1979).

7. Yang, Y.S., Ph.D. Thesis, University of Wisconsin (1980).

8. Elworthy, P.H. and Mysels, K.J., J. Coll. Interf. Sci., 21, 331 (1966).

9. Mittal, K.L. and Mukerjee, P., in "Micellization, Solubilization, and Microemulsions", p.1, K.L. Mittal, ed., 1, Plenum, New York (1977).

10. Fendler, J.H., "Membrane Mimetic Chemistry", Wiley, New York (1982).

11. Fendler, J.H. and Fendler, E.J., " Catalysis in Micellar and Macromolecular Systems", Academic Press, N.Y. (1975).

12. Reiss-Husson, F. and Luzzati, V., J. Phys. Chem., 68, 3504 (1964).

13. Gruen, D.W.R., Progr. Colloid and Polymer Sci., 70, 6 (1985).

14. Hartley, G.S. "Aqueous Solutions of Parafin Chain Salts", Hermon, Paris (1936).

15. Huisman, H.F., Proc. K. Ned. Akad. Wet. Ser. B., 67, 388 (1964).

16. Mukerjee, P., Ber. Bunsenges. Phys. Chem., 82, 931 (1978).

17. Dill, K.A., J. Phys. Chem. 86, 1498 (1982).

18. Mukerjee, P., Koll. Z.Z. Polym., 236, 76 (1970).

19. Kurz, J.L., J. Phys. Chem., 66, 2239 (1962).

20. Mukerjee, P., in "Micellization, Solubilization, and Microemulsions", p. 171, K.L. Mittal, ed., 1, Plenum, New York (1977).

21. Aniansson, G.E.A., Prog. Coll. Polym. Sci., 70, 2 (1985).

22. Aniansson, E.A.G., et al, J. Phys. Chem., 80, 905 (l976).

23. Mukerjee, P., in "Solution Chemistry of Surfactants", p. 153, K.L. Mittal, ed., 1, Plenum, New York (1979).

24. McBain, M.E.L. and Hutchinson, E., "Solubilization and Related Phenomena", Academic Press, New York (1955).

25. Koltoff, I.M. and Stricks,W., J. Phys. Coll. Chem., 52, 915 (1948).

26. Koltoff, I.M. and Stricks,W., J. Phys. Coll. Chem., 53, 424 (1949).

27. Williams R.J., Phillips J.N., Mysels K.J.,Trans. Farad. Soc.51, 728 (1955).

28. Mukerjee, P., Cardinal, J.R. and Desai, N.R., in "Micellization, Solubilization, and Microemulsions", p. 241, K.L. Mittal, ed., 1, Plenum, New York (1977).

29. Almgren, M., Grieser, F., Thomas, J.K., J. Am. Chem. Soc., 101, 279 (1979).

30. Klevens, H.B., Chem. Rev., 47, 1 (1950).

31. Elworthy, P.H., Florence, A.T. and MacFarlane, C.B., "Solubilization by Surface Active Agents," Chapman and Hall, London (1968).

32. Florence, A.T., in "Techniques of Solubilization of Drugs", S. Yalkowsky, ed., Dekker, N.Y. (1982).

33. Atwood, D. and Florence, A.T., "Surfactant Systems," Chapman and Hall, New York (1983).

34. Robb, I., ed. "Microemulsions", Plenum, N.Y. (1982).

35. Venable, R.L., and Nauman, R.V., J.Phys. Chem., 68, 3498 (1964).

36. Jacobs, P.T. and Anacker, E.W., J. Coll. Interf. Sci. 43, 105 (1973).

37. Stearns, R. S., Oppenheimer, H., Simon, E. and Harkins, W.D., J. Chem. Phys., 15, 496 (1947).

38. Klevens, H.B., J. Phys. Coll. Chem., 54, 283 (1950).

39. Harkins, W.D., and Oppenheimer, H., J. Am. Chem. Soc., 79, 808 (1949).

40. Missel, P.J., Mazer, N.A., Benedek, G.B. and Young, C.Y., J. Phys. Chem., 84, 1044 (1980).

41. Anaker, E.W., Rush, R.M. and Johnson, J.S., J. Phys. Chem., 68, 81 (1964).

42. Hoskins, J.C. and King, A.D., J. Coll. Interf. Sci., 82, 260 (1981).

43. Koltoff and Graydon, J. Phys. Coll. Chem., 55, 699 (1951).

44. Chaiko, M.A., Nagarajan, R. and Ruckenstein, E., J. Coll. Interf. Sci., 99, 168 (1984).

45. Hayase, K. and Hayano, S., Bull. Chem. Soc. of Japan, 50, 83 (1977).

46. Riegelman, S., Allawalla, N.A., Hrenoff, M.K. and Strait, L.A., J. Coll. Sci., 13, 208 (1958).

47. Rehfeld, S., J. Phys. Chem. 74, 117 (1970).

48. Rehfeld, S., J. Phys. Chem. 75, 3905 (1970).

49. Cardinal, J. and Mukerjee, P., J. Phys. Chem. 82, 1614 (1978).

50. Mukerjee, P., and Cardinal, J., J. Phys. Chem. 82, 1620 (1978).

51. Ramachandran, C., Pyter, R.A. and Mukerjee, P., J. Phys. Chem. 86, 3198 (1982).

52. Pyter, R.A., Ramachadran, C. and Mukerjee, P., , J. Phys. Chem. 86, 3206 (1982).

53. Eriksson, J.C. and Gillberg, G., Acta Chem. Scand., 20, 2019 (1966).

54. Fox, K.K., Robb, I.D. and Smith, R., Faraday Trans. I, 68, 445 (1972).

55. Jobe, D.V., Reinsborough, V.C. and White, P.J., Can. J. Chem., 60, 279 (1982).

56. Kalyansundarum,K. and Thomas, J.K., 99, 2039 (1977).

57. Mukerjee, P., Ramachandran, C., Pyter, R.A., J. Phys. Chem. 86, 3189 (1982).

58. Rehfeld, S.J., J. Phys. Chem., 71, 738 (1967).

59. Gumkowski, M.J., M.S. Thesis, University of Wisconsin (1983).

60. Smith, M.B. and Alexander, A.E., in "Proc. 2nd Int. Cong. Surface Activity", Vol. 1, p. 311, Butterworth, London (1957).

61. Mukerjee, P. and Manabe, M., unpublished work.

62. Mukerjee, P., Pure and Appl. Chem., 52, 1317 (1980)

63. Nakagawa, T. and Tori, K., Kolloid Z.Z., 1968 132 (1960).

64. Wishnia, A., J. Phys. Chem., 67, 2079 (1963).

65. Blatt, E., Sawyer, W.H. and Ghiggino, K.P., J. Phys. Chem., 88, 3918 (1984)

66. Dipple, A., Polynuclear Aromatic Carcinogens in "Chemical Carcinogens", ACS monograph 173, (Searle, C.E. ed.), American Chemical Society, Washington D.C., 1976.

67. Halper, L.A., Timmons, C.O., Zisman, W.A., J. Coll. Interf. Sci., 38, 511 (1972).

68. Leci, C.L., Garti, N. and Sarig, S., J. Cryst. Growth, 51, 85 (1981).

69. Mukerjee, P. and Handa, T., J. Phys. Chem., 85, 2298 (1981).

70. Pyter, R.A., Ph.D. Thesis, University of Wisconsin (1980).

71. Graham, D., J. Phys. Chem., 66, 1815 (1962).

72. Starkweather, H.W., Macromolecules, 10, 1161 (1977).

73. Lando, J.L. and Oakley, H.T., J. Coll. Interf. Sci., 25, 526 (1967).

74. Bauer, N. and Levin, S.Z., in "Technique in Organic Chemistry", Vol. I, p. 157, Interscience, New York (1959).

75. Ben-Naim, A. and Wilf, J., J. Phys. Chem., 84, 583 (1984).

76. Rubio, R.G., Menduina, C., Renuncio, J.A.R. and Diaz Peña, M., J. Chem. Soc. Faraday Trans. I, 80, 1425 (1984).

77. Harris, K.R. and Dunlop, P.J., J. Chem. Thermodyn., 2, 805 (1970).

78. Jain, D.V.S., Gupta, V.K. and Lark, B.S., J. Chem. Thermodyn., 5, 451 (1973).

79. Rubio, R.G., Renuncio, J.A.R. and Diaz Peña, M., Intern. J. Thermophys., 3, 325 (1982).

80. Rubio, R.G., Renuncio, J.A.R. and Diaz Peña, M., Thermochemica Acta, 65, 69 (1983).

81. Barker, J.A., Aust. J. Chem., 6, 207. (1953).

82. Tucker, E.E. and Christian, S.D., J. Phys. Chem., 83, 426 (1979).

83. Yoshida,Z., Osawa, E., J. Am. Chem. Soc., 87, 1467 (1965).

84. Yoshida,Z., Osawa, E., J. Am. Chem. Soc., 88, 4019 (1966).

85. Linse, P., Diss. Farad. Soc. 17, 179 (1982).

86. Engberts, J.B.F.N., Diss. Farad. Soc., 17, 179 (1982).

87. Abraham, M.H., J. Chem. Soc., Faraday Trans. I, 80, 153 (1984).

88. MacKay, D. and Shiu, W. Y., J. Phys. Chem. Ref. Data, 10, 1175 (1981).

89. Bohon, R.L. and Claussen, W.F., J. Amer. Chem. Soc., 73, 1571 (1951).

90. Ben-Naim, A.,Wilf, J., and Yaacobi, M., J. Phys. Chem., 77, 95 (1973).

91. Hildebrand, J.H., Prausnitz, J.M. and Scott, R.L., "Regular and Related Solutions", Van Nostrand Reinhold, New York (1970).

92. Green, W.J. and Frank, H.S., J. Soln. Chem., 8, 187 (1979).

93. Guggenheim,E.A. and Adam, N.K., Proc. Roy. Soc. A., 139, 218 (1933).

94. Butler, J.A.V., Proc. Roy. Soc. A, 135, 348 (1932).

95. Belton, J.W. and Evans, M.G., Trans. Faraday Soc., 41, 1 (1945).

96. Guggenheim,E.A., Trans. Faraday Soc., 41, 150 (1945).

97. Hoar, T.P. and Melford, D.A., Trans. Faraday Soc., 53, 315 (1957).

98. Prigogine,I. and Melford, D.A., J. Coll. Sci., 7, 122 (1952).

99. Defay, R., Prigogine, I., Bellemans, A. and Everett, D.H., "Surface Tension and Adsorption, John Wiley, New York (1966).

100. Handa, T. and Mukerjee, P., J. Phys. Chem., 85, 3916 (1981).

101. Kaelble, K.H., "Physical Chemistry of Adhesion," Wiley, New York (1971).

102. Gaines, G.L., Jr., J. Phys. Chem. 73, 3143 (1979).

103. Gaines, G.L., Jr., Trans. Faraday Soc., 65, 2370 (1969).

104. Girifalco,L.A., and Good, R.J., J. Phys. Chem., 61, 904 (1957).

105 Fowkes, F.M., J. Phys. Chem., 84, 510 (1980).

106. Eberhart, J.G., J. Phys. Chem., 70, 1183 (1966).

107. Romagosa, E.E., and Gaines, G.L., Jr., J. Phys. Chem., 73, 3150 (1969).

108. Schmidt, R.L., Randall, J.C. and Clever, H.L., J. Phys. Chem. 70, 3912 (1966).

109. Edmons, B. and McLure, I.A., J. Chem. Soc. Faraday Trans., 1., 78, 3319 (1982).

110. Jasper, J.J., J. Phys Chem. Ref. Data, 1, 841 (1972).

111. Flory, P.J., "Principles of Polymer Chemistry", Chapter 12, Cornell University Press., Ithica, (1953).

112. Letcher, T.M., J. Chem. Thermodyn., 7, 969 (1975).

113. Shewmaker, J.E., Vogler, C.E. and Washburn, E.R., J. Phys. Chem., 58, 945 (1954).

114. Gillap, W.R., Weiner, W.D. and Gibaldi, M., J. Am. Oil. Chem. Soc., 44, 71 (1967).

115. Mellan, I., "Compatibility and Solubility", Noyes Development Corp., Park Ridge, N.J. (1968).

116. Aveyard, R., Trans. Faraday Soc. 64, 2778 (1967).

117. Schatzberg,P., J. Phys. Chem., 67, 776 (1963).

118. Goldman, S., Can. J. Chem., 52, 1668 (1974).

119. Aveyard, R. and Briscoe, B.J., J. Chem. Soc. Farad. Trans. I, 68, 478 (1972).

120. Croxton, C.A., "Statistical Mechanics of the Liquid Surface", Wiley, New York (1980).

121. Rusanov, A.I., J. Coll. Interf. Sci., 85, 157 (1982).

122. Gunnarson, G., Jonsson, B. and Wennerstron, H., J. Phys. Chem., 84, 3114 (1980).

123. Isrealachvili, J.N., Mitchell, J.J., and Ninham, B.N., J. Chem. Soc., Faraday Trans., 2, 72, 1525 (1976).

124. Nagarajan, R. and Ruckenstein, E., J. Coll. Interf. Sci., 71, 580 (1979).

125. Ericksson, J.C., Ljungguen, S. and Henriksson, U., J. Chem. Soc., Faraday Trans., 2 81, 833 (1985).

126. Matheson, I.B.C. and King, A.D., Jr., J. Coll. Interf. Sci., 66, 464 (1978).

127. Hoskins, J.C. and King, A.D. Jr., J. Coll. Interf. Sci., 82, 260 (1981).

128. Bolden, P.C., Hoskins, J.C. and King, A.D. Jr., J. Coll. Interf. Sci., 91, 454 (1983).

129. Ownby, D.W. and King, A.D., Jr., J. Coll. Interf. Sci., 101, 271 (1984).

130. Prapaitrakul, W. and King,A.K. Jr., J. Coll. Interf. Sci., 106, 186(1985).

131. Christian, S.D., Tucker, E.E. and Lave, E.H., J. Coll. Interf. Sci., 84, 423 (1981).

132. Aveyard, R. and Haydon, D.A., Trans. Faraday Soc., 61, 2255 (1965).

133. Hartly, G.S., in "Wetting and Detergency", Chemical Publishing Co. of New York, N.Y. (1937).

134. Kling, W., and Lange, H., Proc. Second Cong. Surf. Activity, London, 1, 295 (1957).

135. Haydon, D.A. and Taylor, F.H., Phil. Trans. Roy. Soc., Ser. A., 252, 225 (1960).

136. Abraham, M.H., J. Am. Chem. Soc., 14, 2087 (1982).

137. Jadot, R., J. Chim. Phys. Chim. Biol., 69, 1036 (1962).

138. Wilhelm, E. and Battino, R., Chem. Rev., 73, 1 (1973).

139. Hayduk, W., and Cheng, S.C., Can. J. Chem. Eng., 48, 93 (1970).

140. Handa, Y.P., D'Arcy, P.J., and Benson, G.C., Fluid Phase Equil., 8, 181 (1982).

141. Goates., J.P., Ott, J.B., and Grigg, R.B., J. Chem. Thermodyn., 13, 907 (1981).

142. Ott, J.B., Marsh, K.N. and Stokes, R.H., J. Chem. Thermodyn., 13, 371 (1981).

143. Gomez-Ibanez, J.D., and Liu, C.T., J. Phys. Chem., U67U, 1388 (1963).

144. Schneider, R.L., Eastman Organic Chem. Bull., 47, 1 (1975).

145. Letcher, T.M., J. Chem. Thermodyn., 11, 435 (1979).

146. Goates., J.P., Ott, J.B., and Grigg, R.B., J. Chem. Thermodyn., 11, 497 (1979).

147. Temper, K.K., and Anderson, S.T., Ann. Rev. Med., 36, 309 (1985).

148. Tolman, R.C., J. Chem. Phys., 17, 333 (1949).

149. Fisher, L.R., and Isrealachvili, J.N., Coll. and Surf., 3, 303 (1981).

150. Mukerjee, P., J. Phys. Chem., 74, 3824 (1970).

151. Haydon, D.A. and Taylor, F.H., Trans. Farad. Soc., 58, 1233 (1962).

152. Pierotti, R.A., J. Phys. Chem., 69, 281 (1965).

153. Brooks, J.H. and Pethica, B.A., Trans. Farad. Soc., 61, 571, (1965).

154. Mukerjee, P., J. Phys. Chem., 66, 943 (1962).

155. Corkill, J.M., Goodman, J.F. and Walker, T., Trans. Faraday Soc., 63, 768 (1967).

156. Tanaka, M., et.al., J. Coll. Interf. Sci., 46, 132 (1974).

157. Tartar, H.V., J. Coll. Interf. Sci., 14, 115 (1959).

158. Melrose, J.C., in "Applied Thermodynamics", p. 249, (D.E. Gushee, ed.), ACS Publications, Wash. D.C. (1968).

159. Mukerjee, P., J. Phys. Chem., 65, 740 (1961).

160. Lianos, P. and Zana, R., J. Phys. Chem., 84, 339 (1980).

161. Stigter, D., J. Coll. Interf. Sci., 23, 379 (1967).

162. Overbeek, J. Th. G. and Stigter, D., Rec. Trav. Chim., 75, 1263 (1956).

163. Stigter, D. and Overbeek, J.Th.G., Proc. Intern. Cong. Surface Activity Second, London 1957, Vol I, p. 311.

164. Lucassen-Reynders, E.H., ed., "Anionic Surfactants", p. 1 Marcel Dekker, N.Y. (1981).

165. Davies, J.T., Proc. Roy. Soc., Ser. A., 208, 244 (1951).

166. Nagarajan, R. and Ruckenstein, E. in "Surfactants in Solution" (K.L. Mittal, Ed.), Plenum, New York (1983).

167. Lucassen-Reynders, E.H., J. Phys. Chem., 70, 1777 (1966).

168. Rodakiewicz-Nowak, J. and Goralezyk, D., J. Coll. Interf. Sci. , 103, 290 (1985).

169. Jho, C. and King, A.D., Jr., J. Coll. Interf. Sci. , 79, 365 (1981).

170. Aveyard, R. and Mitchell, R.W., Faraday Trans., 65, 2645 (1969).

171. Vilallonga, F.A., Koftan, R.J., and O'Connell, J.P., J. Coll. Interf. Sci., 90, 539 (1982).

172. Stilbs, P., J. Coll. Interf. Sci., 80, 608 (1981).

173. Abu-Hamdiyyah, M. and Rahman, I.A., J. Phys. Chem., 89, 2377 (1985).

174. Tucker, E.E. and Christian, S.D., Faraday Symp., 17, I (1982).

175. Brady, A.P. and Huff, H., J. Phys. Chem., 62, 644, (1957).

176. Carlfors, J. and Stilbs, P., J. Coll. Interf. Sci., 103, 332 (1985).

177. Abuin, E.B. and Lissi, E.A., J. Coll. Interf. Sci., 95, 198 (1983).

178. Treiner, C. and Chattopadhyay, A.K., J. Coll. Interf. Sci., 98, 447 (1984).

179. Zana, R., Yiv, S., Strazielle, C. and Lianos, P., J. Coll. Interf. Sci., 80, 208 (1981).

180. Mukerjee, P. and Mysels, K.J., J. Am. Chem. Soc., 77, 2937 (1955).

181. Isirikyau, A.A. and Kiselev, A.V., J. Phys. Chem, 66, 210 (1962).

182. Isirikyau, A.A. and Kiselev, A.V., J. Phys. Chem, 65, 601 (1961).

183. Simon, S.A., McDaniel, R.V. and McIntosh, T.J., J. Phys. Chem., 86, 1449 (1982).

184. Hirose, C. and Sepulveda, L., J. Phys. Chem., 85, 3689 (1981).

185. Deno, N.C. and Spink, C.H., J. Phys. Chem., 67, 1347 (1963).

186. McDevit, W.F. and Long, F.A., J. Am. Chem. Soc., 74, 1773 (1952).

187. Lianos, P., Viriot, M-L. and Zana, R., J. Phys. Chem., 88, 1098 (1984).

188. King, M.B. "Phase Equilibrium In Mixtures", Pergamon, Oxford (1969).

189. Bergen, R.C., Jr. and Long, F.A., J. Phys. Chem., 60, 1131 (1956).

190. Krasnoshchekova, R. and Gubergrits, M., Coll. J. of the USSR, 45, 300 (1983).

191. Sepulveda, L. and Sato, R., Makromal. Chem., 179, 765 (1978).

192. Mukerjee, P. Mysels, K.J. and Kapauan, P., J. Phys. Chem., 71, 4166 (1967).

193. Wen, Y.H. and Hung, J.H., J. Phys. Chem., 74, 170 (1970).

194. Heller, W., Klevens, H.B. and Oppenheimer, H., in J. Chem. Phys., 14, 565 (1946).

195. Mysels, K.J., Mukerjee, P. and Abu-Hamdiyyah, M.J., J. Phys. Chem., 67, 1943 (1963).

196. Meder, W.J., Vold, R.D. and Vold, M.J., in "Techniques of Organic Chemistry", A. Weissberger (ed.), Vol. 1, "Physical Methods of Organic Chemistry", Third ed., Part 1, Chapter 11, Interscience, N.Y. (1959).

197. Daniels, F., et.al., "Experimental Physical Chemistry", McGraw Hill, New York (1970).

198. Hildebrand, J.H., Fisher, B.B., Benesi, H.A., J. Am. Chem. Soc., 72, 4348 (1950).

199. Mukerjee, P. and Mysels, K.J., ACS Symp. Series No. 9, 239 (1975).

200. Stigter, D., Williams, R.J. and Mysels, K.J., J. Phys. Chem., 59, 330 (1955).

201. Hayashi, S. and Ikeda, S., J. Phys. Chem., 84, 744 (1980).

202. Ikeda, S., Hayashi,S., and Imae, T., J. Phys. Chem., 85, 106 (1981).

203. Young, C.Y., Missel, P.J., Mazer, N.A. and Benedek, G.B., J. Phys. Chem., 82, 1375 (1978).

204. Hwang, S.T. and Kammermayer, K., "Membranes in Separations, Techniques in Chemistry", Vol VII, A. Weissberger, ed., Wiley (1975).

205. Schott, H., J. Phys. Chem., 70, 2966 (1966).

206. Mukerjee, P. and Williams, N.A., unpublished work; Williams, N.A., M.S. Thesis, University of Wisconsin (1980).

207. Almgren, M. and Swarup, S., J. Phys. Chem., 86, 4212 (1982).

208. Heriz, E.L. and Posey, C.D., J. Chem. Eng. Data, 9, 35 (1964).

209. Ozeki, S. and Ikeda, S., J. Phys. Chem., 89, 5088 (1985).

210. Imae, T., Abe, A., Taguchi, Y. and Ikeda, S., J. Coll. Interf. Sci., 109, 567 (1986).

211. Funasaki, N., Yang, Y.S. and Mukerjee, P., unpublished work.

212. Mukerjee, P. and Handa, T., unpublished work.

213. Eastman, J.W. and Rehfeld, S.J., J. Phys. Chem., 74, 1438 (1970).

214. Evans, D.F., J. Chem. Phys., 23, 1429 (1955).

215. Mauser, H., and Kretschmer, R., Z. Phys. Chem., 80, 21 (1972).

216. Rao, C.N.R., "Ultra-Violet and Visible Spectroscopy", Second ed., Plenum, New York (1967).

217. Bayliss, N.S., J. Chem. Phys., 18, 292 (1950).

218. Cordes, E.H. and Dunlop, R.B., Acc. Chem. Res., 2, 329 (1969).

219. Singer, S.J. and Nicolson, G.L., Science, 175, 720 (1972).

220. Russell, J.C. and Whitten, D.J., J. Am. Chem. Soc., 104, 5939 (1982).

221. Russell, J.C., Wild, U.P. and Whitten, D.G., J. Phys. Chem., 90, 1319 (1986).

222. Menger, F.M. and Chow, J.F., J. Am. Chem. Soc., 105, 5501 (1983).

223. Banks, R.E., ed., "Organofluorine Chemicals and Their Industrial Applications", Ellis Horwood Ltd., Chichester, England, (1979).

224. Mukerjee, P. and Yang, Y.S., J. Phys. Chem., 80, 1388 (1976).

225. Grunwald, E. and Haley, J.F. Jr., J. Phys. Chem., 72, 1944 (1968).

226. Covington, A.K., Freeman, J.G. and Lilley, T.H., J. Phys. Chem., 74, 3773,

227. Robin, M.B., "Higher Excited States of Polyatomic Molecules," Vol II, Academic Press, New York (1975).

228. Szyper, M. and Zuman, P., Analytica Chemica Acta, 85, 357 (1976).

229. Timmons, C.J., ed., "UV Atlas for Organic Compounds", Vol. 5, (1967).

230. Jaffe, H.H. and Orchin, M., "Theory and Applications of Ultra Violet Spectroscopy", Wiley, New York (1962).

231. Rusoff, I.I., Platt, J.R., Klevens, H.B. and Burr, G.O., J. Am. Chem. Soc., 67, 673 (1945).

232. Closson, W.D. and Haug, P., J. Am. Chem. Soc. 86, 2384 (1964).

233. Closson, W. D., Orenski, P.J. and Goldschmidt, B.M., J. Org. Chem. 33, 416 (1968).

234. Closson, W. D., Orenski, P.J. and Goldschmidt, B.M., J. Org. Chem. 32, 3160 (1967).

235. Ralston, A.W., "Fatty Acids and Their Derivatives", Wiley, New York, (1948).

236. Morrison, R.T. and Boyd, R.N., "Organic Chemistry", Third Edition, Allyn and Bacon, Boston (1981).

237. Steigman, J. and Shane, N., J. Phys. Chem., 69, 968 (1965).

238. Pitzer, K.S. and Kim, J.J., J. Am. Chem. Soc., 96, 5701 (1974).

239. Khoo, K.H., J. Chem. Soc., Faraday Trans. I, 82, 1 (1986).

240. Robinson, R.A. and Stokes, R.H., "Electrolyte Solutions", Academic Press, New York (1959).

241. Murkerjee and Chan, unpublished work.

242. Henne, A.L. and Fox, C.J., J. Am. Chem. Soc., 73, 2323 (1951).

243. Randles, J.E.B., and Tedder, J.M., J. Chem. Soc., 1218 (1955).

244. Hood, G.C., Redlich, O. and Reilly, J., J. Chem. Phys., 23, 2229 (1955).

245. Kurz, D.L. and Farrar, J.M., J. Am. Chem. Soc., 90, 6057 (1969).

246. Mukerjee, P. and Ray, A., J. Phys. Chem., 70, 2150 (1966).

247. Gratzner, W.B. and Beaven, G.H., J. Phys. Chem., 73, 2270 (1969).

248. Mukerjee, P., J. Phys. Chem., 66, 943 (1962).

249. Mukerjee, P. and Ray, A., J. Phys. Chem., 70, 2d144 (1966).

250. Mukerjee, P. and Banerjee, K., J. Phys. Chem., 68, 3567 (1964).

251. Shinoda, K., Hato, M. and Hayashi, T., J. Phys. Chem., 76, 909 (1972).

252. Mukerjee, P., Korematsu, K., Okawauchi, M. and Sugihara, G., J. Phys. Chem., 89, 5308 (1985).

253. Hoffman, H. and Ulbricht, W., Z. Phy. Chemn. (Neae Fole) 106, 184 (1977).

254. Mysels, K.J. and Mysels, E., J. Coll. Sci., 20, 315 (1965).